Nigerian Journal Of Materials Science and Engineering (NJMSE)

Vol. 7 Number 2 ISSN 214-453-2 December 2016

Materials Science and Technology Society of Nigeria (MSN)

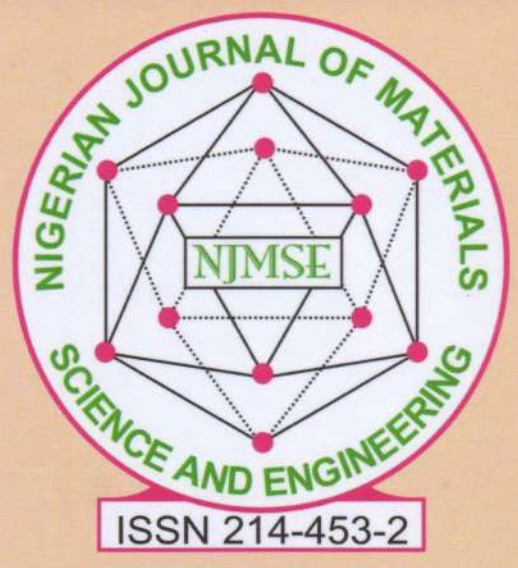

An International Journal of the Materials Science and Technology Society of Nigeria

Nigerian Journal
of
Materials Science and Engineering
[NJMSE]

ISSN: 214-453 2

A Publication of Materials Science and Technology Society of Nigeria (MSN)
[Formerly Materials Society of Nigeria (MSN)]

Nigerian Journal of Materials Science and Engineering (NJMSE)

Volume 7, No. 2; December 2016

Published by

Materials Science and Technology Society of Nigeria (MSN)
National Headquarters
Engineering Materials Development Institute (EMDI)
KM 4, Ondo Road, Akure

njmse@msn.ng; http://www.msn.ng

Printed by
Materials Science and Technology Society of Nigeria (MSN)

EDITORIAL COMMENT

The Nigerian Journal of Materials Science and Engineering is geared towards encouraging researchers to showcase and publish their work in all areas of Materials Science and Engineering, Physics and Chemistry, Nanomaterials and Nanotechnology, Biomaterials and other related fields.

Thanks to our numerous Authors and Reviewers, that made it possible for us to move at a pace that has bridged the gap that had been created by lack of financial support from our various donors. On behalf of the entire Board, I wish to sincerely apologise to our contributing authors, reviewers and researchers for the slight delay in publishing their articles in this Volume 7, Number 2.

You will find in this volume, just as in previous volumes, interesting quality articles to enhance knowledge in the frontiers of Materials Science and Engineering.

The Editorial Board is once again grateful to all reviewers for the time and intellect expended in reviewing the articles sent to them. We thank all authors who sent in their manuscripts for choosing to publish with us. We look forward to their continuous patronage.

We thank the National Executive Board of MSN for supporting and sponsoring the production of this volume.

Prof. F. E. Okieimen
Editor-in-Chief

Table of Contents

NIGERIAN JOURNAL OF MATERIALS SCIENCE AND ENGINEERING
NJMSE
ISSN 214-453-2

SYNTHESIS AND CHARACTERIZATION OF ZEOLITE-GOETHITE NANOCOMPOSITE

H. I. ADEGOKE*, M. O. BELLO AND A. F. DOLAPO
Department of Chemistry, University of Ilorin, P.M. B.1515, Ilorin, Nigeria
[adegoke.hi@unilorin.edu.ng, 07069365290]

ABSTRACT
In recent years, nanocomposite materials have received much interest in nanotechnology. This new trend in nanotechnology is aimed at producing materials of unique properties. In view of this, zeolite-goethite nanocomposite was synthesized to reinforce zeolite properties. Zeolite was synthesized hydrothermally from sodium aluminate, sodium silicate and sodium hydroxide at 100 ºC for 24 h. The composite was synthesized using in-situ method by adding aqueous solution of the synthesized zeolite during the synthesis of goethite. The structure, morphology and surface area of the zeolite and the composite were investigated using Fourier Transform Infrared (FTIR), Scanning Electron Microscopy (SEM), X-ray Diffraction (XRD) and Brunnauer Emmet Teller (BET) surface area analyzer respectively. The FTIR spectra and SEM micrographs confirmed the formation of zeolite–goethite composite with the surface area increase from 163.491 m^2/g for zeolite to 304.839 m^2/g for zeolite-goethite nanocomposite. It is evident that properties of zeolite can be improved upon by compositing with other materials like goethite. It can also be employed as an adsorbent for different environmental applications as revealed by the surface area.

Keywords: *Zeolite; Zeolite-goethite; Nanocomposite; Characterization; Hydrothermal method*

INTRODUCTION

Nanocomposite is referred to as a multiphase solid material which one of the phases has one, two or three dimensions of less than 100 nanometers (nm), or structures having nano-scale repeat distances between the different phases that make up the material (Tyagi and Tyagi, 2014). This new nanotechnological product has attracted considerable attention recently because of their distinctive physical and chemical properties. Nanocomposites are high performance materials which exhibit unusual property combinations and unique design possibilities (Carmago *et al*., 2009).

The hybrid composites have characteristics such as flexibility, easy processabilty; lightness strength, dimensional stability, chemical inertness, and thermal stability are bestowed on them from their components. Application volume for composite materials have grown steadily and have a large appreciation in the removal of toxic ion from water (Montes-Hernandez et al., 2013; Li *et al*., 2011), preparation of electrochemical sensor, immunosensor for pesticides detection, membrane for alkaline fuel cells, catalyst, energy, sensors, medicine, construction, bio-applications, food and water treatments (Taher *et al*; 2011; Hossein *et.al*., 2013).

Zeolites are microporous crystalline hydrated aluminosilicate materials consisting of SiO_4 and AlO_4 tetrahedra which are connected by oxygen atom (Rocha *et al*., 1998). Their framework structure contains interconnection of channels that are filled with cations usually from group IA or IIA which can be exchanged with other cations (Olad *et al*., 2011). These physico-chemical properties along side with others like crystallinity, thermal stability, well-defined cage structure of molecular size give natural and synthesized zeolites various application possibilities in different technological processes (Doula, 2007, Shyaa *et. al*., 2015). Zeolites have been widely used in catalysis, adsorption and ion exchange, it is becoming increasingly important in several environmental applications such as water purification, particularly for the removal of ammonia, heavy metals, radioactive species and organic substances (Bogdanov *et. al*., 2009).

Iron, its compounds and iron oxide nanoparticles are of considerable interest because of their biological and chemical properties. Iron oxides are widespread in the earth crust and play an important role in nature. Recently they are widely utilized in nanocomposite for various applications such as magnetic storage, medicine, chemical industries and water purification (Mohapatra *et. al.,* 2010). Goethite is one of the most common iron oxy-hydroxides in natural systems, they are commonly found in all types of soils throughout the world. It is frequently formed during weathering of other iron bearing minerals and is often the cause of the yellowish-brown colour of many soils. Goethite can occur naturally and can be synthesized (Hua *et al*., 2012).

In order to improve the capacity of zeolite they are composited or modified with other substance. Modification of zeolites can be realized using several methods, such as acid or base treatment, ion exchange and surfactant functionalization (Kugbe *et al*., 2008; Mihajlovic *et al*., 2014, Doula, 2007). Recently, zeolites were modified by oxides or hydroxides of metals, such as Al, Fe and Mn (Barquist, 2009). In this work, we synthesized and characterized goethite nanoparticle on the surface of zeolite and produced zeolite/goethite nanocomposite directly using *in-situ* method under a very basic condition.

MATERIALS AND METHODS

All chemicals used for the work were of analytical grade. The sodium hydroxide, sodium metasilicate, sodium aluminate and ferric nitrate for the synthesis were purchase from Sigma-Aldrich.

Synthesis of Zeolite

Zeolite was prepared according to the procedure reported by Hashemian *et al* (2013) from sodium metasilicate and sodium aluminate in the presence of sodium hydroxide. 40 ml of 0.225 M sodium hydroxide was added to each of 8.25 g of sodium aluminate and 15.48 g of sodium metasilicate in two separate containers. These mixtures were stirred for 30 min for the solution to become homogenous after which they were simultaneously transferred into a Teflon container, resulting in the formation of a creamy gel. The Teflon container was sealed in an autoclave (hydrothermal bomb) and heated at 100 °C for 24 h. After cooling, the precipitate was dialyzed, filtered using a vaccum filter and dried in the oven at 100 °C.

Synthesis of Zeolite-Goethite Nanocomposite

The zeolite-goethite nanocomposite was prepared by the procedure reported by (Mihajlovic et al 2014, Kragovica *et al.,* 2012). A suspension was made by mixing 20.0 g of the synthesized zeolite in 100 cm^3 of freshly prepared 1M Fe $(NO_3)_3.9H_2O$ solution in a polyethylene flask. The KOH solution was added rapidly made up to 180 cm^3 under stirring. The suspension was diluted with deionized water to 2000 cm^3 and held in a closed polyethylene flask at 70 °C for 60 h. Finally, the obtained precipitate was dialyzed to remove the anions and then dried at 105 °C.

Characterization Methods and Instruments

Instrumental characterization techniques such as Fourier transform infrared (FT-IR) spectroscopy, Scanning Electron Microscope (SEM), X-ray Diffraction (XRD) (CPI diffractometer model) and the Brunnauer Emmet Teller (BET). GX - FT-IR spectrophotometer (Model) were used for identification of surface functional groups, the SEM (SCOTech Mel-30000) was applied to observe morphology while the surface area was examined using BET. XRD pattern was used to observe the crystallinity of the sample. Other physicochemical properties like pH, colour, texture, bulk density and point of zero charge (pzc) were also observed. The point of zero charge (pzc) of the zeolite-goethite nanocomposite was determined by the batch equilibration technique (salt addition method) in which $NaNO_3$ solution of different ionic strengths: 0.1, 0.01, 0.001 mol/dm^3 were used as electrolyte solutions. The initial pH values (pH_i) of the electrolyte solution (25cm^3 of each in a series) of the predetermined concentration were adjusted by the addition of 0.1mol/dm^3 of HNO_3 or NaOH in the pH range of 3.5 to 10.5. Then 0.05 g of zeolite and the zeolite-goethite composite was added to each sample (At the ratio of solid: liquid=1:500). After 24 h of equilibration at room temperature under constant shaking, the suspension was filtered and then the pH of the filtrate was determined (pH_f). The initial pH versus the difference between the initial and finial pH values (ΔpH) was plotted. The pzc was taken as the point where ΔpH = 0 (Mihajlovic *et al* 2014; Kragovica *et al*., 2012).

RESULTS AND DISCUSSION

Physicochemical properties of zeolite and zeolite-goethite nanocomposite

The result of the physicochemical properties of zeolite and zeolite-goethite nanocomposite is presented in Table 1. The golden-brown colour of goethite imparts on the initial colour of the synthesized zeolite to make the colour of the composite brownish. The texture is however not affected by the introduction of goethite filler into the zeolite matrix. For the pH, the pH medium for the synthesis of both the zeolite and goethite is alkaline. This is likely to be based on the pH medium of the precursors.

Bulk density is a significant property which tends to correlate with other properties like porosity and cation exchange capacity. The bulk density of the zeolite-goethite nanocomposite gives higher value (0.6288g/cm^3) compared to zeolite alone (0.39778g/cm^3). This is an indication of the improvement shown on the nanocomposite material.

Point of zero charge (pzc) is the pH at which the surface of material has net neutral charge. From Figs. 1(a) and (b), the value obtained at the intersection of the pH_i with the ΔpH = 0 gives the point of zero charge of the sample (Cardenas-Pena *et al*., 2012). As observed from Fig. 1(a), point of zero charge (pzc) of zeolite nanoparticle is 8.5 ± 1 while that of zeolite-goethite nanocomposite is found to be 9.5 ± 1. The higher pzc value obtained for zeolite-goethite nanocomposite is an indication of increase in alkalinity of its surface (Mihajlovic *et al.,* 2014) caused by introduction of goethite. Similar observation (i.e higher pzc value for Fe (III) modified zeolite, 7.5 ± 0.1 compared to natural zeolite, 6.8 ± 0.1) was also reported by Kragovic *et al* (2012).

Table1: Properties of zeolite and zeolite-goethite nanocomposite

Properties	Zeolite	Zeolite-goethite nanocomposite
Colour	Whitish	Brownish-red
Texture	Smooth	Coarse
pH	10.0	9.0
Bulk density	0.39778 g/cm^3	0.6288 g/cm^3
Point of zero charge	8.5 ± 1	9.5 ± 1

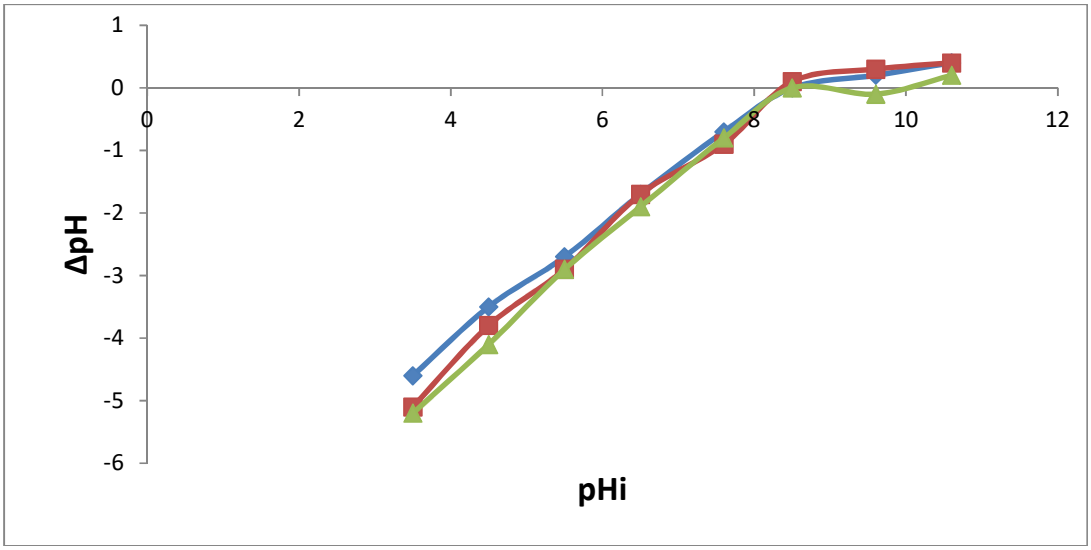

Fig.1a: Point of zero charge of zeolite-nanoparticles at 0.001, 0.01 and 0.1mol/dm^3

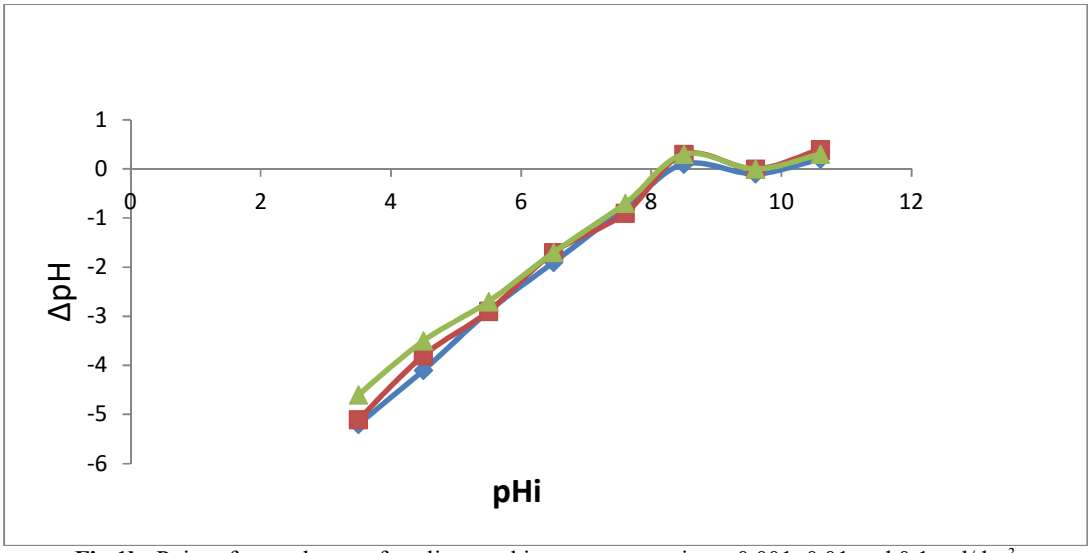

Fig.1b: Point of zero charge of zeolite-goethite nanocomposite at 0.001, 0.01 and 0.1mol/dm^3

Instrumental Characterization

Characterization of nanocomposite materials gives proper and better understanding of the materials towards its properties and applications.

FT-IR Spectroscopy

The FT-IR spectra of zeolite and zeolite-goethite nanocomposite are shown in Figures 2a and 2b respectively. The spectra show an absorption in the region of 1004 cm^{-1} in the zeolite and 997 cm^{-1} in the zeolite-goethite nanocomposite indicate terminal silanol groups [Si-O(Si) and Si-O(Al)] on the external surface of the samples (Huiping *et al*., 2014; Thuadaij and Nuntiya, 2012). Hossein *et al*., (2013) positioned that absorption in the regions of 900 to 1200 cm^{-1} resulted from stretching and bending modes of Si-O or Al-O in framework. The peak that is broad and strong at 3450 cm^{-1} in spectra (2a) for zeolite and 3423 cm^{-1} in spectral (2b) for the composite correspond to O-H stretching (Hossein *et al*., 2013; Ru´ız-Baltazar *et al*., 2015). The peak in the region of 1654 cm^{-1} and 1645 cm^{-1} corresponds to O-H bending vibration for zeolite and zeolite-goethite nanocomposite respectively. The three bands at 462, 559 and 694 cm^{-1} in 2(a) and 447, 555, and 640 cm^{-1} in 2(b) are associated with the asymmetric and symmetric stretching modes of internal tetrahedral (Kugbe *et al*., 2008, Khandanlou *et al*., 2015, Hossein *et al*., 2013; Thuadaij and Nutiya, 2012). Figure 2a and 2b also showed that zeolite and its composite spectra do not significantly differ from one another in the spectral regions 400 to 4000 cm^{-1}. This fact indicates that zeolite structure has not changed much in the reaction to form the composite.

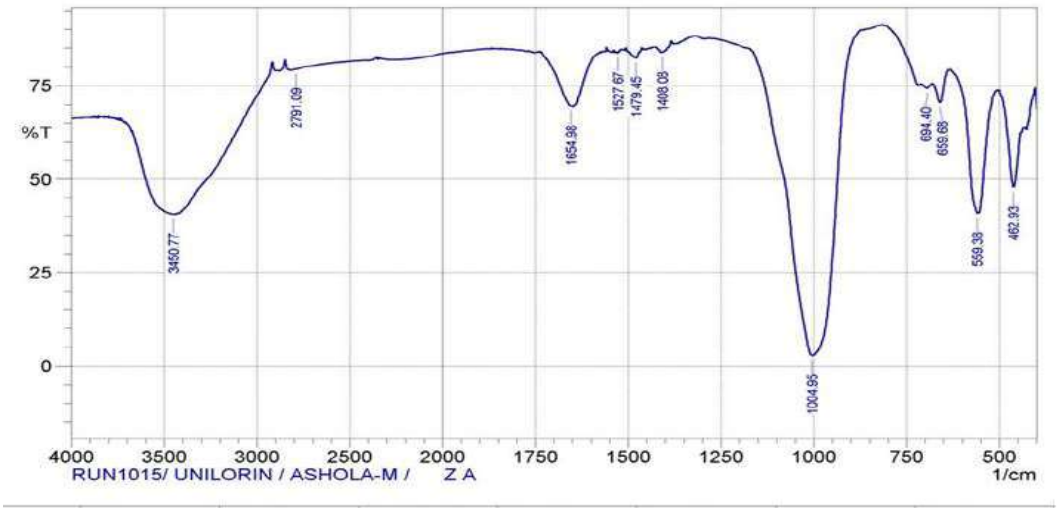

Fig 2a: The FTIR Spectrum of the zeolite nanoparticle

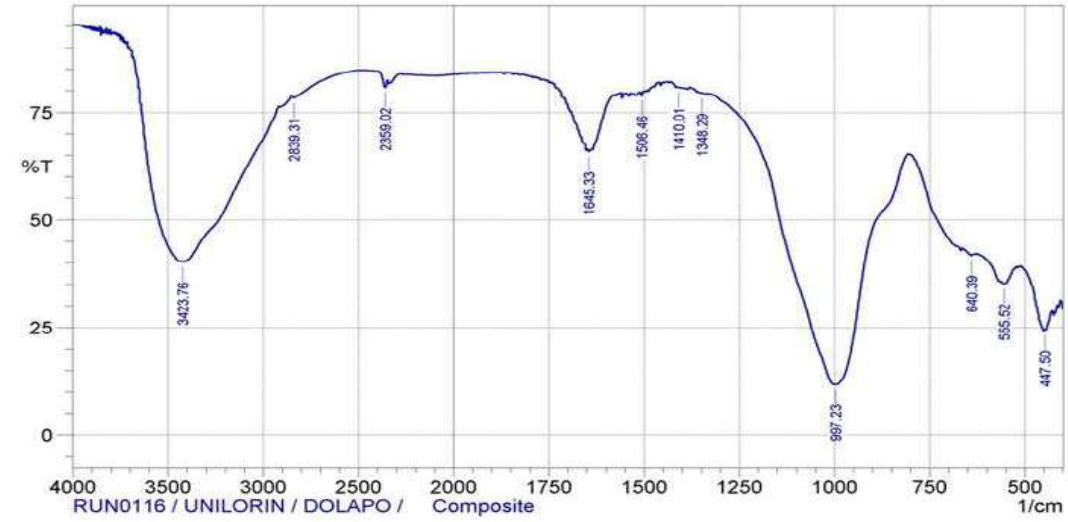

Fig 2b: The FTIR Spectrum of the zeolite-goethite nanocomposite

Scanning Electron Microscopy

The synthesized nanoparticle morphology was characterized by scanning electron microscope (SEM) using SCOTech Mel-30000 Scanning Electron Microscope. The SEM images for the surface morphology of both the zeolite and zeolite-goethite nanocomposites are shown in Figs. 3a and b. The surface morphology of zeolite, Fig. 3 (a) shows abundant small nearly spherical but scattered particles. While its goethite composite, Fig. 3 (b) indicates the deposition of goethite particles on the surface of zeolite and thereby forming an aggregate of particle with numerous pores. With this, it is evident that composite material of zeolite and goethite was successfully prepared (Kugbe *et al*., 2008)

Brunnauer Emmet Teller (BET)

The specific surface area (SSA_{BET}) of both materials, zeolite and zeolite-goethite nanocomposite was determined with low-temperature adsorption/desorption method based on the Brunnauer Emmet Teller theory multilayer adsorption. The result showed that zeolite-goethite nanocomposite has larger surface area, 304.838 m^2/g compared to that of zeolite, 163.491 m^2/g. Also from the t-plot micropore analysis, zeolite has smaller value of external surface area, micropore area and micropore volume as shown in Table 2. There is a significant increase in the external surface area and the micropore volume on the composite material. This observation can be assumed that the particles of iron oxide (goethite) were precipitated on the surface of zeolite forming aggregates (Mockovčiaková *et al*., 2006). The negative value of micropore volume in the zeoliote-goethite composite may however cause by noise and can be assumed to zero value.

X-ray Diffraction (XRD)

The XRD pattern of the zeolite sample is shown in Figure 4. XRD analysis shows the crystalline phases of the sample. There are pronounced peaks at 2Θ values of 15, 25, 32, 35 and 42°. The result is in good agreement with literature data of Ozdemir and Sabriye, (2013).

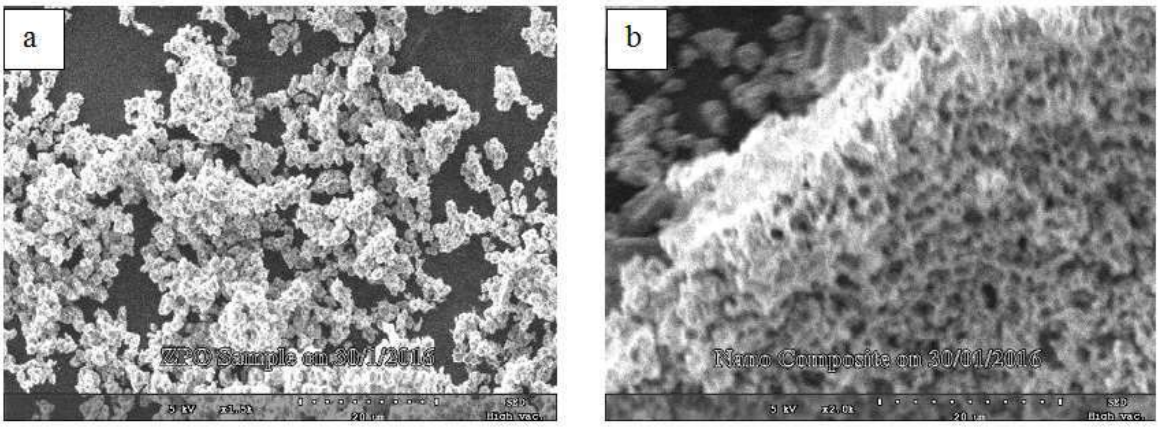

Fig. 3: SEM micrographs of (a) zeolite (b) zeolite-goethite nanocomposite

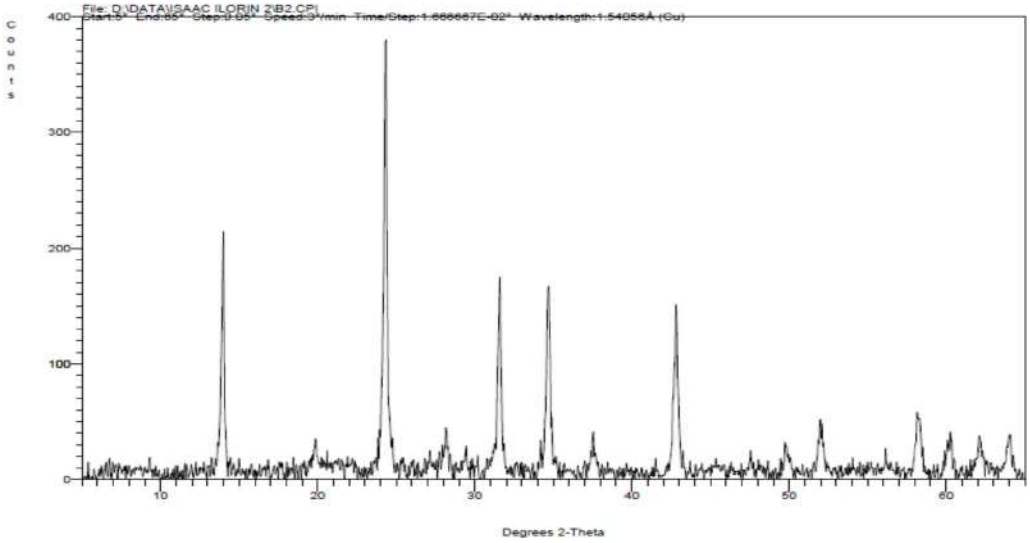

Fig 4: X-ray diffraction pattern of synthesized zeolite

Table 2: BET parameters of zeolite and zeolite-goethite composite

Materials	$SSS_{(BET)}$ (m^2/g)	External surface area (m^2/g)	Micropore area (m^2/g)	Micropore volume (cm^3/g)
Zeolite	163.491	163.491	0.00	0.00
Zeolite-goethite	304.838	261.154	42.684	-0.080

CONCLUSION

The zeolite and zeolite-goethite nanocomposite were synthesized and characterized towards its application as a possible adsorbent material for removal of pollutant from water. The zeolite-goethite nanocomposite was prepared from iron (III) trioxonitriate (V) and Potassium hydroxide aqueous solutions with aqueous solution of the synthetic zeolite by using *in-situ* method under basic condition. The obtained results of Fourier transform infrared spectroscopy (FT–IR), scanning electron microscopy (SEM), confirmed the formation of zeolite-goethite nanocomposite. This is a clear indication that properties of zeolite can be improved upon by compositing with other materials like goethite. Consequently, the synthesized zeolite materials can be employed as an adsorbent for different environmental applications as revealed by the surface area.

REFERENCES

Barquist K. N. (2009). Synthesis and environmental adsorption applications of functionalized zeolites and iron oxide/zeolite composites. Online Thesis and Dissertations of University of Iowa. Available on http://ir.uiowa.edu/cgi/viewcontent.cgi?article=1519&context=etd Retrieved on 28/03/2017

Bogdanov B., Georgiev D., Angelova K. and Hristov, Y. (2009). Synthetic Zeolites and Their Industrial and Environmental Applications Review. International Science Conference, Natural and Mathematics Science, IV, 1-5

Cardenas-Pena A. M., Ibanez J. G., Medrano R.V., (2012). Determination of the Point of Zero Charge for Electrocoagulation Precipitates

from an Iron Anode. International Journal of Electrochemical Science, 7, 6142 – 6153

Carmago P. C., Satyanarayana K. G. and Fernando Wypych F. (2009). Nanocomposites: Synthesis, Structure, Properties and New Application Opportunities. Materials Research, 12(1), 1-39

Doula M. K. (2007). Synthesis of a clinoptilolite–Fe system with high Cu sorption capacity, Journal of Chemosphere 67, 731–740.

Hashemian S., Hosseini S. H., Salehifar H., Salari K., (2013). Adsorption of Fe(III) from aqueous solution by Linde Type A-zeolite. American Journal of Analytical Chemistry, 4, 123-126

Hossein J., Mohd H., Shah I., Md J. H., Roshanak R. M. , Kamyar S., Soraya H., Yoon K., Roshanak K., Elham G. and Sepideh S. (2013). Synthesis and Characterization of Zeolite/Fe3o4 Nanocomposite by Green Quick Precipitation Method. Digest Journal of Nanomaterials and Biostructures, 8 (4), 1405 – 1413.

Hua M., Zhang S., Pan B., Zhang W., Lv L., Zhang Q., (2012). Heavy metal removal from water/wastewater by nanosized metal oxides: A review. Journal of Hazardous Materials, 212, 317– 331

Huiping S., Huaigang C., Zepeng Z. and Fangqin C., (2014). Adsorption properties of zeolites synthesised from coal fly ash for Cu (II). Journal of Environmental Biology, 35, 983-988.

Khandanlou, R., Ahmad, M. B., Fard Masoumi, H. R., Shameli, K., Basri, M. and Kalantari, K. (2015). Rapid Adsorption of Copper(II) and Lead(II) by Rice Straw/Fe_3O_4 Nanocomposite: Optimization, Equilibrium Isotherms, and Adsorption Kinetics Study. PLoS ONE, 10(3), e0120264. http://doi.org/10.1371/journal.pone.0120264

Kragovica M., Dakovica A., Sekulica Z., Trgob M., Ugrinab M., JelenaPeric J. G., Gattac D. (2012). Removal of lead from aqueous solutions by using the natural and Fe(III)-modified. Applied Surface Science, 258, 3667–3673

Kugbe J., Matsue N., Henmi T., (2008); Synthesis of Linde Type A Zeolite-Goethite Nanocomposite as an Adsorbent for Catonic and Anionic Pollutants. Journal of Hazardous Materials, 164, 929-935.

Li S., Zhou P. and Ding L. (2011). Adsorption Application for Removal of Hazardous Chloroform from Aqueous Solution by Nanocomposites Rectorite/Chitosan Adsorbent. Journal of Water Resource and Protection, 3, 448-455

Mihajlovic M. T., Lazarevic S. S., Jankovic-Castvan I. M., Jokic B. M., Janackovic D. T., Petrovic R. D. (2014). A Comparative study of the removal of Lead, Cadmium and Zinc ions from aqueous solutions by natural and Fe(III)-Modified zeolite. Journal of Chemical Industries and Chemical Engineering Quarterly. 20 (2), 283−293

Mockovciakova A., Orolinova Z., Matik M., Hudec P. and Kmecova E. (2006). Iron Oxide Contribution to the Modification of Natural Zeolite. Acta Montanistica Slovaca, 11(1), 353-357

Mohapatra, M. and Anand S., (2010). Synthesis and applications of nano-structured iron oxides/hydroxides – a review, International Journal of Engineering, Science and Technology, 2 (8), 127-146

Montes-Hernandez G., Renard F., Chiriac R., Findling N., Ghanbaja J. and Toche F. (2013). Sequential precipitation of a new goethite–calcite nanocomposite and its possible application in the removal of toxic ions from polluted water. Chemical Engineering Journal, 214, 139-148

Olad A., Khatamian M. and Naseri B. (2011). Removal of Toxic Hexavalent Chromium by Polyaniline Modified Clinoptilolite Nanoparticles. Journal of the Iranian Chemical Society, 8, 141-151

Ozdemir O.D. and Sabriye P. (2013) Zeolite X Synthesis with Different Sources. Int. Journ. of Chemical, Environmental and Biological Sciences (IJCEBS) 1 (1), 229-232.

Rocha J. Ferreira P., Lin Z., Brandao P., Ferreira A., and Pedrosa de Jesus J. D. (1998). Synthesis and Structural Characterization of Microporous Yttrium and Calcium Silicates. Journal of Physical Chemistry, B, 102, 4739-4744

Ruiz-Baltazar A., Esparza R., Gonzalez M., Rosas G. and Pérez R. (2015) Preparation and Characterization of Natural Zeolite Modified with Iron Nanoparticles. Journal of Nanomaterials, 1-8

Shyaa A. A., Hasan O. A., Abbas A. M. (2015). Synthesis and characterization of polyaniline/ zeolite nanocomposite for the removal of Chromium (VI) from aqueous solution. Journal of Saudi Chemical Society, 19, 101–107.

Taher A. S., Ahmed A. E., Daifallah M. A., Abdullah M. A. and Salem S. A. (2011). Synthesis and Characterization of Magnetite Zeolite Nanocomposite, International Journal of Electrochemical Science, 6, 6177 – 6183.

Thuadaij P. and Nuntiya A. (2012). Effect of the SiO_2/Al_2O_3 ratio on the synthesis of Na-x zeolite from Mae Moh fly ash. Science Asia, 38, 295–300

Tyagi M. and Tyagi D. (2014). Polymer Nanocomposites and their Applications in Electronics Industry International Journal of Electrical and Electronics Engineering, 7(6), 603-608

NIGERIAN JOURNAL OF MATERIALS SCIENCE AND ENGINEERING
NJMSE
ISSN 214-453-2

ZEOLITE NAY FROM KANKARA KAOLIN USING COMMERCIAL GRADE CHEMICAL: EFFECT OF CRYSTALLIZATION TIME AND TEMPERATURE

O. A. AJAYI[1], J. MAMMAN[1] AND S. S. ADEFILA[2]
[1]Department of Chemical Engineering, Ahmadu Bello University, Zaria. Kaduna State. Nigeria.
[2]Engineering Environmental Management Services, Suite 5 1st Floor, Plot 1469, Ahmadu Bello Way, Garki, Abuja.
[segeaj@gmail.com and aoajayi@abu.edu.ng]

ABSTRACT
Zeolite Y was synthesized using commercial sodium hydroxide and Kankara kaolin as starting material in the presence of sodium silicate formed from kaolinite clay. Synthesis was done at 90°C, 95°C and 100°C for crystallization time of 12, 18, 24 and 36 hours. Results showed that commercial sodium hydroxide could be used to successfully produce zeolite Y from Kankara kaolin when gelling ratios of $\frac{H_2O}{Na_2O} = 30, \frac{Na}{Na+K} = 0.8$ *and* $\frac{Na_2O}{SiO_2} = 0.7$ *are used. Zeolite Y with the best crystallinity was produced at 90°C for 18 hours. Crystallisation of zeolite materials from kaolin and low grade NaOH is quite different from commercial zeolite because the sources of Si and Al are relatively less reactive due to the presence of competitive cation ions, like* K^+, Mg^{2+}, *present in the monomer. Additionally, the sodium silicate, selectivity induces the formation of zeolite NaY and eliminate the processes of induction and nucleation. Cost analysis per unit catalyst, showed an overwhelming $185.524 difference between imported high grade chemicals and local chemicals in favour of locally obtained chemicals. The as-synthesized zeolite was characterized using XRF, XRD and SEM analyses. The resulting NaY zeolite can find application in refining process, as shown by the XRD results.*

Keywords: *NaY, Crystallization, dealumination, Kankara kaolin, sodium silicate*

INTRODUCTION

Zeolites are crystalline solids with micropores having engineered dimension capable of handling variety of chemicals and are highly selective to targeted products. They are aluminosilicate minerals containing regular arrays of pores and cavities that can accommodate a wide variety of cations (positively charged ions), such as Na^+, K^+, Ca^{2+}, as well as small molecules, such as water. Due to their immense importance as catalysts, adsorbents, and ion exchange material, there is great interest in the process by which different zeolites and relative molecular sieves are formed. This is so important, in order to control their phase distribution, composition, structures and macroscopic properties. Over 150 synthetic and 40 naturally occurring zeolites are known (Marcus and Cormier, 1999). Initially only natural zeolites are used but more recently, synthetic forms have been made on an industrial scale giving rise to tailor made zeolites that are highly replicable. Structurally, zeolites are framework alumino-silicates, which are based on infinitely extending three dimensional Al_2O_3 and SiO_2 tetrahedral linked to each other by sharing all the oxygen (Breck, 1974; Richardson, 1989). They can be represented by the empirical formula:

$$M_{2/n}O \bullet Al_2O_3 \bullet xSiO_2 \bullet yH_2O$$

In this oxide formula, x is generally equal to or greater than 2 since tetrahedral AlO4 are joined only to tetrahedral SiO4 and n is the valency of the cation. They are traditionally formed from high grade chemicals such as sodium silicate, sodium aluminate and sodium hydroxide (Cundy and Cox, 2005). However, the preparation of synthetic zeolites from chemical sources of silica and alumina is expensive. Such costs may be reduced by the use of clay minerals, volcanic glasses (perlite and pumice), rice husks, diatomite, fly ash or paper sludge ash as starting materials (Adamczyk and Bialecka, 2005; Querol *et al*., 1997; Saija *et al*., 1983; Tanaka *et al*., 2004; Walek *et al*., 2008; Wang *et al*., 2008), though with rather less crystallinity and sometime associated allowable unwanted phases. Zeolite has also been developed by the transformation of one zeolite type into other zeotypes (Rios *et al*., 2007; Sandoval *et al*., 2009). Apparently, some mineral ores and waste materials could serve as good source for the necessary monomers for zeolite synthesis (Barrer, 1988; Chandrasekhar and Pramada, 1999; Murat *et al*., 1992; Tavasoli, *et al*., 2014 and Atta *et al*., 2007). Amongst different zeolite groups, faujasites, particularly zeolite Y has attracted lots of interest due to its application in the fluidized catalytic cracking unit of refineries. Factors affecting synthesis of zeolite Y includes: nature of reactant, chemical composition and pre-treatment, overall homogeneity of the mixture, ageing, pH (alkalinity), seeding and conditions of crystallization (i.e. temperature and time). Numerous studies have been and are still undertaken to deepen understanding of the formation, kinetics and mechanisms of zeolite Y formation from alkaline precursor solutions (Liu *et al*, 1998) Wang *et al*., (2008), investigated the role of NaOH in zeolite synthesis and concluded that NaOH concentrations determine compositions, molar ratio of prepared initial gel, and then affect structural formation, morphology, particle size distribution and in some cases, type of zeolite formed. Ajayi (2012), identified inadequate depolymerisation of the aluminosilicate by sodium hydroxide used as one amongst several factors affecting the successful synthesis of zeolite Y from Kankara kaolin. Imported high grade chemicals are mostly used to help solve this problem. However, these high-grade chemicals are very expensive and it takes several weeks running to months to arrive the country, impeding the swiftness of the research. This work

attempts to address the trade-off between quality/purity of chemicals used and pace/cost of research. Throughout this research, locally obtained chemicals were used to reduce cost of production of zeolite Y, without affecting its end application as catalyst for refining process, while investigating the effects of crystallization time and temperature on the final product phase.

METHODOLOGY

Raw kaolin obtained from Kankara, Katsina State, Nigeria, was wet beneficiated for 3 days and the slurry sieved to get rid of coarse particles with a 53 µm sieve. The fine suspension thus obtained was allowed to settle and the supernatant water decanted. The sediment was dried at atmospheric condition and in an oven at 100ºC for 6 hours, milled and calcined in a furnace at 750°C for 6 hours to obtain metakaolin, a more reactive phase of kaolin. The metakaolin was dealuminated to obtain Si/Al ratio adequate for zeolite Y synthesis. 80g of dealuminated metakaolin was measured and mixed with the required amount of water from the mole ratio $\frac{H_2O}{Na_2O} = 30$ and then thoroughly mixed with a high torque mixer for ten minutes. The required mass of sodium hydroxide from the mole ratio $\frac{Na}{Na+K} = 0.8$ *and* $\frac{Na_2O}{Sio_2} = 0.7$ were prepared and added to the mixture. Sodium silicate synthesis from Kankara clay by our group was added, while keeping the silica-alumina ratio of the mixture at level good enough for the targeted zeolite Y. The resulting gel was placed in a polypropylene bottle and aged for five days. The aged gel was placed in an oven at 90°C. After specified crystallization reaction time of 12 to 36 hours, the samples were removed washed and dried. The same procedure was thereafter repeated for same reaction times but at temperatures of 95 and 100°C. The products obtained were subjected to characterization.

Characterization techniques

Chemical composition was conducted using X-ray fluorescence (XRF) technique (PW 1400 spectrometer, Philips). The structural analysis was carried out using X-ray diffraction (XRD) patterns were recorded on a PW 1840 diffractometer (Philips), with Ni filtered Cu kα radiation at 40 kV and 40 mA. The measurements were carried out with a step width of 0.03_ 2h and scan rate of 1 s per step. The morphology was recorded by scanning electron microscopy (SEM) using a JEOL 6400.

RESULTS AND DISCUSSION

Beneficiation, as expected reduces the silica content from 58.3 to 55.768, which was achieved through floatation and dissolution of free silica, the molar Si/Al reduced from 2.55 to 2.3 as a result, which is still rather higher than theoretical value. Dealumination increased the Si/Al ratio to about 4.5 which is within the range stipulated for the synthesis of Zeolite Y from kaolin, which was later altered to 4.7 with introduction of freshly prepared kaolinite derived sodium silicate. The structural and morphological analyses of the kaolinite clay and sodium silicate were already discussed in an earlier paper (Ajayi, 2016).

Zeolite synthesis -Crystallization Conditions

Figures 1-3 show formation of faujasite zeolite comprising mainly of Y and traces of X and undepolymerized quartz. From the composition of the phases it could be safely deduced that the NaOH used depolymerised a high percentage of the silica in the precursor, despite the presence of quartz noticed. The peaks at 2 theta position of about 6.3 agrees with the principal peak of Na-Y (Treacy and Higgins, 2007). From Figure 1, it can be deduced that crystallization at 90°C for 18hrs had a relatively higher intensity for the zeolite Y characteristic peak.

Figure 3 shows that at 100°C Na-Y was synthesized along with Na-X and spikes of ZSM-5, ZSM-11 and TNU-7 and quartz. It was noted remarkably, that there was a progressive increase in the number of phases attributed to zeolite Y from Figure 1 to 3 which implies that a slight increase in the temperature between 90°C to 100°C affects the phases of zeolites Y formed (Li *et al.*, 2010). Additionally, the intensity of quartz was noticed to improve with increase in temperature, justifying the speculation of metastability of zeolite Y and formation of thermodynamically favoured product. (Bouchiba *et al.*, 2011).

Effect of crystallization time and temperature on crystallinity of zeolite

The crystallinity of zeolite Y phase increased as depicted in Figure 4 between 12-18 hours of crystallization time for all temperatures. This trend agrees with literature that crystallinity increases with time (Sang *et al.*, 2006).

The disordered form of the aluminosilicate in the gel favours the formation of zeolitic material than its already ordered counterpart, quartz, in Figure 5, hence the sharp increase in crystallinity for Na-Y. Above 18 hours the trend slopes downward, indicating decrease in crystallinity with time. This inconsistency could be attributed to the effect of impurities and/or metastability of formed zeolitic materials for prolonged crystallization time.

The sample with the highest crystallinity was gotten at 18hours at 90°C. The SEM image for this sample is shown in Figure 6, depicting its high crystallinity after other associated zeolitic phases.

Table 1. Composition of Kaolin

Oxide	SiO_2	Al_2O_3	Na_2O	SO_3	Fe_2O_3	CaO	K_2O	ZnO	PbO	MnO	Si/Al (mol)
RKK[1]	58.300	32.200	0.120	0.189	3.160	0.150	1.260	0.176	0.043	0.090	2.55
BK[2]	55.768	40.750	0.074	0.185	1.320	0.113	0.981	0.175	0.042	0.019	2.3
DK[3]	71.895	24.470	0.106	0.258	0.908	0.103	1.516	0.065	0.039	0.009	4.499

[1]Raw Kankara Kaolin [2]Beneficiated Kaolin [3]Dealuminated Metakaolin

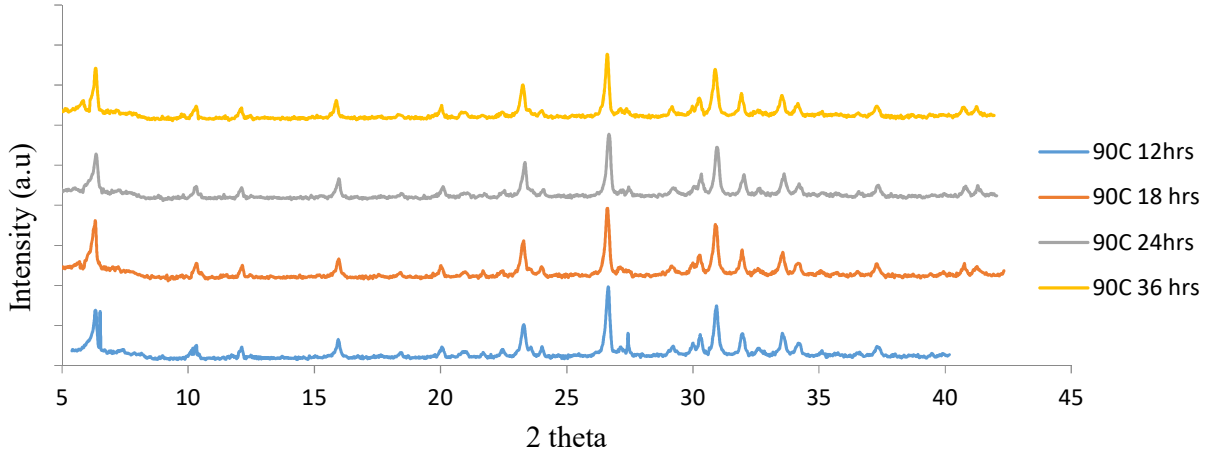

Fig.1. XRD patterns of zeolites synthesized at 90º C

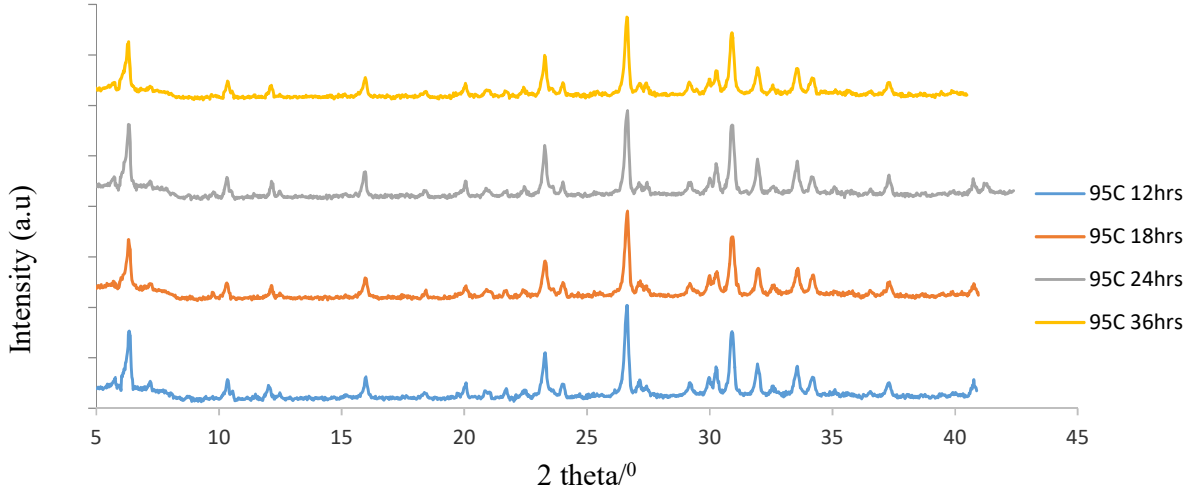

Fig.2. XRD patterns of zeolites synthesized at 95º C

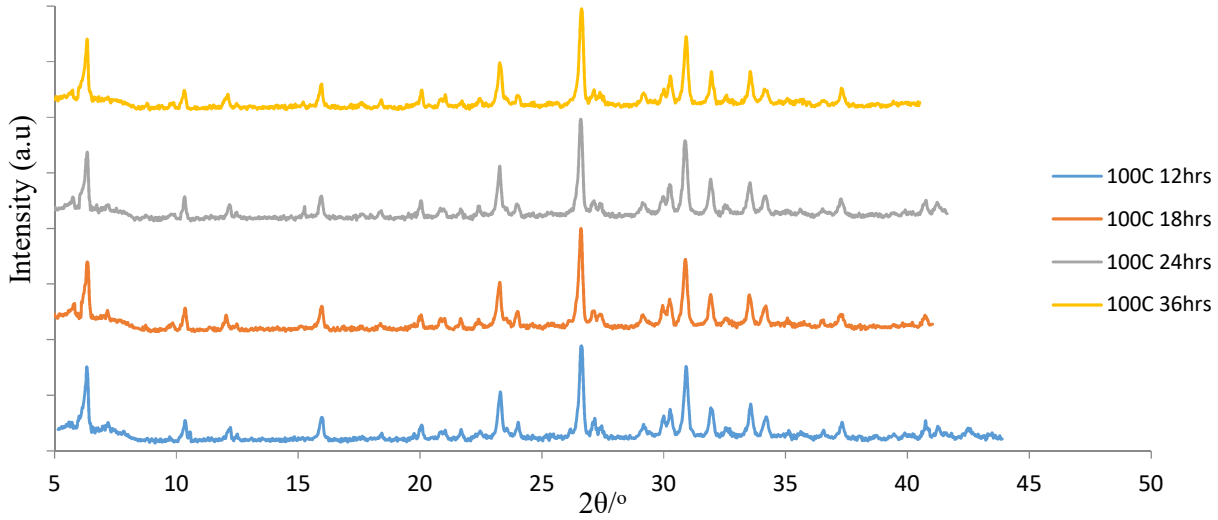

Fig. 3.XRD patterns of zeolites synthesized at 100º C

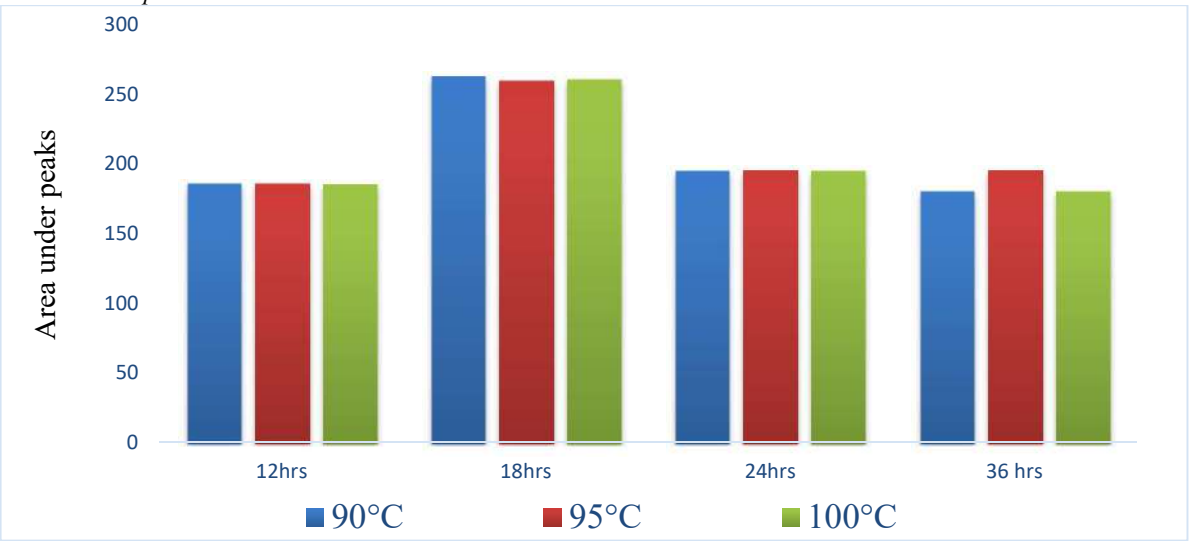

Fig.4. Na-Y phase at 90º – 100º C for various time

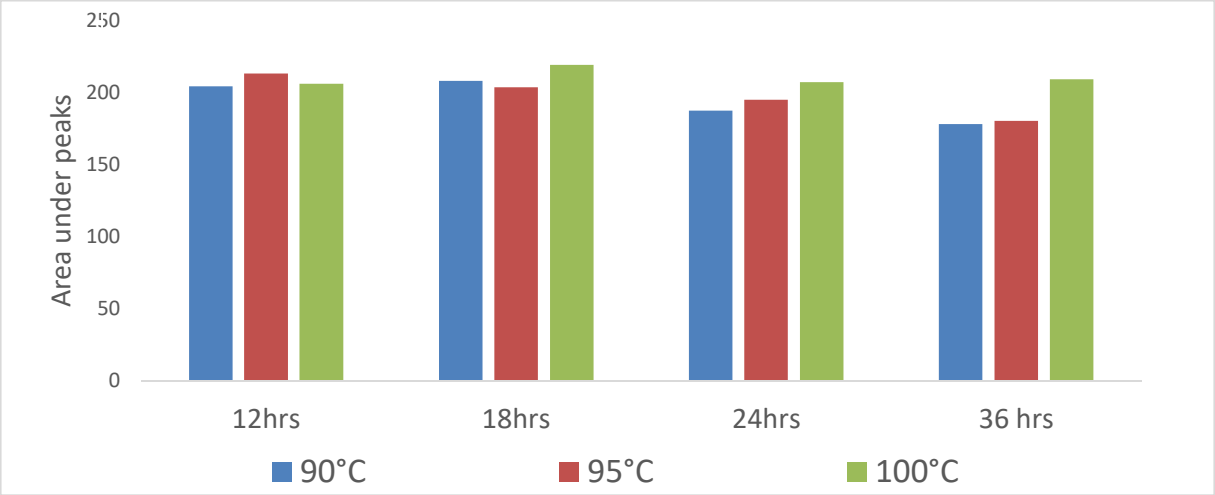

Fig.5. Unconverted (quartz phase) at 90º – 100º C for various times.

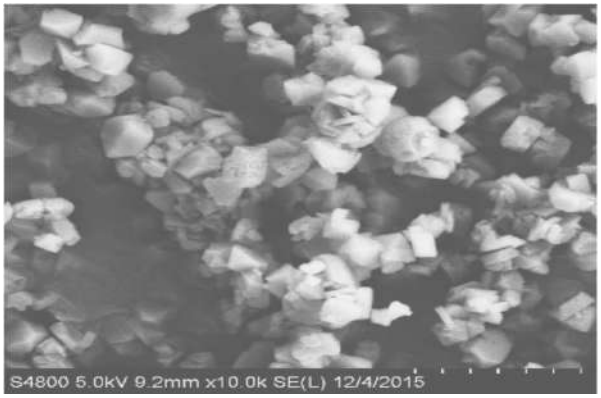

Figure 6: SEM image for as-synthesized zeolite at 900C for 18hrs

The product (whose SEM is shown in Figure 6) compositional ratios were determined and shown in Table 2. The silica to alumina ratio of zeolite Y was within the range of 3-5 from literature (Magee, and Mitchell). Comparing compounded ratios and product ratios, there was an increase in Na/(Na+K) from 0.8 to 0.947, Previous works of Breck, 1974 and Ajayi *et. al*., (2013), concluded that the closer this ratio is to one, the lesser the eclipsing effect of potassium. They also opined that a reduced Na_2O/SiO_2 and Si/Al favours the formation of zeolite Y.

Reduction in ratios Na_2O/SiO_2 and Si/Al were seen from 0.7 to 0.162 and 4.99 to 3.01, respectively. The reduction in Na_2O/SiO_2 suggests that the sodium hydroxide used was active enough to depolymerize about 77% of the inherent SiO_2. This was responsible also for the reduction noticed in molar ratio of Si/Al. The aforesaid give credence to the successive synthesis of zeolite Y using low-cost locally obtained chemicals.

Table 2. Mineral composition of zeolitic product

Oxides	**Na_2O**	**MgO**	**Al_2O_3**	**SiO_2**	**SO_3**	**K_2O**	**CaO**	**TiO_2**	**Mn_2O_3**	**Fe_2O_3**
(w/w%)	12.28	0.37	30.87	53.20	0.231	1.011	0.110	0.358	0.015	1.492

Gel composition: Na/(Na+K)=0.8 ***Product Composition***: Na/(Na+K)=0.947
Na_2O/SiO_2=0.7 Na_2O/SiO_2=0.162; Si/Al=4.99 Si/Al=3.01

Table 3. Zeolitization Process Economy

Unit process	**Chemical**	**Cost and Sources of Chemicals ($)**	
		Commercial chemicals	Sigma-Aldrich chemicals
Dealumination	H_2SO_4 (1L)	21.21	152.958
Gelation	NaOH (500g)	9.696	63.472
Total Cost ($)		30.906	216.43

From Table 3, the cost on unit weight basis is $0.85/gram of zeolite Y produced. Though reagent grade chemicals are purer and may give better results, the high cost of reagent grade chemicals and it not being readily available was a source of concern. A difference in cost of $185 is significant enough to cause concern to Nigerian researchers and tilt them towards the use of commercial chemicals which hitherto were considered not good enough for zeolite Y production. The results from XRD and SEM confirms the applicability of the synthesized zeolite in cracking process, since the commercial FCC zeolite are often blended with amorphous material, which is not necessary for the one presented here. The differential cost difference of $185 is much when we take into consideration the quantity of this zeolite used in FCC unit and also their life span during the process.

CONCLUSION

Zeolite NaY was successfully synthesized from kaolin using industrial grade NaOH in the presence of sodium silicate sourced from kaolin. The use of commercial grade sodium hydroxide in the synthesis of zeolite was successful as it was able to depolymerize silica in Kankara Kaolin, besides saving cost, it ensured that the research went without delay for arrival of chemicals from overseas. The ratios employed for chemicals used ensured adequate depolymerisation and help to conceal the effect of impurities such potassium which constitute a nuisance in the synthesis of zeolite Y from Kankara kaolin. The process economy tends to favour investment in local production of zeolite NaY using this route, for about $185 can be saved per unit cost of production.

REFERENCES

Adamczyk, Z., Bialecka, B., 2005. Hydrothermal synthesis of zeolites from polish coal fly ash. Pol. J. Environ. Stud. 14 (6), 713–719.

Ajayi, O.A (2012). Development of large pore zeolites from kaolinite clay. Ph.D Thesis, ABU, Zaria.

Ajayi, O. A. Mamman, J and Adefila, S.S (2016). Comparative Synthesis of Sodium Silicate from Rice Husk and Kaolin. Paper submitted to Nigerian Journal of Materials Science and Engineering (NJMSE).

Atta, A.Y., Ajayi, O.A., Adefila, S.S., (2007). Synthesis of Faujasite zeolites from Kankara kaolin clay. J. Appl. Sci. Res. 3 (10), 1017–1021.

Barrer, R.M (1988). Zeolite Synthesis: An Overview. Chapter in a book titled: Surface Organometallic Chemistry: Molecular Approaches to Surface Catalysis, Volume 231 of the series NATO ASI Series, pp 221-244, Published by Springer, Netherland. DOI: 10.1016/j.matlet.2005.10.110

Bouchiba, N., M.L.A. Guzman Castillo, A. Bengueddach, F. Fajula and F. Di Renzo (2011). Zeolite metastability as a function of the composition of the surrounding solution: The case of faujasite and zeolite omega. Microporous and Mesoporous Materials 144 (2011) 195–199. DOI: 10.1016/j.micromeso.2011.04.015

Breck D.W. (1984). *Zeolite molecular sieves*. New York: John Wiley & Sons.

Chandrasekhar, S., Pramada, P.N., 1999. Investigation on the synthesis of zeolites NaX from Kerala kaolin. J. Porous. Mater.6 (4), 283–297.

Cundy, C. and Cox, P. (2005*)* The hydrothermal synthesis of zeolites: precursors, intermediates and reaction mechanism. Microporous and Mesoporous Materials, 82 (1-2). pp. 1-78. ISSN 1387-1811 DOI: 10.1016/j.micromeso.2005.02.016

Li, Q., Zhang, Y., Cao, Z., Gao, W., and Cui, L (2010). Influence of synthesis parameters on the crystallinity and Si/Al ratio of NaY zeolite synthesized from kaolin. Petroleum Science Volume 7, Issue 3, pp 403–409. DOI: 10.1007/s12182-010-0085-x

Liu, C., Gao, X., Ma, Y., Pan, Z. and Tang, R. (1998). Study on the mechanism of zeolite Y formation in the process of liquor recycling. Microporous and Mesoporous Materials Volume 25, Issues 1–3, pp 1–6.

Magee, J.S. and M.M. Mitchell (1993). Fluid Catalytic Cracking: Science and Technology, Technology & Engineering, pp 109-110, Published by Elsevier, Netherland

Marcus, B.K., Cormier, W.E., 1999. Going green with zeolites. Chem.Eng. Prog. 95 (6), 47–53.

Murat, M., A. Amokrane, J. P.bastide and l. Montanaro (1992). Synthesis of zeolites from thermally activated Kaolinite: Some observations on nucleation and growth. Clay Minerals 27, 119-130

Querol, X., Plana, F., Alastuey, A., Lopez-Soler, A., 1997. Synthesis of Na-zeolites from fly ash. Fuel 76, 793–799.

Richardson, J.T., 1989. Principles of Catalysts Developments. Plenum Press, New York and London.

Rios, C.A., Williams, C.D., Maple, M.J., 2007. Synthesis of zeolites and zeotypes by hydrothermal transportation of kaolinite and metakaolinite. BISTUA 5 (1), 15–26.

Saija, L.M., Ottana, R., Zipelli, C., 1983. Zeolitization of pumice in ash-sodium salt solutions. Mater. Chem. Phys. 8, 207–216.

Sandoval, M.V., Henao, J.A., Rios, C.A., Williams, C.D., Apperley, D.C., 2009. Synthesis and characterization of zeotype ANA framework by hydrothermal reaction of natural clinker. Fuel 88, 272–281.

Sang, S., Liu, Z., Tian, P., Liu, Z., Qu, L and Zhang, Y (2006). Synthesis of small crystals zeolite NaY. Materials Letters 60, 1131.

Tanaka, H., Miyagawa, A., Eguchi, H., Hino, R., 2004. Synthesis of a pure-form Zeolite A from coal fly ash by dialysis. Ind. Eng. Chem.Res. 43, 6090–6094.

Tavasoli, M., Kazemian, H., Sadjadi,S. and Tamizifar, M (2015). Synthesis and Characterization of Zeolite NaY using Kaolin with Different Synthesis Methods. Clays and Clay Minerals. DOI: 10.1346/CCMN.2014.0620605

Treacy, M. M., and Higgins, J. B. (2007). *Collection of Simulated XRD Powder Patterns for Zeolites Fifth (5th) Revised Edition*. Elsevier.

Walek, T.T., Saito, F., Zhang, Q., 2008. The effect of low solid/liquid ratio on hydrothermal synthesis of zeolites from fly ash. Fuel 87, 3194–3199.

Wang, C. F., Li, J. S., Wang, L. J., & Sun, X. Y. (2008). Influence of NaOH concentrations on synthesis of pure-form zeolite A from fly ash using two-stage method. *Journal of Hazardous Materials*, *155*(1), 58-64.

Wang, C.F., Li, J.S., Wang, L.J., Sun, X.Y., 2008. Influence of NaOH concentrations on synthesis of pure-form zeolite A from fly ash using two-stage method. J. Hazard. Mater. 155, 58–64.

ISSN 214-453-2

EVALUATION OF BAGASSE ASH FOR APPLICATION IN GLASS MANUFACTURE

J. T. TAGWOI[1], A. D. GARKIDA[1], E. A. ALI[1], F. ASUKE[2], AND D. S. YAWAS

[1]Department of Industrial Design, Ahmadu Bello University, Zaria, Nigeria.
[2]Department of Metallurgical and Materials Engineering A. B. U. Zaria, Nigeria.
[3]Department Mechanical Engineering A. B. U. Zaria, Nigeria.
[jtagwoi@yahoo.com 08033883986]

ABSTRACT

Bagasse ash results from burning bagasse, a matted cellulose fiber residue from sugarcane that has been processed in sugar mills. In this paper, Bagasse ash has been chemically characterized in order to evaluate the possibility of its use in glass manufacture. The result of X-ray fluorescence (XRF) showed the ash to contain SiO_2 - 31.67%, K_2O - 31.41%, P_2O_5 - 8.14%, MgO - 4.89%, CaO - 3.92%, Na_2O - 3.17%, Fe_2O_3 - 1.23% the ash was normalized as no LOI was carried out. Qualitative and quantitative X-ray diffractometry (XRD) for determination of composition and presence of crystalline material, showed the presence of silica in free and various combined states and potassium magnesium carbonate. Scanning electron microscopy (SEM/EDS) at 100µm and 300µm showed clusters of spherical and rod-like microstructure at different spectra.

Keywords: *Silicates waste, Bagasse Ash*

INTRODUCTION

In recent years, research interest has been directed towards the need of low cost alternatives to raw materials needed in production and manufacture sectors. In this case, the high presence of silica in bagasse ash, as well as oxides of potassium, sodium, magnesium, phosphorus and calcium has necessitated the interest in bagasse ash research. Although, the number of possible glass composition is unlimited, the bulk of commercial glasses are based on silica which is a primary glass former [1-3].

Sugarcane bagasse ash (SCBA), is a product of combustion of bagasse. The sugarcane is crushed and the juice extracted resulting in bagasse [4] an industrial waste which is being used worldwide as fuel. The combustion yields ashes containing high amounts of unburned matter, silicon, potassium, aluminium and phosphorus oxides as the main components [5-8].

Castaldelli et al. [9] in their work demonstrated that sugarcane bagasse ash is an interesting source for preparing alkali-activated binders; it is composed mainly of silica. They further suggested that this by product can be used as a mineral admixture in mortar and concretes [1-2].

Analysis of wood ashes, including stems of plants, grass, straw and millet stalk are grouped as fluxes of the amphoteric and acidic type [10]. The most common fluxes are the alkali oxides e.g. Na_2O and PbO. Most windows in offices and houses and container glasses contain soda. Potassium oxide is also used extensively in commercial glasses [3]. This research therefore intends to look into the suitability of bagasse ash for use in glass making.

MATERIAL AND METHODS

Sample Preparation

Sugarcane bagasse obtained from Unguwar Wakili, Zangon Kataf Local Government Area of Kaduna State, was subjected to burning, which was carried out in two stages. The first stage being an open air firing followed by a controlled firing in a muffle furnace at 700°C at a resident time of 2hrs.

The sugarcane bagasse ash (SCBA) obtained was ground in a porcelain mortar and screened with the aid of a mechanical electric sieve shaker, a set of standard US/BSS sieves meeting the requirement of Tek-907k. The ash which passed through a sieve of mesh size 0.4mm was collected and used for the study.

The sample was subjected to various characterization techniques to determine the chemical composition, crystalline pattern and microstructural configuration, using X-ray Fluorescence (XRF), X-ray Diffraction (XRD) and Scanning Electron Microscopy (SEM)/ Energy Dispersive X-ray spectrometer (EDS), respectively.

Determination of Chemical Composition

X-ray Fluorescence (XRF) analysis was used to determine the chemical composition. The sample was prepared with boric acid as powder briquettes. 1g of the sample was mixed with 6g lithium tetra borate flux to make stable formula for trace elemental analyses; the sample was then mixed with PVA binder and pressed into pellets. SCBA sample was analyzed for Silica, Lime and oxides of Sodium, Magnesium, Potassium, Aluminium, Phosphorus, Sulphur, Titanium, Chromium, Iron amongst others.

Determination and Identification of Crystal Phases

X-Ray diffraction (XRD) method was employed for the determination and identification of crystal phases; this was done using a back loading technique. This was carried out using a PAN analytical X´pert pro powder diffractometer with X´celerator detector and a fixed divergence slit type.

The various phases formed were determined using X´pert High Score Plus Software. Phases identified are shown in (graphical representations) Figure 2 and Table 2.

Morphological study

Scanning Electron Microscopy, equipped with an Energy Dispersive Spectrometer (SEM/EDS) model number JEOL JSM 7500F was used to examine the microstructure. A small quantity of the sample was placed on the sample holder, then transferred into the machine. The sample was irradiated to produce emissions that were translated into a micrograph for morphological identification.

RESULTS AND DISCUSSION

Chemical Analysis

The chemical composition of Bagasse ash (as determined by XRF) shown in Table 1, the ash contain SiO_2 31.67%, K_2O 31.41%, P_2O_5 8.14%, MgO 4.89%, CaO 3.92%, Na_2O 3.17%, Fe_2O_3 1.23%, Al_2O_3 1.49% the ash was normalized as no LOI was carried out. $Si\ O_2$ is a glass network former which can readily form a single component glass. A vast bulk of commercial glasses are based on silica as the glassformer. While silica itself forms excellent glass, with a wide range of applications, the use of pure silica for production of windows, containers, bottles and other commercial applications would be very expensive due to the high melting temperature (< 2000ºC) required to produce vitreous silica. K_2O 31.41% and Na_2O 3.17% are alkali oxides and network modifiers, replacing silica by alkali oxides causes the thermal expansion coefficient α of the resulting glass to increase, producing more non-bridging oxygen, which break the connectivity of the glass network, softening the structure of glass. They met the need of the requirement for addition of flux in order to reduce the processing temperature to within practical limits as well as leading to a decreased cost of glass formation. 8.14% P_2O_5 a glass network former which, just like SiO_2, can readily form a single component glass, 1.23% Fe_2O_3 is an indication of high iron content in the ash, this is way above the permissible 0.1-0.3% Fe_2O_3 content for production of colorless glass. Fe_2O_3 is a common impurity that also acts as an unintentional colorant in silicate glasses.

Crystallization Phases and Microstructural Configuration

A qualitative and quantitative XRD analysis result as shown in Figure 1 and Table 2 revealed that bagasse ash contains silica in its free state as well as in combined state. Figure 2 shows Silica to have the highest peak. The primary minerals present are Calcium Silicate Ca_2SiO_4, Moissanite SiC, Potassium Magnesium Carbonate $K_2Mg(CO_3)_2$, Potassium silicate K_4SiO_4, Fosterite Mg_2SiO_4, Potassium Silicate $K_2Si_4O_9$ and Quartz SiO_2, in quantities that suggest a near balance in their proportions.

The SEM analysis given in Figure 3a and 4a show an interlocked mass of agglomeration of particles which are mostly spherical with a few rod like presentations. The EDS analysis in Figures 3b show a high presence of Si, O, Mn, Mg and K and 4b show presence of Si, O, Mn, Mg and K further revealing the major elemental composition of the mineral present in Bagasse ash at spectrum 1.

Table 1. Chemical composition of Bagasse Ash determined by XRF

Oxides	BA
SiO_2	31.67
Na_2O	3.17
CaO	3.92
Mg0	4.89
Al_2O_3	1.49
K_2O	31.41
Fe_2O_3	1.23
SO_3	0.21
TiO_2	0.21
P_2O_5	8.14
BaO	0.14
SrO	0.04
ZrO_2	0.06
Cl	11.06
ZnO	0.12
MnO	0.25
CuO	0.01
Cr_2O_3	0.01
CdO	0.01
HfO_2	0.01
Rb_2O	0.09
Br	0.01

Table 2. Quantitative XRD Analysis of Bagasse Ash

Chemical Formula	Compound Name	SCORE
$Ca_2\ Si\ O_4$	Calcium Silicate	20
Si C	Moissanite-4\ITH\RG, syn	16
$Si\ O_2$	Silicon Oxide	19
$K_2\ Mg\ (\ C\ O_3)_2$	Potassium Magnesium Carbonate	15
$K_4\ Si\ O_4$	Potassium Silicate	5
Mg2 $Si\ O_4$	Forsterite	14
$K_2\ Si_4\ O_9$	Potassium Silicate	11

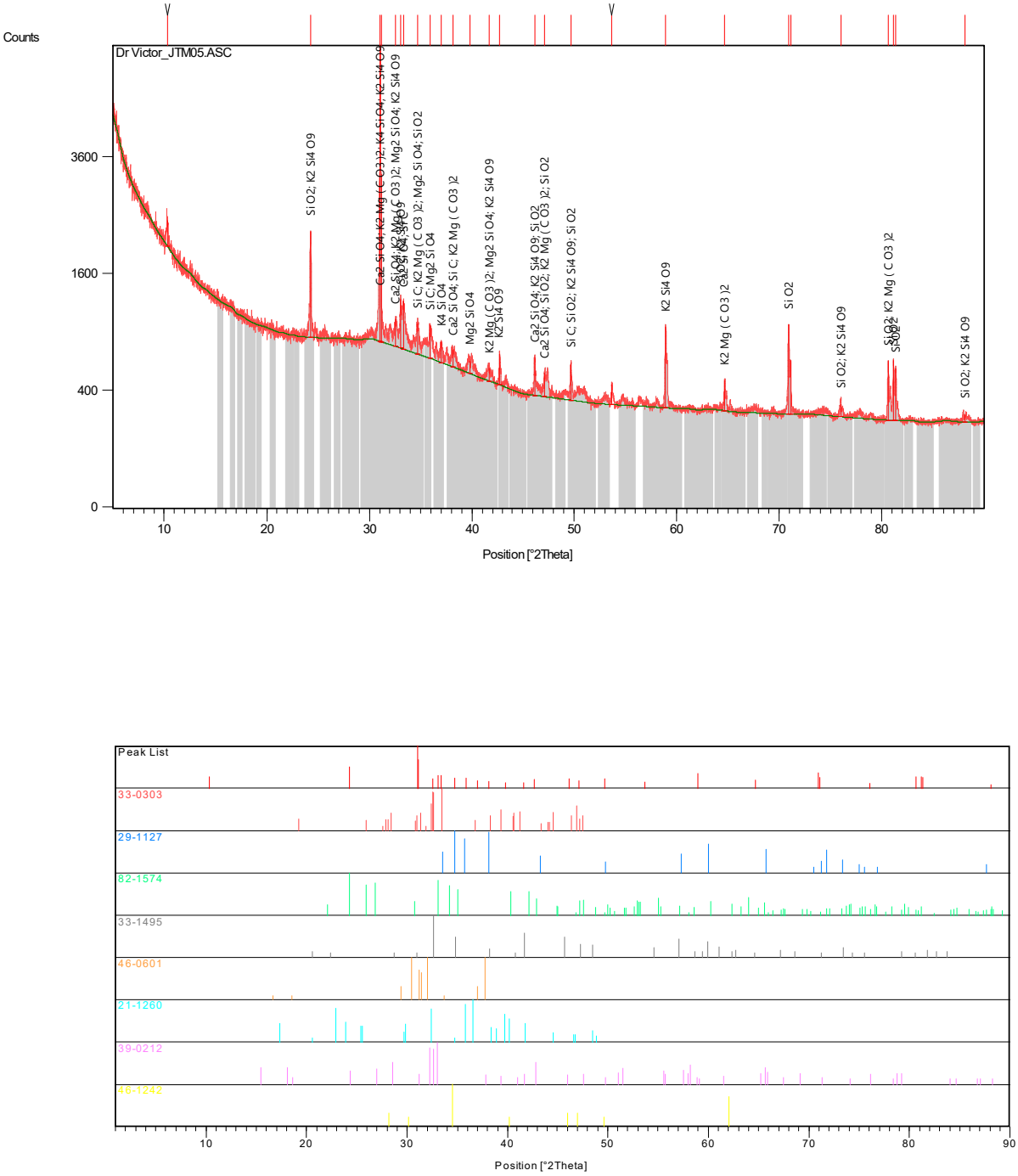

Figure 1. Qualitative XRD Analysis of Bagasse Ash

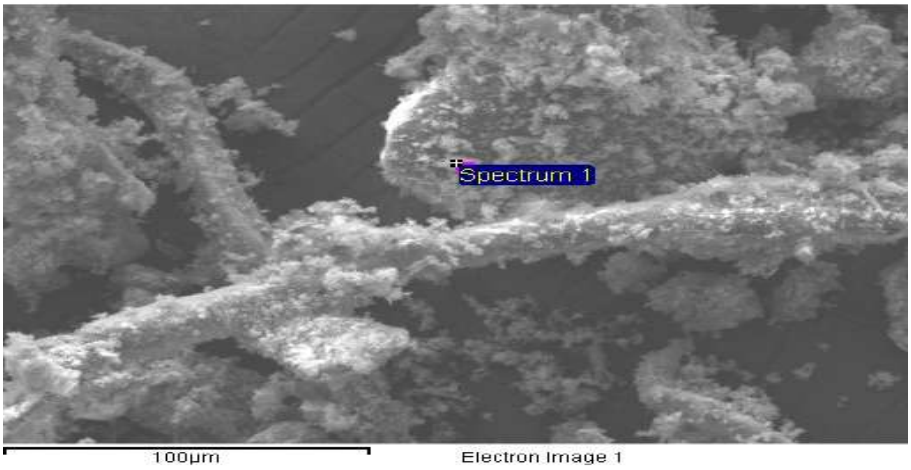

Figure 3a. SEM micrograph showing an agglomeration of irregular spherical dusty patterns

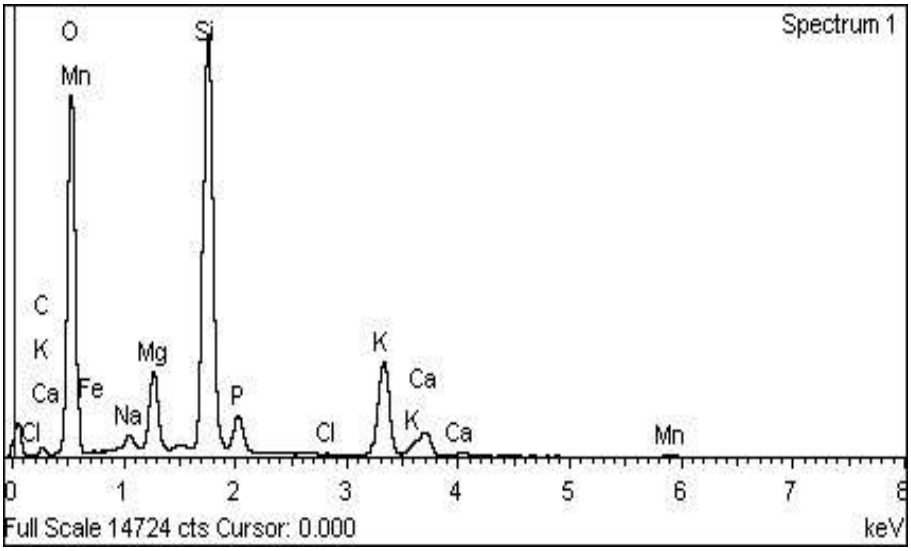

Figure 3b. EDS Analysis of Bagasse Ash showing the elements present at spectrum 1

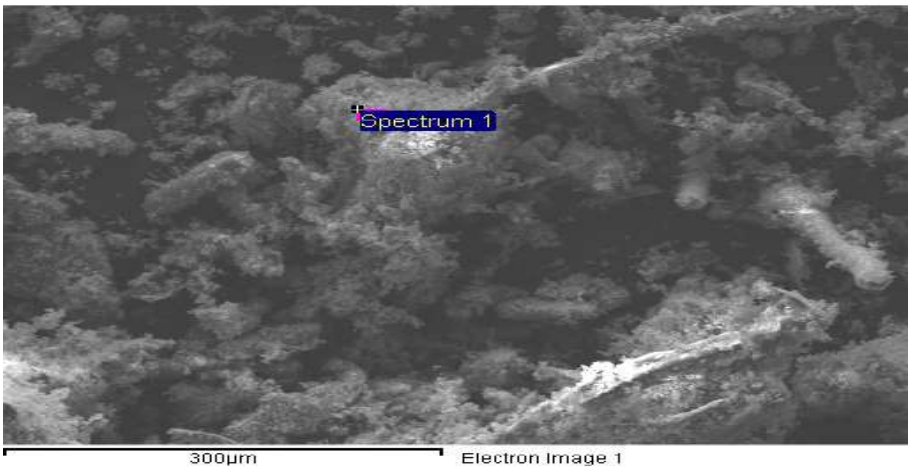

Figure 4a. SEM micrograph showing an agglomeration of disordered patterns

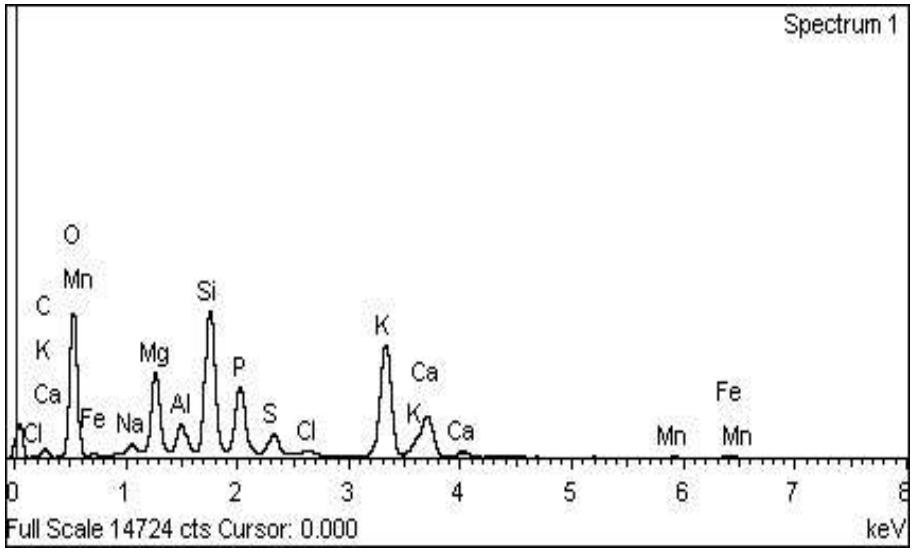

Figure 4b. EDS Analysis of Bagasse Ash showing the elements present at spectrum 1

CONCLUSION

The results of the analyses have shown Bagasse Ash to be a good source of Silica 31.67% and Potash 31.41%, with an ability to form a Silicate Glass (Potassium Silicate System), in the presence of glass modifiers. When used alongside other glass forming oxides, it will be an excellent fluxing agent in glass making by major reductions in the viscosity of the melt and the glass transformation temperature, this will reduce the energy used, thereby lower the cost in glass production. The ash also has a relatively high content of Fe_2O_3, though an impurity, will aid in the production of colored glasses. Bagasse Ash is therefore, a good source of Silica and Potash for the making of Alkali Silicate Glasses.

REFERENCES

1. Cordeiro, G. C., Toledo Filho, R. D., Tavares, L.M. and Fairbairn, E. M.R., Pozzolanic Activity and Filler Effect of Sugarcane Bagasse Ash in Portland Cement and Lime mortars: Cement and Cement Composites. Elsevier Ltd. 2008 Vol 30 issue 5 pp 410-418.
2. Ganesan K., Rajagopal K. and Thangavel K., Evaluation of Bagasse ash as Corrosion Resisting Admixture for Carbon Steel in Concrete, Anti corrosion Methods and Materials. Elsevier Ltd. 2007 Vol. 54(4), pp. 230-6.
3. Shelby, J.E., Introduction to Glass Science and Technology. Royal Society of Chemistry, Cambridge UK. 2005. PP 29
4. Govindarajan, D. and Jayalakshmi, G., XRD, FTIR and SEM Studies on Calcined Sugarcane Bagasse Ash Blended Cement. Arch. Phy. Res. 2011 2 (4): 38-44.
5. Ajay, G., Hattori, K., Ogata, H. and Mandula, Properties and Reactivity of Sugarcane Bagasse Ash. (12th International colloquium on structural and geotechnical engineering, 2007) Vol 1 Pp.1-5
6. Payá, J., Monzó, J., Borrachero, M., Díaz-Pinzón, L. and Ordóñez, L., Sugar-cane Bagasse ash (SCBA): studies on its properties for reusing in concrete production. Journal of Chemical Technology and Biotechnology. 2002. 77(3) 321–325
7. Stanmore, B. R., Generation of energy from sugarcane bagasse by thermal treatment, Waste and Biomass Valorization, 2010 pp 177-89
8. Hariharan V., Shanmugam M., Amutha K. and Sivakumar G., Preparation and Characterization of Ceramic Products Using Sugarcane Bagasse ash Waste. Research Journal of Recent Sciences. ISSN 2277-2502. (International Science Congress Association 67. 2014). Vol. 3(ISC-2013), pp. 67-70.
9. Castaldelli, V. N., Akasaki, J. L., Melges, J. L.P., Tashima, M. M., Soriano, L., Borrachero, M. V., Monzó, J. and Jordi Payá, J., Use of Slag/Sugar Cane Bagasse Ash (SCBA) Blends in the Production of Alkali-Activated Materials. Materials 2013 6, 3108-3127; doi:10.3390/ma6083108
10. Ewule, E. E., Potentials of Ash as a Ceramic Raw Material. International Journal of Science Laboratory Technology JOSCILT. Glass technology. 2007 Vol 1(2) pp 11-15.

NIGERIAN JOURNAL OF MATERIALS SCIENCE AND ENGINEERING
NJMSE
ISSN 214-453-2

OPTIMAL DESIGN OF THE SAME LENGTHS OF GLASS CONDENSERS

C. M. GONAH[1], C. E. GIMBA[2], A. D. GARKIDA[3] AND D. S. YAWAS[4]
[1 &3]Department of Industrial Design, Faculty of Environtl Design, Ahmadu Bello University, Zaria
[2]Department of Chemistry, Faculty of Science, Ahmadu Bello University, Zaria
[4]Department of Mechanical Engineering, Faculty of Engineering, Ahmadu Bello University, Zaria
[nomhat2003@gmail.com]

ABSTRACT
The study explored solid modelling for possible optimization of conventional laboratory heat exchangers. 240mm, 360mm, 480mm, 600mm and 720mm lengths conventional and unconventional Allihn, Graham, Liebig and Zigzag condensing models were designed and fabricated. An automated coolant system for test running the condensing models was sketched, constructed and used for test running the models using tap water as purification liquid in distillation flasks and coolant from the automated system for condensing vapour. Distillation temperatures range between 93-110^oC; while differences between inlet and outlet temperatures were between 6-10^oC. Optimal designs for 240mm, 360mm, 480mm, 600mm and 720mm based on distillation rates were Model Nos. 43=BZBZBWB (TA) with distillation rate (WDR) of 477mLs/hr, 38=SBSBS (TB) WDR of 458mLs/hr, 18=BSB (TB) WDR of 438mLs/hr, 18=BSB (TB) WDR of 422mLs/hr and 38= SBSBS (TB) WDR of 428mLs/hr respectively. The models could potentially be used for separation, purification, extraction and teaching aids in science and engineering laboratories and tertiary institutions of higher learning.

INTRODUCTION

Heat exchangers are complicated devices [1] broadly classified into surface and direct contact condensers. In a surface condenser, the coolant is separated from the vapour by tubular heat transfer. The coolant and the condensed vapour leave the device by separate exits. The temperature of the coolant is increased, so the device is also a heater. On the other hand, a direct contact condenser, both the coolant and vapour stream are physically mixed. Both the compressed vapour and the coolant leave the condenser as a single exhaust stream. It should be noted that actual applications of heat exchangers determine the design, size and materials selected for construction. Therefore, design is critical to maximum and effective heat transfer from the exhaust incoming vapour entering the heat exchanger to the circulating coolant, determined by the heat exchanger, pressure, coolant flow rate, coolant inlet temperature, and maintenance of correct and thermal gradient [1,3-4].

Stewart [5] highlighted that the commonest figure-of-merit for most heat exchangers is the efficiency; which is usually a focal point of optimization in both industrial and laboratory scale processes [3, 6-8]. Largest part of optimization researches conducted on heat exchangers concentrate more on theoretical methods with attention to large plants. Majority of these theoretical researches are basic in nature and have constraints that make their applications to a real world design problem impractical. Besides, theoretical detailed models of heat exchangers have been developed with good accuracy compared to experimental data; however, most of these models are rarely employed even industrially [3,9].

Jensen [10] and Anonymous 11-12] viewed that Liebig, Allihn and Graham glass condensers in spite of being the commonest heat exchangers in most of the teaching and research laboratories; there is still little or no improvement in terms of efficiency apart from Friedrichs and Dimroth condensers. The latter were improvements on coil condensers, but are rarely available or even used in most laboratories. Their unpopularity is not unconnected to their complexity, high cost of production, maintenance cost and coupled with the fact that they are not better off than Graham condenser.

Despite the advances in science and medicine which have reduced the demand for scientific glassware, new and modified methods of scientific research are still being developed daily and most of the experimental instruments involved are glassware which must be researched, designed, redesigned, fabricated, modified and maintained for improved performance. Moreover, laboratory glass ware (SGT), which is the bedrock of scientific glass instruments, especially heat exchangers do not receive the desired attention indigenously, where custom designed and fabricated laboratory glassware have usually been imported [13-17].

The study aimed to improve the performance of conventional laboratory heat exchangers for optimum and effective removal of latent heat in the exhaust vapours stream entering the heat exchangers, as well as their heat transfers into the circulating coolants, determined by the heat exchangers' pressures, coolant flow rates, and coolant temperatures. The research was delimited to design and fabrication of 240mm conventional and unconventional surface glass condensing Allihn, Graham, Liebig and Zigzag models.

MATERIALS AND METHOD

Conventional and unconventional 240mm, 360mm, 480mm, 600mm and 720mm condensing models were designed, fabricated and characterized using an improvised automated coolant system. Characterization of the condensing models was carried out in Glass Technology Laboratory, Department of Industrial Design, Ahmadu Bello University, Zaria. A simple

distillation principle and procedure were adopted for the experiment. Five SEARCHTECH electric heating mantles, twelve 1000mls Wurtz (distillation) flasks, twelve 10mls and twelve 100mls graduated cylinders for collecting and measuring distillates and four 250mls volumetric flask for measuring liquids into distillation flasks. Twelve of 250mls conical flasks were used for collecting distillates. Two of 300literes GP tanks with accessories, an electric water pump, a water level sensor, eight clamps and stands, a table of 150cm by 128cm and a height of 101.5cm, two S-TEK electric blowers of 350watts and metallic frame housing for the two GP tanks.

A system of four simple distillation sets were assembled and run concurrently (Figure 1). A set was made up of a laboratory jack, a heating mantle, 1000mls distillation flask, a condenser, two thermometers, two rubber bungs, a delivery adaptor and two distillate collectors (two 50mls measuring cylinders). Tap water was employed as both distillation solvent and coolant in the characterization test because of its availability, economy and position as a universal solvent. Besides, water has a high specific heat index of one than many common materials, for example, glass with specific heat index of 0.12. It takes much more heat to raise the temperature of a volume of water than the same volume of air and other common materials. This was why water was employed as a coolant. To avoid the risks of water bumping over the flasks, the distillation flask was 2/3 filled with tap water and 50 glass beads were put in it.

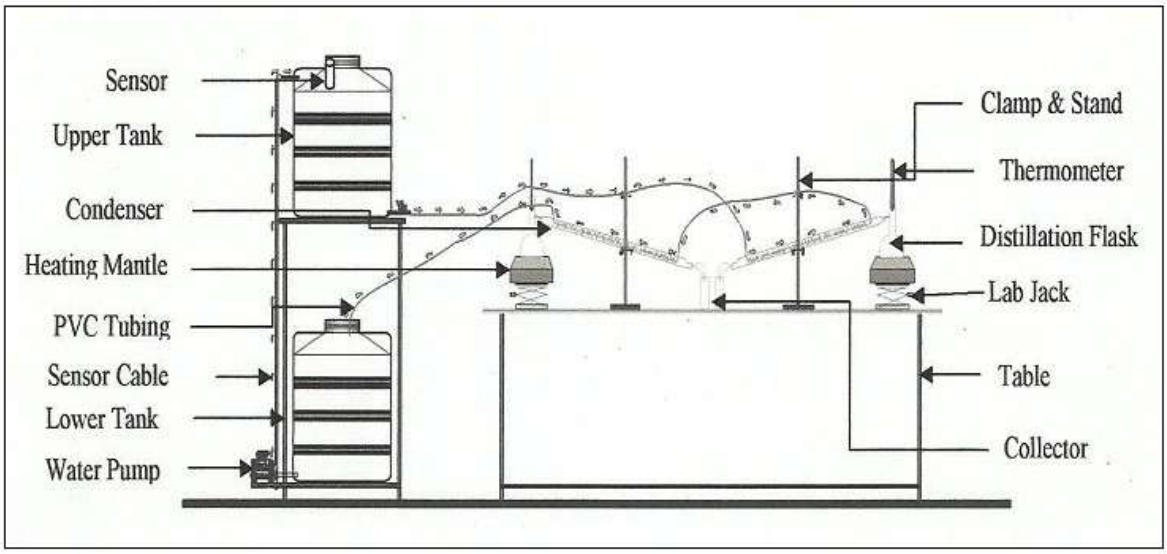

Figure 1: Automated Coolant Recycling and Distillation System [3]

Coolant flowed through the four distillation sets. The upper and the lower water tanks served as the source and destination of the coolant respectively. The flow was a continuous process; four distillation sets were assembled which operated concurrently. Two distillation sets per side were arranged in series with common coolant supply pumps from a split main pump coming from the upper 300litres GP tank. The outlet-coolant for one set became the inlet coolant for the second set, and then the coolant returned to the lower tank from the outlet of the second set through PVC tubing by gravity force. 750mls tap water and 50 glass balls or beads were put into each 1000mls Wurtz flasks. With the aid of rubber bungs, the glass condensing models were fitted to the stems of the Wurtz flasks, thermometers were inserted into the mouths of the four Wurtz flasks and adaptor deliveries to distillate collectors with the aid of rubber bungs and corks. Coolants were first turned on, followed by turning SEARCHTECH Instrument heating mantles on. Distillates were collected in 50mls measuring cylinders. Readings of distillates were taken in every five minutes for one hourly basis per glass condensing models.

RESULTS AND DISCUSSION

Graph and chart are employed to underscore the differential distillation of condensing models of 240mm, 360mm, 480mm, 600mm and 720mm of different designs (Figures 2-6). 48 designs of the same lengths are compressed to a single graph and bar chart for easy-to-understand format that clearly and effectively communicate the highest and lowest distillates at a glance. Numbers 1-48 on the abscissa on the coordinate plane on the graphs represent condensing models of 240mm, 360mm, 480mm, 600mm and 720mm lengths, viz: 1=LIEBIG (TA), 2=LIEBIG (TB), 3=LIEBIGWB (TA), 4=LIEBIGWB (TB), 5=ALLIHN (TA), 6=ALLIHN (TB), 7=ALLIHNWB (TA), 8=ALLIHNWB (TB), 9=GRAHAM (TA), 10=GRAHAM (TB), 11=GRAHAMWB (TA), 12=GRAHAMWB (TB), 13=ZIGZAG (TA), 14=ZIGZAG (TB), 15=ZIGZAGWB (TA), 16=ZIGZAGWB (TB), 17=BSB (TA), 18=BSB (TB), 19=BSBWB (TA), 20=BSBWB (TB), 21=SBS (TA), 22=SBS (TB), 23=SBSWB (TA), 24=SBSWB (TB), 25=ZBZ (TA), 26=ZBZ (TB), 27=ZBZWB (TA), 28=ZBZWB (TB), 29=BZB (TA), 30=BZB (TB), 31=BZBWB (TA), 32=BZBWB (TB), 33=BSBSB

(TA), 34=BSBSB (TB), 35=BSBSBWB (TA), 36=BSBSBWB (TB), 37=SBSBS (TA), 38=SBSBSWB (TB), 39=SBSBSWB (TA), 40=SBSBSWB (TB), 41=BZBZB (TA), 42=BZBZB (TB), 43=BZBZBWB (TA), 44=BZBZBWB (TB), 45=ZBZBZ (TA), 46=ZBZBZ (TB), 47=ZBZBZWB (TA) and 48=ZBZBZWB (TB).

Optimal designs for 240mm, 360mm, 480mm, 600mm and 720mm based on distillation rates were Model Nos. 43=BZBZBWB (TA) with distillation rate (WDR) of 477mLs/hr, 38=SBSBS (TB) WDR of 458mLs/hr, 18=BSB (TB) WDR of 438mLs/hr, 18=BSB (TB) WDR of 422mLs/hr and 38= SBSBS (TB) WDR of 428mLs/hr respectively (Figures 2-6). Model Nos. 38=SBSBSWB (TB) WDR of 443mLs/hr, 45=ZBZBZ (TA) WDR of 426mLs/hr, 21=SBS (TA) WDR of 423mLs/hr and 22=SBS (TB) WDR of 420mLs/hr ranked next in descending order to the optimum design of the 240mm; the same ranking was done for other designs of the same lengths.

Therefore, models Nos. 33= ZBZBZ (TA) WDR of 445mLs/hr, 28= ZBZWB (TB) WDR of 436mLs/hr, 27= ZBZWB (TA) WDR of 432mLs/hr and 17= BSB (TA) WDR of 431mLs/hr for 360mm lengths; 17= BSB (TA) WDR of 431mLs/hr, 34= BSBSB (TB) WDR of 425mLs/hr, 41= BZBZB (TA) WDR of 419mLs/hr and 46= ZBZBZ (TB) WDR of 413mLs/hr from 480mm lengths; 33= BSBSB (TA) WDR of 413mLs/hr, 27=ZBZWB (TA) WDR of 411mLs/hr, 42= BZBZB (TB) WDR of 410mLs/hr and 28= ZBZWB (TB) WDR of 403mLs/hr from 600mm lengths; 17= BSB (TA) WDR of 413mLs/hr, 18= BSB (TB) WDR of 412mLs/hr, 22= SBS (TB) WDR of 411mLs/hr and 41= BZBZB (TA) WDR of 409mLs/hr from 720mm lengths are all in descending order. Least efficient designs based on distillation rates for 240mm, 360mm, 480mm, 600mm and 720mm lengths were models Nos. 10= GRAHAM (TB) WDR of 179mLs/hr, 10= GRAHAM (TB) WDR of 271mLs/hr, 38= SBSBSWB (TB) WDR of 247mLs/hr, 13= ZIGZAG (TA) WDR of 260mLs/hr and 6= ALLIHN (TB) WDR of 253mLs/hr respectively.

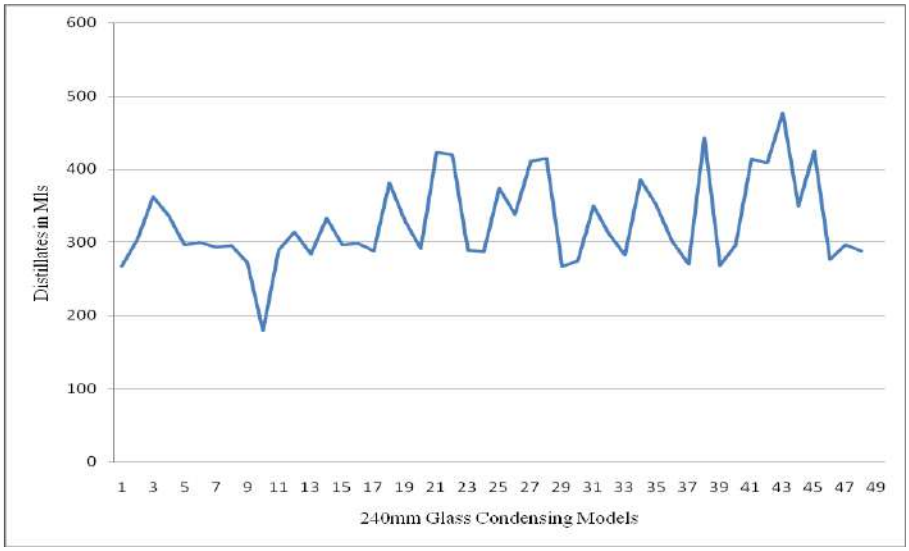

Figure 2: 43 BZBZBWB (TA) Graph Optimum Design of 240mm

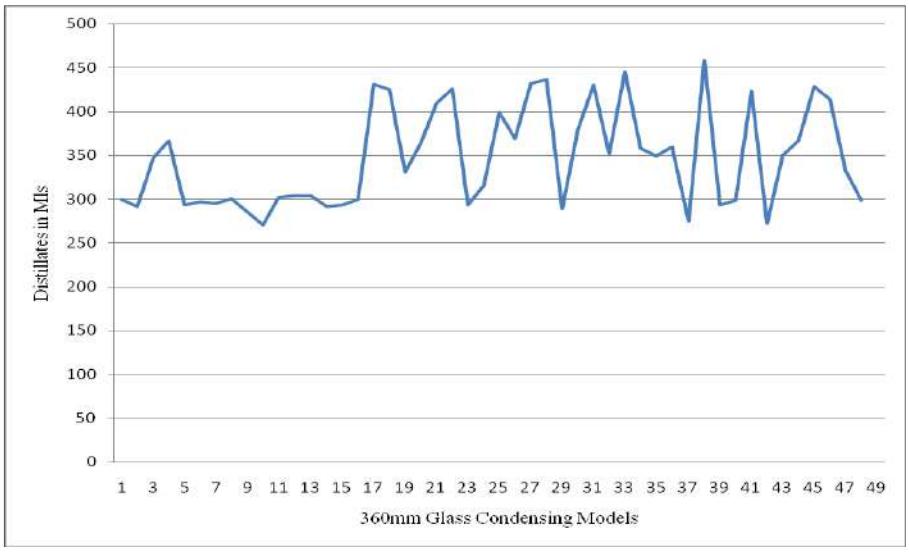

Figure 3 : 38 SBSBS (TB) Graph Optimum Design of 360mm

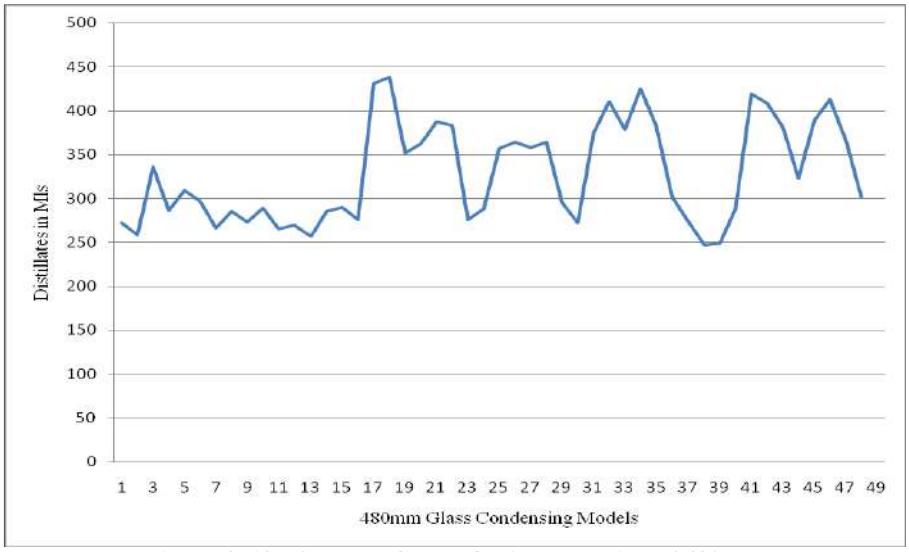

Figure 4: 18 BSB (TB) Graph Optimum Design of 480mm

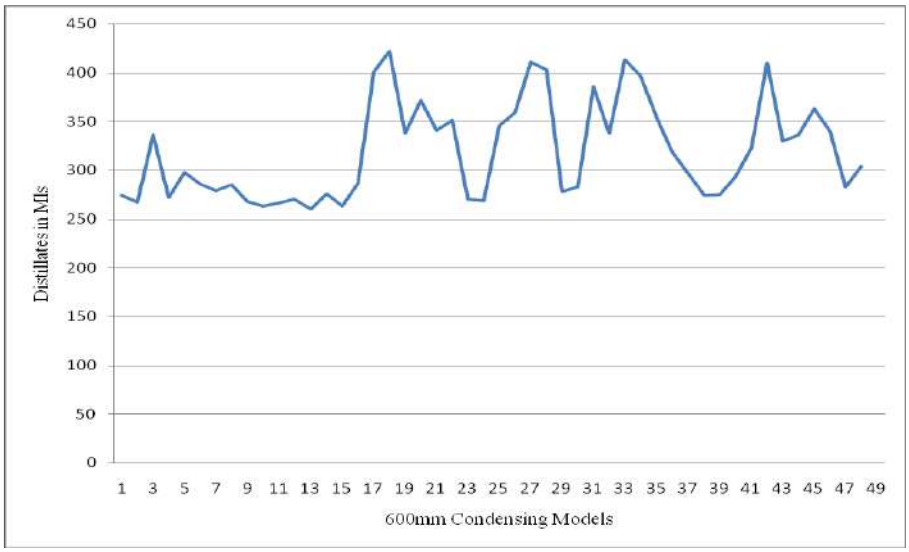

Figure 5: 18 BSB (TB) Graph Optimum Design of 600mm

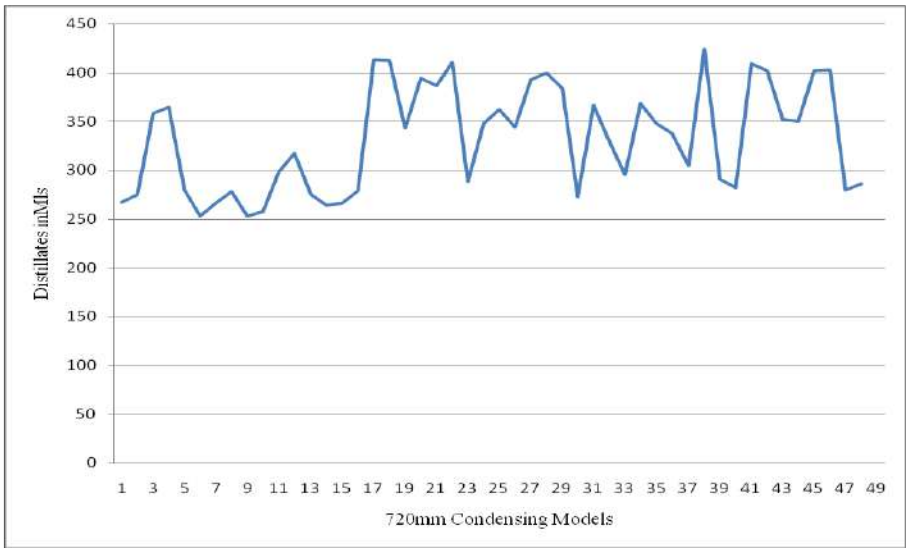

Figure 6: 38 SBSBS (TB) Graph Optimum Design of 720mm

Efforts were made to ensure optimal operating factors throughout the experiments. However, design, accuracy of fabrication according to specified design, length, coolant and mode of coolant flow, fouling factor from accumulation of deposits on heat transfer surface, leak-tight, power supply and handling skills of the researchers could have contributed more or less to the performance of the condensers.

CONCLUSION

Based on the above, optimal designs should be emphasized in choice of condensers. This will save time, cost, maximize profit, reduce losses and sustains, perhaps the business. Further research should be carried out on re-fabricating the solid models with attention to spiral pitches, bulb sizes and spacing. Again, the current models should further be characterized by differential distillation of two or more mixed liquids.

REFERENCES

1. Y. A. Cengel, R. H. Turner and J. M. Cimbala. Fundamental of Thermal Fluid Sciences, 2008. McGraw- Hill Companies, 3rd Ed., London.P. 968.
2. W. L. Badger and J. T. Banchero. Introduction to Chemical Engineering, 2005. Tata McBraw-Hill Pub. Co. Ltd, New Delhi, New Yorek. Pp120-399, 257-463.
3. C. M.Gonah. AutoCAD Drawing of a Coolant Recycling Distillation System. Unpublished PhD Research, Optimization of Laboratory Heat exchangers by Solid Modelling, 2013. Glass Technology, Department of Industrial Design, Faculty of Environmental Design, Ahmadu Bello University, Zaria.
4. W. C. McCabe, J. C. Smith and P. Harriott. Unit Operations of Chemical Engineering, 2005. McGraw Hill Intl. Ed., Singapore. Pp299-486, 663-703.
5. E. W. Stewart and and S. V. Shelton, S. V. Finned-Tube Condenser Design Optimization Using Thermo Economic Isolation, 2003. Unpublished Ph.D. Dissertation; George W. Woodruff School of Mechanical Engineering, Georgia Institute of Technology, Atlanta, Ga 30332-0405,USA.
6. T. F. Edgar, D. M. Himmelblau and L. S. Lasdon. Optimization of Chemical Processes, 2001. *McGraw Hill*, New York, pp20-24
7. D. Mikielewiez, J. Wajs and M. A. Glinkski. Model of Dry Out in Annular Flow, Proceeding, 2007. 6th International Conference on Multiphase Flow, ICMF, Leipzig, Germany, pp10.1, 18.7
8. Rao, S.S. Engineering Optimization: Theory and Practice, 2003. New Age International Ltd; Delhi, pp1-30 www.lynxsys.net/bookreview/bkrv960802.pdf.
9. A. Ford. Modeling the Environment, 2009. Island Press, Washington D.C. PP.1-36. http://serc.carleton.edu/introgeo/models/WhatIsAModel.html 28/05/2014
10. W. B. Jensen. The Origin of the Liebig Condenser . Journal of Chemical Education. 2006. (83), p23. http://jchemed.chem.wisc.edu/Journal/Issues/2006/Jan/abs23.html. 24/02/2012.
11. Anonymous. "Condensor." CU Boulder Organic Chemistry, Undergraduate Courses, 2011b. http://orgchem.colorado.edu/equipment/glassware/cond.html. 17/11/ 2011.
12. N. J. Niancoli. Kinetic Theory Applied: Evaporation, 2005. Vapour Pressure, and Boiling Point. Physics for Dorks, 3rd Ed. Pearson.pp.1, 2.
13. C. M. Gonah, C.M. Analysis and Synthesis of Scientific Glass Technology Studios, 2011. Ahmadu Bello University, Zaria. Unpublished Seminar Term Paper - INDE 908: Industrial Design Advanced Studio Theory; Course Lecturer: Dr. S.U. Dakyes. Ph.D/Env-Design/10575/2007- 08; pp2-23.
14. A Macfarlane and G. Martin. Beyond The Ivory Tower, Glass: A World History, 2004. Chicago Univ. Press, Chicago, pp.1-229. http://www.alanmacfarlane.com/12/04/2012
15. H. K. Mensah. Development of the Art of Glassblowing in Ghana; Prospects and Challenges of Selected Glassblowing. A Thesis Submitted to the School of Graduate Studies, KNUST in Partial Fulfillment of the Requirements for the Award of the Degree of Master of Philosophy in African Art and Culture, 2009. Faculty of Fine Art, College of Art and Social Sciences. Ghana.
16. Organomation Associates. Extraction Glassware - Liquid/Liquid for *ROT-X-TRACT-L; 2007.* Online Catalog (Organomation Associates), p125 *w*ww.organomation.thomasregister.com 10/04/2012.
17. Salem Community College, USA. Scientific Glass Technology Programme Entry Requirements, 2012. Salem Community College, USA. Salem Community College *Website,USA*. 856, 299, pp21-31.http://www.salemcc.edu/glass/programs/scientific.php 11/04/2012

ISSN 214-453-2

ESSENTIAL QUALITY ASSESSMENT OF SOME SELECTED FLAT BED-SHEETS FROM FOREIGN AND LOCALLY MADE - MATERIALS

M. B. MUSA, E. B. ILIYA AND P. T. ADOKWU
Department of Polymer and Textile Science, Ahmadu Bello University, Zaria. Nigeria
[mmbukharisal@yahoo.co.uk; +2348036139168]

ABSTRACT
A comparative analysis was carried out for essential quality parameters of five different bed sheets fabrics; Two foreign and three locally produced flat bedsheet fabrics. These fabrics were compared on parameters such as fabric thickness, air permeability, water absorption, fabric flammability, abrasion resistance, tensile strength, crease recovery, fabric shrinkage, stain removal, fabric handle, fabric sett, fabric drape, yarn count and yarn crimp using the appropriate techniques and apparatus. The results obtained show that the locally produced fabric exhibited comparably better end-use performance characteristic in terms of air permeability, water absorption, flammability, and drape. The foreign flat bed sheets are better in terms of crease recovery, handle, tensile strength, yarn crimp and shrinkage. These fabrics are therefore valued for their end-use performance.

Keywords: *air permeability, abrasion resistance, flammability, crease recovery, handle, yarn crimp and shrinkage*

INTRODUCTION

The quality of a textile material depends largely on the nature of raw material used and also the kind of manufacturing processes it has undergone (Adokwu, 2016). Generally, the quality of a textile fabric is judged by its physical appearance, handle and to some extent price, however, technically, the structure and properties of the fabric have to be considered in quality assessment of a textile fabric.

Nigerian people generally prefer foreign (textile) goods over the home made materials. This is because of the belief that the performance properties of the foreign made textiles are better than those produced locally (Raji et al., 2007). The quality (value) of a textile material is often determined by the feel (handle), aesthetic properties, comfortability during use, serviceability and probably past experience (Musa et al 2011). The main objective of the present work is to determine the basis or otherwise for the Nigerian's preference of foreign goods over locally made materials from technical point of view.

In this work, analysis and comparism of essential quality parameters of five flat bed sheet (two foreign and three locally produced) materials were carried out using standard procedures.

MATERIALS AND METHODS

MATERIAL

Five bed sheet materials were analysed and used in this research work, two foreign textile bed sheet and three locally produced textile bed sheet. All the textile fabrics are cotton materials, they are designated as **F^1, F^2, L^1, L^2 and L^3** throughout this work.

$$Foreign\ produced\ bed\ sheet \begin{cases} F^1 \dfrac{17 \times 17}{1.7 \times 1.7}\ Plain \\ F^2 \dfrac{14 \times 13}{1.72.1}\ Plain \end{cases}$$

$$Localy\ produced\ bed\ sheet \begin{cases} L^1 \dfrac{18 \times 14}{1.3 \times 2.6}\ Plain \\ L^2 \dfrac{19 \times 17}{1.2 \times 4.4}\ Plain \\ L^3 \dfrac{19 \times 16}{1.3 \times 4.1}\ Plain \end{cases}$$

EQUIPMENT

Shirley Air Permeability Tester, Martindale Wear Abrasion Tester, Shirley Crease Recovery Instrument, Cussick Drape Tester, Shirley Crimp Tester, Essdiel Thickness Gauge, Instron Tensile Strength Tester Model 1026, Digital Weighing Balance, Microscopic Lens, Stop Watch, Counting Glass, Stirring Rod, Beakers, Grey Scale for assessing Stain, Bunsen Burner, Meter Rule, Scissors, Dissecting Needle, Thermometer, Volumetric Flask, Measuring Cylinder, Burette.

EXPERIMENTAL METHODS

The five samples were evaluated for those properties required for satisfactory end use performance. All the tests were carried out in accordance with the British Standard Hand Book II (1974), after conditioning the samples in an atmosphere for textiles i.e. 65 ± 2% relative humidity and temperature of $20 \pm 2\ ^{O}C$ for at least 24 hours.

FABRIC THICKNESS

The test for fabric thickness was carried out in accordance with British Standard Hand book II (1974), the apparatus used was *Essdiel thickness guage.* Five tests were carried out for each sample and the mean value calculated, as show in Figure 1.

AIR PERMEABILITY

Air permeability test was carried out in accordance with the British Standard Hand Book II. The apparatus used was the *Shirley air permeability tester.* For each sample five tests were carried out on different portions. The test area was 5.02cm^2 and at the pressure head of 10 mm of water. The air permeability was obtained using the following formula;

$$\text{Fabric air permeability} = \frac{\text{mean rota meter reading}}{\text{test area}} \quad \ldots\ldots\ldots (1)$$

The average value of the rotameter readings was calculated and the average volume of air and the air resistance was calculated and shown in Table 2

WATER RESISTANCE

The test for water resistance for the five flat bed sheets under study were carried out in accordance with British Standard Hand Book II (1974). The test (sample) fabric was mounted onto an embroidery hoop and placed to face upper most on the hoop support. 250 ml of water contained in a beaker was poured onto the surface of the fabric inclined at an angle of 45^o through a funnel with tiny holes. The water was poured quickly and steadily to ensure a continuous flow of spraying once it has commenced.

After the spraying from the funnel had stopped, the test fabric was tapped twice with a solid object with the fabric faced down in a horizontal position. After the tapping, with the fabric still on the hoop, a spray rating was then assigned to the tested fabric by visually comparing the appearance of the sprayed sample with that of the nearest corresponding standard ratings given. The resultsare shown in Table 3.

FABRIC FLAMMABILITY

The vertical strip test principle was employed in this work. The test fabric was cut to a dimension of 21 cm X 2.5 cm and was suspended in a drought free cabinet (where air does not flow freely) and held at the top end over the top most wire by clips. The flame from a candle stick was put below the lower end of the fabric. Using: *asbestos platform, clip wire a stop watch*, the time (seconds) it took the flame to consume the fabric from its lower to top end was noted and used for fabric flammability grading. The results for five fabric sample were as shown in Table 4.

ABRASION RESISTANCE

The abrasion resistance test of each sample was carried out using the break method as outline in the British Standard Hand Book II (1974). *Using the Martindale abrasion tester*. The average loss in weight per 50 rubs was obtained from the graph figure, and the reciprocal of percentage loss in weight was used as the resistance to abrasion. The results are shown in Figure 2.

TENSILE STRENGTH

The tensile strength test was carried out in accordance with British Standard Hand book II (1974),using the *zwick/Roel Tensile testing machine.* For each test fabric, five strips from sample were cut each of dimension 12 cm X 2.5 cm. Each sample was axially extended until it broke under the applied load. Readings were taken and the values are shown in Table 5

CREASE RECOVERY

This test was carried out in accordance with the British Standard Hand Book II (1974), with the aid of *Shirley Crease instrument.* 3 rectangular strips of 3 cm X 7 cm dimensions were cut from each of the samples in both weft and warp directions. The Crease load was 20 Newton for 30 seconds; the results are shown in Figure 3.

FABRIC SHRINKAGE

The percentage shrinkage of a fabric is an indication of its dimensional stability. The specimen was conditioned and a pen was used to mark out the dimension of 10 cm X 10 cm. The sample was then immersed in a tray of 10 cm square and 2 cm deep containing water at room temperature. The specimen was submerged for 2 hours and was carefully removed, and laid on a piece of glass and dabbed with an absorbent cloth, so as to remove excess water. It was then allowed to dry in open air. After being thoroughly dried, the dimensions were re-measured and the percentage shrinkage for both warp and weft direction was calculated and the results presented in Figure 4

FABRIC STAIN REMOVAL.

The stain removal test for the five samples under investigation were carried out using the *ISO 105-A03: 1987,BS 1006-A03:1990 SDC* Standard Methods 5th Edition A03 Grey scale for assessing change in colour. The samples were stained with palm oil, groundnut oil and engine oil and placed in a container containing 2.5 g/l soap and 2.5 g/l Na_2CO_3 solution previously heated to a temperature of 60 ± 2^{O}C, so as to give a liquor ratio of 50:1. The specimen was removed, rinsed, dried and assessed. The assessment of the staining of the adjacent fabric was carried out using Grey scale. The results obtained are shown in Table 6.

FABRIC HANDLE

The pieces of five different samples were given to about 22 people to comment on the feel and physical appearance. Their view were compared and used to determine the fabric handle and visual assessment and the results obtained are shown in table 7.

FABRIC SETT

The *1cm counting glass* method as outlined in British Standard Hand Book II (1974) was used. With this method, the number of warp and weft thread per centimeter for each fabric under analysis were determined by placing the glass on the fabric before counting. Ten determinations were carried out on each sample and the mean value were calculated and recorded in Table 8

FABRIC DRAPE

A piece of five fabric 30 cm in diameter each were cut out from each sample and tested for drape characteristics on a *Cussick drape tester* according to

British Standard Specification. The fabric pieces were allowed to hang under the action of gravity,and then the shadow of the fabric on the ring paper was traced out. The weight of the ring paper (M_2)was determined.The outline was traced and then cut and the inner part weighed to give (M_1). The average values of M_1 and M_2 were obtained. The drape coefficient was therefore calculated thus:

Drape coefficient = M_2/M_1 X 100 (%)..... (2)

YARN COUNT

This was carried out in accordance with British Standard Hand Book II (1974). The apparatus used was the *Digital weighing Balance* and *Dissecting pin.* Here 10 cm X 10 cm strips of the samples were prepared from the fabrics under investigation. Ten threads each from warp and weft directions were removed from the strips using the *dissecting pin*. The crimp of the yarn was removed by the crimp tester. The weight of each group was determined and this was used to calculate the yarn count as follows;

$$Tex\ count = \frac{W}{L}\ X\ 100 \text{..... (3)}$$

where *W* =weight of yarns (grain), *L* =Length (meters)
The result is shown in table 9.

YARN CRIMP

The test was carried out in accordance with British Standard Hand book II (1974), using the *Crimp tester* and *dissecting pin*. The fabrics were laid flat, free from tension and creases. A rectangular strip of about 20cm X 20cm was marked out along the warp and weft directions, the yarn samples were carefully removed using a dissection needle. The yarns were tensioned as recommended ten readings were taken for each series of threads and the mean calculated. The percentage crimp was calculated as followed

$$\%\ Crimp = \frac{\text{Straightened yarn length} - \text{lengt of yarn in fabric}}{\text{Length of yarn in fabric}}\ X\ 100 \text{.....(4)}$$

The results obtained are shown in table 3.14

RESULTS AND DISCUSSION

FABRIC THICKNESS

Thickness of a fabric is a factor which depends on the structure of the fabric mass/unit area, and the type of yarn used. Various parameters such as abrasion resistance, dimensional stability, stiffness and thermal insulation are affected by fabric thickness (Musa et al, 2011). The results in the Table 1 were the average thickness values calculated for the respective test fabric. The test sample **L^1** and **L^2** showed the highest value for fabric thickness of **0.384** both, followed by **L^3** with **0.364,** other values were **0.322, and0.332,** for **F^1** and **F^2** respectively. The test sample **F^1** has the least mean thickness of **0.322.** Coefficient of variations of the result were calculated (Table 1) and it was found that the sample **F^1** has the highest values in percent followed by **F^2**, **L^3**, **L^1** and **L^2** in that order. This shows that sample **L^1** and **L^2**can best be used during cold to provide the maximum warmth needed. Due to its high thickness values, it can be used in a situation where fabrics are to be subjected to frequent rubbing with another object. The order of fabric thickness increases as follows: **$F^1 < F_2 < L^3 < L^1 < L^2$** as shown in Figure 1

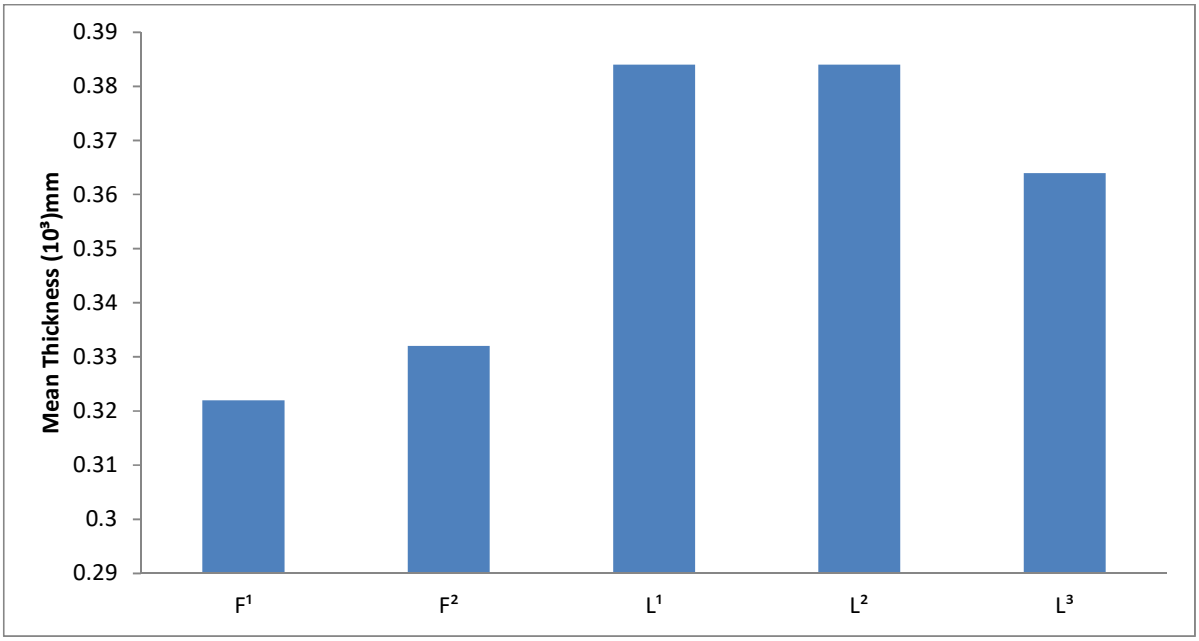

Figure 1: Fabric thickness

Table 1: Thickness coefficient of variation (%)

Test Sample	Mean thickness (mm) $x10^{-2}$	Standard deviation $x10^{-4}$	Coefficient of variation (%)
F^1	0.322	0.0148	4.6
F^2	0.332	0.0116	3.49
L^1	0.384	0.00787	2.05
L^2	0.384	0.0036	0.94
L^3	0.364	0.00837	2.3

AIR PERMEABILITY

Air permeability is a factor which depends on the type of finish fibre and the diameter of yarn used to produce the fabric. The bigger the opening in a fabric, the higher the flow rate of air through the fabric, while the thicker a fabric is, the more difficult it is for air to flow through. Also the construction and finishing techniques affects the air permeability of fabrics such as hot calendaring which flattens the yarn.

Table 2: Air permeability

Sample	Average volume of air cm^3/s (V)	Air resistance $x10^{-3}$ (Sec/cm)
F^1	109.2	0.076
F^2	109.2	0.416
L^1	109.2	0.458
L^2	109.2	0.494
L^3	109.2	0.458

The results shown in Table 2, are the respective average rate of flow of air through the test fabrics. The table also shows the air resistance values as calculated using the formulae for air permeability as given in equation 1. Test sample L^2 showed the highest value of **0.494** followed by L^1 and L^3 with **0.458.** Sample F^1**,** and F^2 have values **0.076** and **0.416** respectively. The resistance for each of the test fabric calculated showed that sample L^2 had the highest air resistance value of **0.494,** Sample F^1 has the least of **0.076**. Air permeability is influenced by fabric density and probably the yarn fineness or yarn count, thus the high air permeability for sample F^1 may be attributed to its yarn count while the low level of air permeability for sample L^2 could be attributed to its high fabric density and its coarser weft yarn.

WATER RESISTANCE

The results in Table 3 was obtained from a scale mockrain shower produced by pouring water through a spray nozzle. Samples L^1, L^2, and L^3, gave a spray rating of '0', indicating a complete wetting of the whole sprayed surface, that is, thus, the local bed sheets have very poor (low) water resistance. While the foreign bed sheets (F^1 and F^2) gave spray rating of 25 indicating wetting of about75 % of the sprayed surface. In other words the local bed sheets have better water absorption as compared to the foreign bed sheets hence better in terms of comfort particularly in temperate environment or during summer periods.

Table 3: Water Resistance

Test Sample	Spray rating
F^1	25
F^2	25
L^1	0
L^2	0
L^3	0

FABRIC FLAMMABILITY

Result shown in Table 4 gave the average burning time of the respective fabric and their flammability grades. It can be observed that the samples are graded **D** with the exception of sample F^1 which is foreign. Test sample F^1 is highly flammable, while the entire local test samples are graded **D** and this refers to the grade assigned to flame proof self-extinguishing fabrics. Thus, the local flat bed sheets are shown to have good flammability rating. This probably was as a result of chemical finishing treatment done to the fabrics which made them to become flame retardant or proof, since all cotton fabrics are flammable.

Table 4: Fabric flamability

TEST SAMPLE	AVERAGE BURNING TIME (Seconds)		FLAMMABILITYGRADE
	Warp direction	Weft direction	
F^1	5.78	5.50	A
F^2	14.00	12.50	D
L^1	18.50	18.25	D
L^2	16.75	14.75	D
L^3	15.75	12.19	D

KEY:
A= Highly flammable 5 seconds B= Flammable 6 – 10 seconds
C= Flame Retardant 10 seconds D= Flame proof self extinguishing above 10 seconds

ABRASION RESISTANCE

Abrasion resistance is a property that allows a material to resist wear. The abrasion resistance of a material helps to withstand mechanical action and tends to protect the removal of materials from its surface (Adokwu, 2016). Fabric abrasion resistance is a factor which affects the durability and performance characteristic of fabrics. The assessment of abrasion of fabrics, usually provides the fabric with the conditions similar to those it will be subjected to, while in use. The

results in Figure 2 show that sample **L^2** had the highest abrasion resistance of **1.234 %** weight loss, while **L^3** has the least abrasion resistance with **6.139** weight loss(%) other results are **5.454, 3.649,** and **3.479** for **F^1, L^1** and **F^2** respectively. Sample **L^2** has the highest abrasion resistance indicating that it will be more durable comparably. This shows that in places where the bed sheets are to be subjected to frequent use, sample **L^2** which lost only very small mass after a considerable number of rubs will be the best.

TENSILE PROPERTIES

Tensile properties are affected by many factors such as chemical composition and internal structures of the fibre. The tensile property is of non-linear type because mostly the less extensible fibre, breaks before an extensible fibre reached its breaking load. Result from Table 5 show that sample **F^2** gave the highest value of breaking load followed by **F^1, L^3, L^2** and **L^1** in that order respectively. The breaking load of the foreign fabric is slightly higher than those of the local ones, which may obviously be attributed to the variations in the strength of the yarns components in the individual samples. This result slightly vary with what was obtained in abrasion resistance both of which may be related to wear life of the fabric. Sample **F^2** with highest breaking strength and higher modulus may remain the most promising in terms of tensile properties.

CREASE RECOVERY

Fabric crease recovery determines the ability of a fabric to recover from deformation. Crease recovery depends on the plastic behavior of the fibre and the geometry of yarn and fabric. The crease recovery angle given in Figure 3 of the test sample showed that sample **F^2** with the highest angle of recovery of **14.6^o** in warp directions while sample **F^1** showed the highest angle of recovery of **12^o** in weft direction. Other results are **14, 9, 6** and **3.33**. for **F^1, L^3, L^2** and **L^1** respectively in warp direction. The crease recovery angle in weft direction for samples **F^2, L^2, L^3** and **L^1** are **10.8, 7.3, 4.5** and **2.03** respectively. Generally, the foreign flat bed sheets recovered better from creasing in both weft and warp direction in relation to their local counterparts thus, will have better easy care property and do not need much ironing after laundering.

FABRIC SHRINKAGE

The percentage shrinkage of a fabric is an indication of its dimensional stability. Figure 4 indicates that both the fabrics samples have low percentage shrinkage highest being 3% which is indeed negligible. However, the foreign bed sheets have relatively better dimensional stability in both warp and weft directions with only 1% shrinkage in both directions. For the local bed sheets the fabric shrinkage is better in the warp directions with the exception of **L^2** indicating that it is more dimensionally stable as compared to **L^1** and **L^3**.

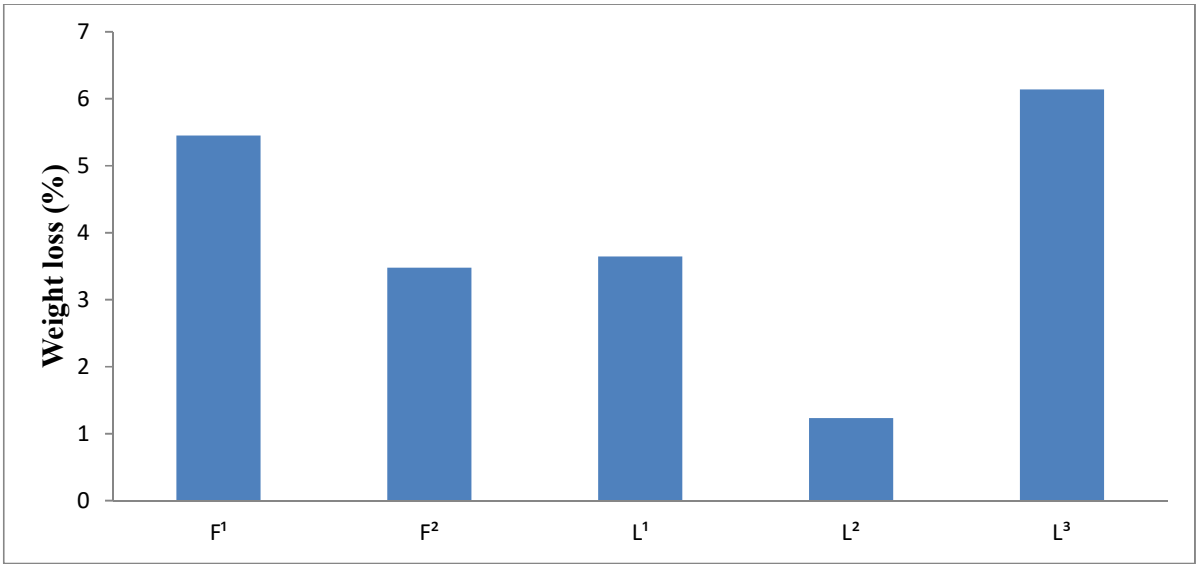

Figure 2: Abrasion Resistance

Table 5: Tensile properties

TEST SAMPLE	BREAKING LOAD (KG)	Applied force (N)	Elongation x10^{-3} (m)	Stress X10^{-5}(n/m^2)	Strain X10^{-2} (M)	Initial modulus (N/M^2)
F^1	14.6	143.1	126.67	4.77	1.267	3.765
F^2	18.16	177.92	64	5.93	0.64	9.265
L^1	9.04	88.6	243.5	2.953	2.435	1.213
L^2	11.84	116.84	188.25	3.868	1.883	2.054
L^3	13.44	131.74	129.42	4.391	1.294	3.393

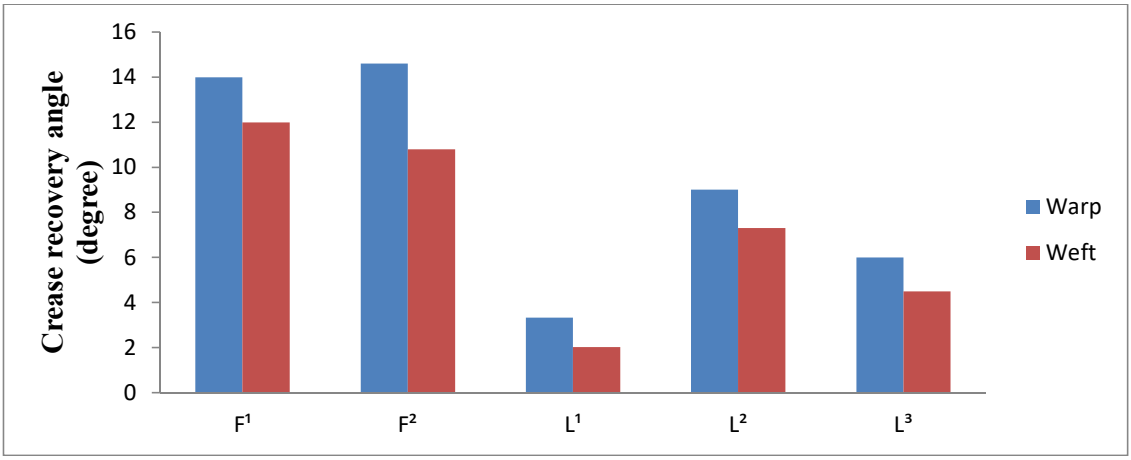

Figure 3: Crease recovery

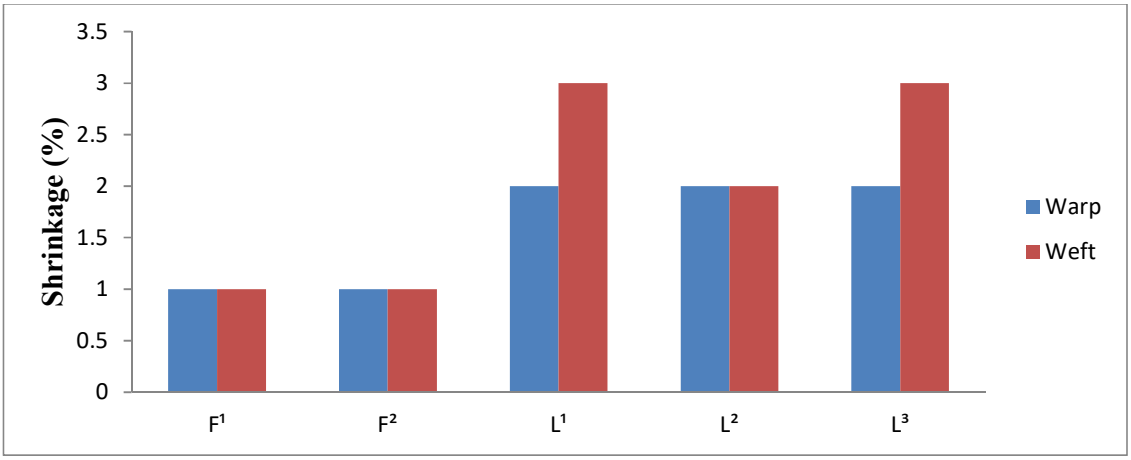

Figure 4 Fabric Shrinkage

STAIN REMOVAL

Table 6: Stain removal

samples	Type of stain	Grade	Remarks
F¹	Groundnut oil	1-2	Poor
	Palm oil	2	Fair
	Engine oil	1	v. poor
F²	Groundnut oil	1-2	Poor
	Palm oil	2	Fair
	Engine oil	1	v.poor
L¹	Groundnut oil	4	v.good
	Palm oil	3-4	v.good
	Engine oil	1	v.good
L²	Groundnut oil	3-4	v.good
	Palm oil	2-3	Fairly good
	Engine oil	3	Good
L³	Groundnut oil	3	v.good
	Palm oil	2-3	Fairly good
	Engine oil	4	v.good

KEY

5 = excellent, 4 = very good, 3/4 = very good, 3 = good, 2/3 = fairly good, 2 = fairly poor, ½ = poor, 1 = very poor

The results obtained for stain removal are shown in table 6 which is based on the effect of fibre on fabric staining and stain removal efficiency. The fabrics specimens after washing and drying, were kept under a standard atmospheric conditions for 24 hours and then compared. Using soap to wash the fabrics, groundnut oil stain is the easiest to remove while engine oil proved difficult especially in the foreign flat bed sheets in the following order.

FABRIC HANDLE

The result obtained recorded and tabulated inTtable 7, from No1-5. The second batch of the fabric handle was carried out in front of Ribadu Hostel 4 female students were able to assess the fabrics. The result were recorded and tabulated from No 6-8 The third batch of fabric handle assessment was carried out in the Department of Polymer and Textile Science where 5 female and 5 male students assess the fabrics based on the handle and appearance and the results obtained were tabulated from No 9-22. All at Ahmadu Bello University, Zaria, Nigeria. Out of the people that assessed the fabric only 10 assessors were male while the rest assessors were female. From the result obtained fabric sample **F¹** and

F^2 has the best handle. This implies that they are the most soft and smooth of all the fabric samples. Never the less the result shows that the handle of the tested sample for both foreign and locally produced bed sheets fabric do not show any significant difference

Table 7: Fabric handle

	SAMPLES/ GRADES				
SAMPLES	**F^1**	**F^2**	**L^1**	**L^2**	**L^3**
1	4	4	3	3	3
2	3	4	4	3	3
3	4	3	3	3	3
4	4	4	3	3	3
5	4	4	3	3	4
6	4	3	3	3	3
7	3	4	3	3	3
8	4	4	3	3	3
9	4	4	3	4	3
10	4	3	3	3	3
11	3	3	3	3	3
12	4	4	4	3	4
13	3	3	3	3	3
14	3	4	4	3	3
15	4	3	3	3	3
16	3	4	3	3	3
17	4	4	3	3	3
18	3	3	3	3	4
19	4	4	3	3	3
20	3	4	3	3	3
21	3	3	3	3	3
22	4	4	3	3	3
Total	79	80	69	67	69
Average	3.59	3.63	3.13	3.04	3.13

Key:
4= fabric is softest in term of handle and appearance
3= fabric is soft interm of handle and appearance
2= fabric is harshest interm of handle and appearance
1= fabric is harsh interm of handle and appearance

.

FABRIC SETT

Table 8: Fabric density

Test sample	End per centimeter (epcm)	Pick per centimeter (ppcm)	epcm x ppcm
F^1	17	14	238
F^2	14	13	182
L^1	18	14	252
L^2	19	17	323
L^3	19	16	304

The cover factor controls the density of a fabric, in relation to air permeability, the higher the fabric sett, the lower the air permeability. Table 8, shows that for all the samples epcm is higher than the ppcm, since the epcm and ppcm are not equal, the fabric samples are unbalanced and the greater numbers of yarns are usually in the warps. Sample **L^2** has a high fabric sett, while sample **F^2** has low values of epcm and ppcm sett,. The foreign fabrics have a relatively low fabric sett, while the locally produced flat bed sheets have high fabric density.

3.12 FABRIC DRAPE

Fabric drape is the extent to which a fabric will deform, when allowed to hang under its own weight. It is largely affected by the yarn twist. The thicker the yarn, the lower the drapeability. The drape coefficient expresses the drapeability of the fabric, and the higher the value of drape coefficient the poorer its drapeability. Figure 5, Shows that sample **L^1** is the stiffest which could be probably attributed to its higher fabric density and probably high yarn twist, sample **F^1** is the smoothest with the list drape coefficient, and will therefore assume a graceful appearance compare to the others.

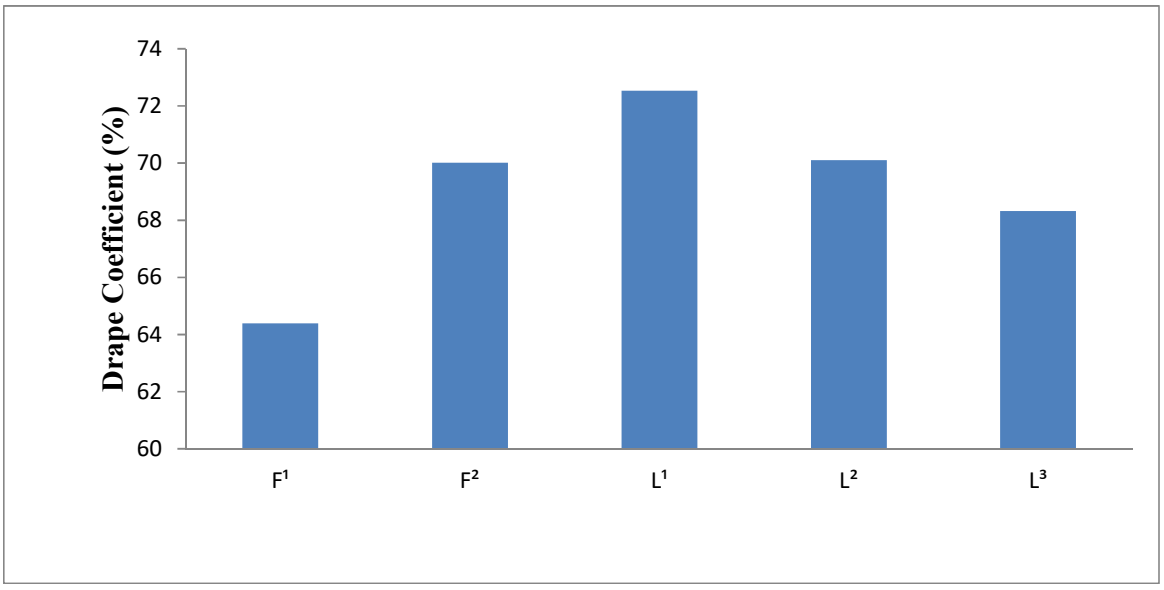

Figure 5: Fabric Drape

YARN COUNT

Table 9: Yarn count

Test sample	Warp Mean Tex	S.D	C.V (%)	Weft Mean Tex	S.D	C.V (%)
F^1	1.7	0.8	7.4	1.7	1.1	10.28
F^2	1.7	0.8	8.27	2.1	1.1	9.91
L^1	1.3	0.316	3.13	2.6	0.5	4.76
L^2	1.2	0.1	3.13	4.4	1.2	10.71
L^3	1.3	0.2	1.96	4.1	0.4	3.84

Key: C.V = Coefficient of Variation, S.D = Standard Deviation

The result in Table 9, shows that sample F^1 having the least mean tex value of 1.7 tex in both warp and weft directions is made from a finer warp and weft threads, which explain the good handle and appearance of sample F^1 as indicated by the fabric handle.

YARN CRIMP

Crimp tends to affect certain fabric characteristic such as cover factor, and thickness, it is a very important parameter in the designing of fabrics for specific end uses. Crimp in either directions, is dependent on fabric structure, though it is largely affected by yarn count and thread density. Figure 6 shows that the weft crimp is generally higher than the warp crimp for all the fabric samples with the exception of sample L^3. This is in agreement with what was obtained in literature (Musa et al, 2011), the higher value of weft crimp is due to the fact that the warp yarn was under greater tension during weaving process on the loom as compared to the weft yarn. So also the weft yarn was more flexible relative to the stiffer warp yarn which was coated with size so as to withstand tension and frictional effects of the healds during weaving action. The crimp of the foreign flat bed sheets is higher than that of the locally produced bed sheets, given the foreign bed sheets a fuller and more compressible feel.

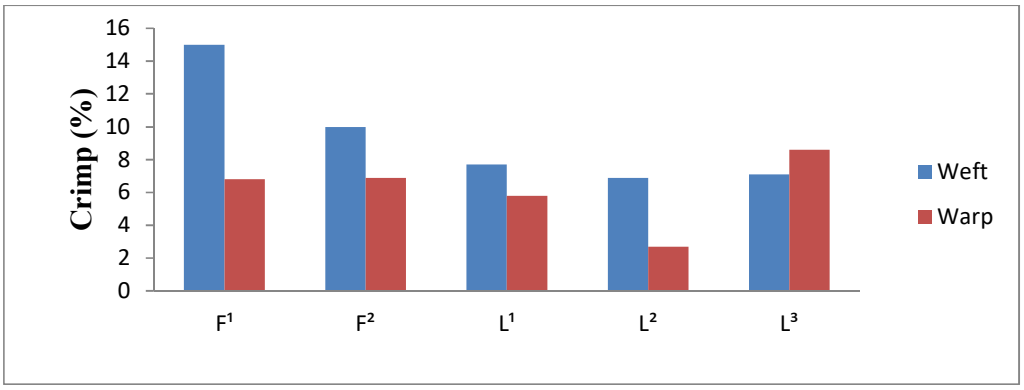

Figure 6: Yarn Crimp

CONCLUSION

The study of the quality parameters of five different materials was carried out successfully. The foreign flat bed sheets are better in terms of crease recovery, tensile properties, handle, drape, yarn crimp and shrinkage, while the locally produced flat bed sheets compete favourably in terms of air permeability, flammability, fabric sett and yarn count. However, the locally produced flat bed sheets are comparably the same with the foreign fabrics considering their abrasion resistance, thickness, and stain removal. Our locally produced flat bed sheets are produced with the aim of suiting our own climatic conditions, usage and aesthetic desires.

REFERENCE

Adokwu.P.T(2016). Comparative analysis of some quality parameters of foreign and local flat bed sheets commercially produced in Nigeria. A final year project presented to the department of Textile Science and Technology, Ahmadu Bello University,Zaria. Nigeria.

British Standard Handbook 11: July (1974). British Standard Institute P (4) :1-224

J.W.S,Hearle, (1992) "journal of textile institute", Vol 83-No 21 pp197,207,208

J.Wiley (1980) "Encyclopedia of Chemical Technology" 2nd Ed Vol 20 pp:48,36

John Wiley and Sons (1960) "Handbook on textile and Quality control" pp:523-535

Koblyakov. A (1989) "Laboratory practice in the study of Textile material" pp:271-364

M. B. Musa, M. K. Yakubu, and E. Danfulani (2011), Qualitative investigation of some locally produced printed fabrics and foreign printed fabrics marketed in Nigeria. Bayero Journal of Pure and Applied Sciences (BAJOPAS), 4(2): 109 – 117

Raji, O. K; Chima, J. F. and Adamu, S. U (2007). A comparative study of selected properties of Nigerian and Foreign made Wax printed Textiles. A conference paper, presented at the 9th annual conference of the National Science and Technology forum. Held at Banquet hall, Kaduna Polytechnic Kaduna, Nigeria. 29th October – 2nd November 2007.

ISSN 214-453-2

HEALTH RISKS ASSESSMENT OF HEAVY METALS IN NOODLES SOLD IN OZORO, DELTA STATE, NIGERIA

*K. EMUMEJAYE, **R. A. DANIEL-UMERI AND ***O. G. EDEMA
*,**Department of Science Laboratory Technology, Delta State Polytechnic, Ozoro, Delta State
***Department of Science Laboratory Technology, Federal Polytechnic, Auchi. Edo State
[ekugbere@gmail.com]

ABSTRACT
The concentrations of some selected heavy metals were assessed by atomic absorption spectrophotometry in noodles sold in the study area. Total of eight different brands of noodles were investigated. The results of heavy metals in samples in mg/kg were in the order: Fe (13.15 – 144.75); Pb (0.00 – 0.55); Cd (0.00 – 0.01); As (0.00 – 0.14); Ni (0.01 – 0.09); Cu (0.02 – 0.33); Zn (1.45 – 8.05) and Cr (0.06 – 0.25). Estimates of daily intakes of metals and health risk index for noodles revealed that the local consumers were safe but were at risk of potential bioaccumulation arising from dietary of Ni, Cd, Cu, Zn in some samples.

Keywords: *Noodles, Heavy metals, Ozoro,Average daily intake, Human health risk*

INTRODUCTION

There is a growing interest in trace/heavy metals and health risk assessment at mining sites and foodstuff across the globe using different techniques (Odumo *et al*., 2011a; 2011b; Kamunda *et al.,* 2016; Wang *et al.,* 2005). The food industry is attracting serious attention on heavy metals due to increasing cases of contamination in agriculture and sea food sources. Also, heavy metals find their way into food during the processing chain.

The pasta industry is growing very fast due to global consumption of noodles. Noodles are produced from rice or wheat flours with other additions such as seasoning, pepper, chicken pieces, salts etc. it lacks some nutritional components such as dietary fiber, therefore it is necessary to add lentil to increase the fiber content.

Previous documentations from Bangladesh, Pakistan and China revealed that wheat and rice from which noodles are made contains heavy metals (Jothi and Uddin, 2014; Huang *et al.,* 2013; Singh *et al.,* 2010; Zeng *et al.,* 2015). Cadmium and lead have been reported to be among the most abundant heavy metals that are toxic. Cadmium and lead exposure may cause kidney and skeletal damage to human body (WHO, 1992; 1995).

Onyema *et al.,* (2014) reported the presence of heavy metals and proximate analysis on instant noodles sold in Nigeria markets. Five common brands of instant noodles were sampled and analysed for proximate and heavy metals using standard analytical methods. The results revealed that Fe and Zn in the samples were within allowable limits of WHO (2003) while Cd, Cr, As, Mn, Ni and Pb occurred at levels slightly above the permissible limits of WHO. Hou and Kruk, (1998) and Omuku *et al.,* (2014) also reported the presence of heavy metals in noodles.

This present study assessed some heavy metal concentrations in noodles and the potential health risks it may pose to the consumers. Suitable models were adopted to estimate the ADI and HRI.

MATERIAL AND METHODS

Study Area

The study area lies within the Niger Delta sedimentary basin which is characterized by both Marine and mixed continental quaternary sediments that are composed of abandoned beach ridges and mangrove swamps (Anoliefo, 1991). The area lies on latitude 5^0 33'23''N and longitude 6^0 14'58''E. The area experiences wet and dry seasons which are typical seasons in Nigeria (Eteng-Inya, 1997; Etu-Efeotor, 1998).

Ozoro is the headquarters of the Isoko North Local Government Area, one of the two administrative units in the Isoko region of Delta State, southern Nigeria. The main economic activity is food crop farming accompanied by some hunting. The staple food crops include cassava and yams. Cassava is the source of most of the food consumed by the Ozoro people. *Garri*, starch meal (*Ozi*) and *Egu* are cassava derivatives. The people are very hospitable. It is one of the largest communities in Isoko land, both in terms of size and population. Ozoro has several schools the most notable one is the Delta State Polytechnic, Ozoro (https://en.wikipedia.org/wiki/Ozoro).

Sampling

A total of eight available brands of noodles were purchased from Ozoro markets in Etevie and main markets and were taken to the laboratory for analysis.

Preparation and digestion of samples

The samples were removed from sachet using a clean scissors and were crushed and ground to fine power on a porcelain crucible.

Digestion of samples was done by a procedure prescribed by ASTM D 1971-95B. 1g of samples with 5ml of Nitric acid and 5ml of Hydrochloric acid was taken in duplicate in flasks with few drops of deionised water added and then heated in a fume hood until the sample was homogenized and brown fumes ceased to evolve. The solution was allowed to cool at room temperature and filtered through whatman filter paper

no.42. Then the volume of the filtrate was made up to 100ml with distilled water for AAS reading. Digestion of blank was also performed in parallel with samples keeping all digestion parameters the same.

Data analysis

Average daily intake of metals (ADI)

Daily intake of noodles in adult and child were estimated by equation (1)

$$ADI = \frac{C_m x D_{fI}}{B_{Awt}} \quad (1)$$

where C_m is heavy metal concentration in noodles (mg kg^{-1}), D_{fI} is average daily intake of noodles (Kg/person), and B_{Awt} average body weight (Kg/person) (Wang et al.2005). The average daily noodle intake for adults and children were estimated to be 0.345 and 0.240 kg/person.day respectively. Body weight for adults was taken as 65kg and children average body weight was estimated to be 35.5kg. The heavy metal intakes were compared with permissible limits for daily intakes for heavy metals set by (WHO, 1993).

Health risk index (HRI)

The knowledge of exposure pathway to the receptor is necessary to be able to assess the health risk of heavy metals to human body. In the present study noodles sold in the market were purchased and the heavy metal concentrations were used to compute the health risk index. HRI values depend on the daily intake of metals (ADI) and oral reference dose (Rf_D). Oral reference dose is an estimated per day exposure of metal to the human body that has no harmful effect during life time (USEPA IRIS, 2006).

The HRI for Cu, Fe, Ni, Zn, Pb, Cd, As and Cr due to consumption of noodles was calculated using equation (2) established by USEPA (1999):

$$HRI = \frac{ADI}{R_{fD}} \quad (2)$$

where ADI has been earlier defined and R_{fD} represents oral reference dose. R_{fD} value for Cu, Fe, Ni, Zn, Pb, Cd, As and Cr is 0.04,0.007,0.02,0.30,0.004, 0.001,0.0003,1.50 (mg/kgbw/day) respectively (USEPA, 2006; 2005). Health risk assessment of contaminants was based on the values of HRI. HRI value that is less than 1 implies no risk and values greater than 1 indicate greater risk level.

RESULTS AND DISCUSSION

Table 1 shows the level of heavy metal concentrations in different brands of noodles sold in the study area. The mean concentrations of all heavy metals ranged from 0.00 -144.75mg/kg. Iron ranged from 13.15-144.75mg/kg and cadmium ranged from 0.00-0.01mg/kg. While other heavy metal values ranged 0.02-0.33, 0.01-0.09, 1.45-8.05, 0.00-0.55, 0.01-0.14 and 0.06-0.25mg/kg for copper, nickel, zinc, lead, arsenic and chromium respectively.

In all samples, the concentration of level of Cr were found to be above WHO permissible limits which are similar to the findings of Onyema et al. (2014). Pb in GPML, GPT and CNS samples were above the WHO permissible limits for Pb. Apart from Cd, Zn and Cu that were within the permissible limits Fe, Pb, Cr and As were above allowable limits set by (WHO, 2003). Our results were slightly higher than those reported in other parts of Nigeria.

Health risk to adults and children

The health risk index (HRI) as shown in Table 2, were less than 1 in adults and children for most metals which indicated that there was no potential risk both the adults and children. However, HRI for Fe in all samples were greater than 1 which implies that the children are at a greater health risk than adults of the same population. Arsenic in some samples has high value of HRI.

Table 1: Heavy metal concentration in noodles sold in the study area

	Heavy metals concentrations in noodles purchased from Ozoro markets in mg/kg							
Brand of noodles	Cu	Fe	Ni	Zn	Pb	Cd	As	Cr
GPML	0.23	46.05	0.02	7.60	0.55	0.00	0.14	0.17
GPT	0.33	144.75	0.09	8.05	0.52	0.01	0.10	0.12
GPS	0.16	13.15	0.03	6.25	0.00	0.00	0.13	0.06
CN	0.06	65.80	0.01	3.65	0.01	0.00	0.05	0.25
CNS	0.08	39.45	0.08	2.20	0.25	0.01	0.05	0.11
ICN	0.05	46.30	0.05	3.45	0.00	0.00	0.03	0.12
DN	0.06	52.65	0.04	2.95	0.00	0.00	0.01	0.09
MGCN	0.02	26.30	0.01	1.45	0.00	0.00	0.01	0.11
WHO[a] limits	NA	10 -50	NA	5 - 22	0.025	0.003	NA	0.05

a (WHO, 2003) NA= not available

Table 2. Health risk assessment of some metals in samples

Brand	Metal	R_{fD}	ADI_{adult}	ADI_{child}	HRI_{adult}	HRI_{child}
	Cu	0.04	0.0012208	0.001555	0.030519	0.038873
	Fe	0.007	0.2444192	0.311324	34.91703	44.47485
	Ni	0.02	0.0001062	0.000135	0.005308	0.006761
	Zn	0.3	0.0403385	0.05138	0.134462	0.171268
GPML	**Pb**	0.004	0.0029192	0.003718	0.729808	0.929577
	Cd	0.001	0	0	0	0
	As	0.0003	0.0007431	0.000946	2.476923	3.15493
	Cr	1.5	0.0009023	0.001149	0.000602	0.000766
	Cu	0.04	0.0017515	0.002231	0.043788	0.055775
	Fe	0.007	0.7682885	0.978592	109.7555	139.7988
	Ni	0.02	0.0004777	0.000608	0.023885	0.030423
GPT	**Zn**	0.3	0.0427269	0.054423	0.142423	0.181408
	Pb	0.004	0.00276	0.003515	0.69000	0.878873
	Cd	0.001	5.308E-05	6.76E-05	0.053077	0.067606
	As	0.0003	0.0005308	0.000676	1.769231	2.253521
	Cr	1.5	0.0006369	0.000811	0.000425	0.000541
	Cu	0.04	0.0008492	0.001082	0.021231	0.027042
	Fe	0.007	0.0697962	0.088901	**9.970879**	**12.7002**
	Ni	0.02	0.0001592	0.000203	0.007962	0.010141
GPS	**Zn**	0.3	0.0331731	0.042254	0.110577	0.140845
	Pb	0.004	0	0	0	0
	Cd	0.001	0	0	0	0
	As	0.0003	0.00069	0.000879	**2.3**	**2.929577**
	Cr	1.5	0.0003185	0.000406	0.000212	0.00027
	Cu	0.04	0.0003185	0.000406	0.007962	0.010141
	Fe	0.007	0.3492462	0.444845	**49.89231**	**63.5493**
	Ni	0.02	5.308E-05	6.76E-05	0.002654	0.00338
CN	**Zn**	0.3	0.0193731	0.024676	0.064577	0.082254
	Pb	0.004	5.308E-05	6.76E-05	0.013269	0.016901
	Cd	0.001	0	0	0	0
	As	0.0003	0.0002654	0.000338	0.884615	1.126761
	Cr	1.5	0.0013269	0.00169	0.000885	0.001127
	Cu	0.04	0.0004246	0.000541	0.010615	0.013521
	Fe	0.007	0.2093885	0.266704	**29.91264**	**38.1006**
	Ni	0.02	0.0004246	0.000541	0.021231	0.027042
CNS	**Zn**	0.3	0.0116769	0.014873	0.038923	0.049577
	Pb	0.004	0.0013269	0.00169	0.331731	0.422535
	Cd	0.001	5.308E-05	6.76E-05	0.053077	0.067606
	As	0.0003	0.0002654	0.000338	0.884615	**1.126761**
	Cr	1.5	0.0005838	0.000744	0.000389	0.000496
	Cu	0.04	0.0002654	0.000338	0.006635	0.008451
	Fe	0.007	0.2457462	0.313014	**35.10659**	**44.7163**
	Ni	0.02	0.0002654	0.000338	0.013269	0.016901
ICN	**Zn**	0.3	0.0183115	0.023324	0.061038	0.077746
	Pb	0.004	0	0	0	0
	Cd	0.001	0	0	0	0
	As	0.0003	0.0001592	0.000203	0.530769	0.676056
	Cr	1.5	0.0006369	0.000811	0.000425	0.000541
	Cu	0.04	0.0003185	0.000406	0.007962	0.010141
	Fe	0.007	0.27945	0.355944	**39.92143**	**50.84909**
	Ni	0.02	0.0002123	0.00027	0.010615	0.013521
DN	**Zn**	0.3	0.0156577	0.019944	0.052192	0.066479
	Pb	0.004	0	0	0	0
	Cd	0.001	0	0	0	0
	As	0.0003	5.308E-05	6.76E-05	0.176923	0.225352
	Cr	1.5	0.0004777	0.000608	0.000318	0.000406
	Cu	0.04	0.0001062	0.000135	0.002654	0.00338
	Fe	0.007	0.1395923	0.177803	**19.94176**	**25.4004**
	Ni	0.02	5.308E-05	6.76E-05	0.002654	0.00338
	Zn	0.3	0.0076962	0.009803	0.025654	0.032676
MGCN	**Pb**	0.004	0	0	0	0
	Cd	0.001	0	0	0	0
	As	0.0003	5.308E-05	6.76E-05	0.176923	0.225352
	Cr	1.5	0.0005838	0.000744	0.000389	0.000496

*Bold figures indicate high health risk values

CONCLUSION

The presence of As and Cr in concentration levels in the samples and high values of HRI in most samples might pose serious health effects in the immediate and long time accumulation of these heavy metals in the human body.

REFERENCES

Anoliefo. G.O (1991), Forcados Blend crude oil effects in Respiratory mechanism, mineral element composition and growth of citrulus vulgaris school unpublished doctoral thesis, University of Benin.

Eteng Inya A., (1997). The Nigerian State, Oil Exploration and Community Interest: Issues and Perspectives. University of Port Harcourt, Nigeria conf paper

Etu – Efeotor J.O (1998). Hydrochemical analysis of surface andground waters of Gwagwalada area of central Nigeria. *Globa J Pure Appl. Sci 4 (2): 153 – 163*.

Hou, G. and Kruk, M. (1998) Asian Noodle Technology. Technical Bulletin 20:10. *International Food Research Journal*, **19**, 309-313.

Jothi,J.S and Uddin, M.B (2014) Detection of heavy metals in some commercial brands of noodles. *European Academic Research 11(6):10667-10679*

Kamunda, C., Mathuthu, M. and Madhuku, M. 2016. Health Risk Assessment of Heavy Metals in Soils from Witwatersrand Gold Mining Basin, South Africa. *Int.J. Environ.Res. Public Health* 13:1-11

Odumo, O.B., Mustapha, A.O., Patel J.P. and Angeyo, H.K. 2011b. Energy Dispersive X – Ray Fluorescence Analysis of Mine Waters from The Migori Gold Mining Belt in Southern Nyanza, Kenya. *Bull environ Contam Toxicol* 86:484-489.

Odumo, O.B., Mustapha, A.O., Patel, J.P. and Angeyo, H.K. 2011a. Multielemental Analysis of Migori (Southwest, Kenya) Artisanal Gold Mine Ores and Sediments by EDX-Ray Fluorescence Technique: Implications of Occupational Exposure and Environmental Impact. *Bull environ Contam Toxicol* 86:484-489.

Omuku, P.E, Onwumelu, H.A and Alisa, C.O (2014) Comparative analysis of selected heavy metals in green leafy vegetables and instant noodles sold in Eke-Awka market, Awka, Anambra state. *Journal of Environmental Science and Water Resources 3(9), pp. 209 – 213.*

Omuku, P.E, Onwumelu, H.A and Alisa, C.O (2014) Comparative analysis of selected heavy metals in green leafy vegetables and instant noodles sold in Eke-Awka market, Awka, Anambra state. *Journal of Environmental Science and Water Resources Vol. 3(9), pp. 209 - 213*

Onyema, C.T., Ekpunobi, U.E., Edowube, A.A., Odinma, S. and Sokwaibe, C.E. (2014) Quality Assessment of Common Instant Noodles Sold in Nigeria Markets. *American Journal of Analytical Chemistry*, **5**, 1174-1177. http://dx.doi.org/10.4236/ajac.2014.517124

Ozoro (n.d) retrieved from https://en.wikipedia.org/wiki/Ozoro on the 4th of August, 2016.

Singh, A., Sharma, R.K., Agrawal, M., Marshall, F.M., (2010). Health risk assessment of heavy metals via dietary intake of foodstuffs from the wastewater irrigated site of a dry tropical area of India. Food Chem. Toxicol. 48, 611–619.

US EPA (1999) Guidance for Performing Aggregate Exposure and Risk Assessments, Office of Pesticide Programs, Washington, DC.

US EPA (2005) Guidelines for Carcinogen Risk Assessment, EPA/630/P-03/001F, Risk Assessment Forum, Washington, DC.

US-EPA IRIS, (2006). United States, Environmental Protection Agency, Integrated Risk Information System. <http://www.epa.gov/iris/substS>.

Wang, X., Sato, T., Xing, B. and Tao, S. (2005), "Health risks of heavy metals to the general public in Tianjin, China via consumption of vegetables and fish". *Sci. Total Environ.(350), 28-37.*

WHO (1992). Cadmium, Environmental Health Criteria, vol. 134, Geneva.

WHO (1995) Reliable Evaluation of Low-Level Contaminants of Food. Workshop in the frameofGEMS/FoodEURO.Available:http://www.who.int/foodsafety/publications/chem/en/lowlevel_may1995.pdf. Accessed 1May2013.

WHO (2003) World Health Organization Provisional Tolerable Weekly Intake of Toxic Heavy Metals.

Zeng, X.,Wang, Z.,Wang,J.,Guo,J., and Chen,X.(2015) Health risk assessment of heavy metals via dietary intake of wheat grown in Tianjin sewage irrigation area. *Ecotoxicology doi 10.1007/s10646-015-1547-0*

ISSN 214-453-2

KINETICS STUDIES OF THE REMOVAL OF MANGANESE, CADMIUM AND LEAD FROM AQUEOUS SOLUTION USING COCOA SHELL

A. O. ERUOLA[1], C. C. OJIODU[1] AND R. A. OLOWU[2]

[1]Department of Chemical Science, Yaba College of Technology, P.O. BOX 1775, Sabo - Yaba, Lagos, Nigeria

[2]Chemistry Department, Lagos State University, Ojo - Lagos, Nigeria

[Ojiodu1966@yahoo.com]

ABSTRACT

The kinetics of the removal of manganese cadmium and lead in aqueous solution using cocoa shell as an adsorbent was investigated. The effect of contact time, kinetic of sorption mechanism and the adsorbate concentrations on sorption of Mn^{2+}, Cd^{2+} and Pb^{2+} ions were examined. The kinetic of the sorption mechanism of Mn^{2+}, Cd^{2+} and Pb^{2+} was evaluated using pseudo-first order (Lagergren) rate and the pseudo-second (Ho-model) rate model. The rate limiting sorption step was physisorption and results indicate that pseudo-second order model provides a more appropriate description of the adsorption rate for the metals ions sorption in cocoa shell. The maximum adsorption capacities per unit gram of the adsorbent at equilibrium time, neutral pH, 200 r p m, and temperature of 25 ^0C are 9.02 to 40.04 mg kg^{-1} for Mn^{2+}, 7.02 to 25.89 mg kg^{-1} for Cd^{2+} and 5.25 to 11.01 for Pb^{2+} under 10 to 50 mg kg^{-1} initial metal concentration. Sorption equilibrium isotherm was determined and correlated with Langmuir and Freundlich model. It was found that the Freudlich adsorption model best fitted the isotherm data. It is concluded that cocoa shell can be use as an effective adsorbent for removal of heavy metals from aqueous solution.

Keywords: *Kinetics Cadmium, Manganese, Lead, cocoa shell, sorption.*

INTRODUCTION

Kinetics study is important in any adsorption process and helps to identifying the type of adsorption, reaction pathway, capacity of adsorbent and reaction rate of the system. The kinetic data are essential for scaling up of sorption processes for industrial preparations. Kinetic studies on the adsorption of contaminants using different biomaterials have been reported previously[1,2] . Heavy metals are group of non biodegradable high density elements. They are released by a human of anthropogenic emission in the environment are some of the major pollutants of soil and water resources[3] . Some metals such as copper, zinc and iron are considered bio-essential while others such as cadmium, lead, mercury, manganese and chromium are highly toxic. However, even bi-essential metals may cause physiological and ecological problems if present at significant concentration. Heavy metals ions should be removed at the source in order to avoid pollution of natural water and subsequent metal accumulation in the food chain. Various physical and chemical techniques for removing metals ions from the wastewater include chemical precipitation, adsorption, ion exchange, extraction and membranes processes chemical precipitation is most common utilized conventional technique. However, the application of these methods is often limited due to their inefficiency, high capital investment or operational costs. Consequently, there is a growing requirement for novel, efficient and cost effective techniques for the remediation of metal bearing waste water before their discharge into the environment. Adsorption has been shown to be an economically feasible alternative method for removing heavy metals from waste water and water supply[4] . Biosorption technology, utilizing natural metals or industrial and agricultural wastes to remove metal form aqueous media, often an efficient and cost-affordable alternative compound to traditional chemical and physical remediation and decontamination technique since the cost of this process are rather expensive, the use of agricultural residue or industrial by product have been studied. These agricultural waste materials includes maize bran[5] , coffee husks[6] , rice straw [7] , sugar peat pulp [8] ,olive pomace[9] , apple wastes [10] , palm kernel fibre [11] ,peanut hull [12] , hazelnut husks[13] ,oak sawdust[14] and grape stalks[15].

Despite the relative simplicity and potential cost effectiveness of bio sorption, metal removal using low cost bio-sorbents is relatively improve and need further development before it may be applied routinely in practice and thus considered an alternative to use of ion-exchange resins or activated carbons. Cocoa shell is an abundant agricultural waste product with millions of tons being generated annual polluting the environment in Nigeria. The cocoa shell has been recognized to have significant potential as a biosorbent for metal removal after simple pre-treatment. In this work, we investigated the potential of cocoa shell to act as a bio sorbent for Mn^{2+}, Cd^{2+}, and Pb^{2+} removal from aqueous media.

MATERIALS AND METHODS

Sorbent preparation

The cocoa shell collected locally, dried, grinded into powdered and sieved through 450 µm and 300 µm mesh screens. The portion of the cocoa shell retained on the 300 µm mesh was steeped in dilute nitric acid solution for 8 hours rinsed with deionized water and air dried.

Sorbate preparation

1000 mg kg^{-1} of each of each metal stock was prepared by dissolving calculated amount equivalent of 1.00g of each metal in a specific compound ($MnSO_4.H_2O$,

$CdSO_4$ and $Pb(NO_3)_2$) in 1litre distilled water (1000mg/L). Standard Mn^{2+}, Cd^{2+}, and Pb^{2+} solutions of 10, 20, 40 and 50 mg kg^{-1} were prepared serially by diluting the stock solutions respectively.

Contact time study

Equilibration time for the adsorption and adsorptions model of Mn^{2+}, Cd^{2+}, and Pb^{2+} on cocoa shell was carried out on the metals ions. 30 ml of each selected concentration of salt solutions of heavy metals in distilled water were added each into 1g of cocoa shell meal weighed into shaking bottles at room temperature (25°C) under neutral pH each to determine the time required for each of the metal ion to reach adsorption equilibrium. Two drops of toluene was added to each solution in the bottles to inhibit microbial growth. The shell suspensions were shaken on a mechanical shaker at a speed of 200 rpm for 40, 80, 120, 160 and 180mins. After the specified shaking time, the solution phase was filtered by using filter paper (whatman 110mm and 11mm pore size) for removing the suspended shell particles. A 10 ml of aliquot of supernant were analyzed for residual Mn^{2+}, Cd^{2+}, and Pb^{2+} respectively by Flame Atomic Absorption Spectrophotometer. The adsorbed heavy metal concentration in cocoa shell was taken as the difference between metal added in initial solution and the remaining metal in supernatant solution after equilibration. The time for metal adsorption to reach equilibrium was determined graphically from the plot of adsorption values against time of equilibrium. The adsorbed metal ions individually on cocoa shell per unit adsorbent mass was calculated as follows:

$$Q_e = (C_o - C_e)\, V/\, m \ldots\ldots\ldots (1)$$

C_o is the initial heavy metal concentrations (mg/l); C_e is the concentration of heavy metal at equilibrium (mg/l), m is the cocoa shell mass (m), V is the volume of solution (ml). Calculations were made by using these data and adsorption curves were obtained.

RESULTS AND DISCUSSION

Effect of contact time

The time taken to attain equilibrium for Mn^{2+}, Cd^{2+}, and Pb^{2+} at neutral pH, temperature of 25°C and centrifugation speed of 200 rpm using 1g of cocoa shell is shown in figure 1, 2, 3. It was observed that the amount of Mn^{2+}, Cd^{2+}, and Pb^{2+} adsorbed per unit mass of cocoa shell increased significantly with increase in initial concentration. The adsorbed rate was very rapid in the first few minutes after which the rate decreased sharply and eventually reached a constant peak after at 160 minutes of the adsorption irrespective of concentrations. The two stage sorption mechanism with the first rapid and quantitatively predominant and the second slower and quantitatively insignificant, has been extensively reported in literature[16]. 160 minutes was therefore indicated as the time for Mn^{2+}, Cd^{2+}, and Pb^{2+} adsorption to reach equilibrium. The necessary contact time to reach the equilibrium depends on the initial metal ion concentration. The uptake rate is controlled by the rate at which the metals (Mn^{2+}, Cd^{2+}, and Pb^{2+}) were transported from the exterior to the interior sites of the adsorbent. The adsorption capacity was observed to increase with the initial metal concentration for the series (10, 20, 40 and 50 mg kg^{-1}) for the selected heavy metals .This is due to larger surface area of the cocoa shell at the beginning of adsorption reaction. The amount of the metal ion each in their different series shows the same magnitude in their removal but varies in the adsorption capacity. However, the differential sorption of Mn^{2+}, Cd^{2+}, and Pb^{2+} ions may be ascribed to the difference in their ionic sizes. The ionic sizes of Mn^{2+}, Cd^{2+}, and Pb^{2+} are 0.67, 0.97, and 1.20 respectively. The smaller the ionic size the greater its affinity to reactive sites. The adsorption capacity increased in the substrate with stronger bond for smaller size metal ion indicative that the competition of manganese with ionic radius of 0.67A has higher binding site than cadmium with ionic radius of 0.97A on cocoa shell. The lowest adsorption capacity of lead with weak bond on cocoa shell could be attributed to its highest ionic radius 1.20A. Mn^{2+}, $Cd^{2+}$and Pb^{2+} adsorbed by complexation reaction. This general trend of the sorption is due to the fact that metal ion with smaller ionic radius diffuse faster in aqueous systems and compete better for exchange site than for those with larger sizes. This trend in smaller ionic size was also observed for Cu^{2+},Cd^{2+} and Zn^{2+} using other biological adsorbents[17] . According to Cho *et al*. (2005)[18] metal with smaller hydrolysis constant (Pk_H) has the increasing tendency to hydrolyse because of their larger charge-size function (z^2/r). The Pk_H for manganese to cadmium shows that cadmium will be hydrolyze to a greater extent than manganese indicating a higher binding for manganese > cadmium and lead has the least adsorption. So the adsorption capacities increases from $Mn^{2+} > Cd^{2+} > Pb^{2+}$. The long contact time of 160 minutes observed to reach equilibrium for all the metal ions indicated that the predominant mechanism was physisorptions which encourage easy removal of the adsorbed heavy metals or regeneration of the spent adsorbent.

Effect of initial rate concentration

The initial concentration provides a driving force to overcome all mass transfer resistances of the metals ion in the aqueous and solid phase. This led to higher probability of collision between the metal and active sites of the cocoa shell. The surface adsorption sites become exhausted at some point in time, it reached a constant value in which no more metal is removed from solution [19-20]. At this point, the adsorbed amount of heavy metals on cocoa shell was in a state of dynamic equilibrium[21] . The equilibrium uptake increased with the increasing of initial metal ions at the range of experimental concentration. Initial rate of the sorption capacity was greater for higher initial heavy metals concentrations, because the resistance to each of the metal uptake decreased as the mass transfer driving force increased so the initial rate of adsorption in metals was greater for higher initial adsorbate concentrations (50 mg kg^{-1}) than for the lowest concentration (10 mg kg^{-1}) of metals ions (manganese, cadmium, and lead) on cocoa shell. This agrees with the work of Okiemen et al (1987)[22] work on cadmium, lead, zinc ions in sulphur containing chemically modified cellulosic material lust.

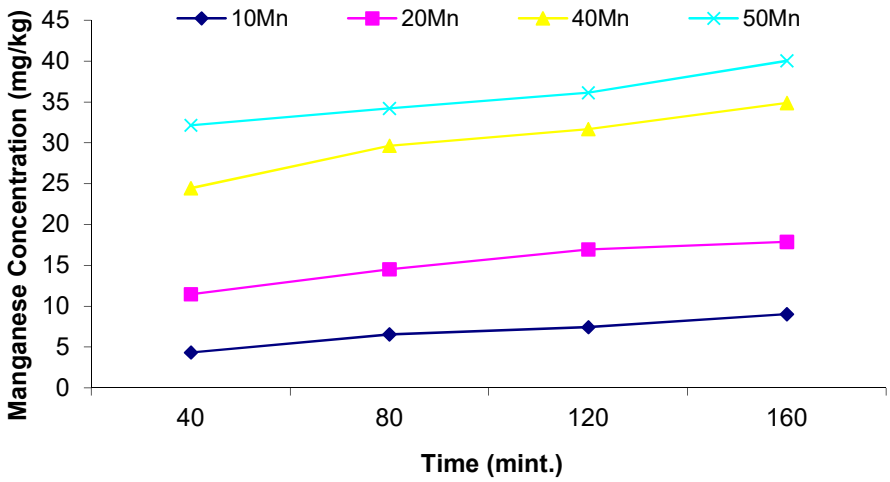

Figure 1: Time of attainment of manganese adsorption equilibrium at pH of 7.0, 10mgkg^{-1} and temperature of 25^{o}C and centrifugation speed of 200 rpm per unit mass of cocoa shell.

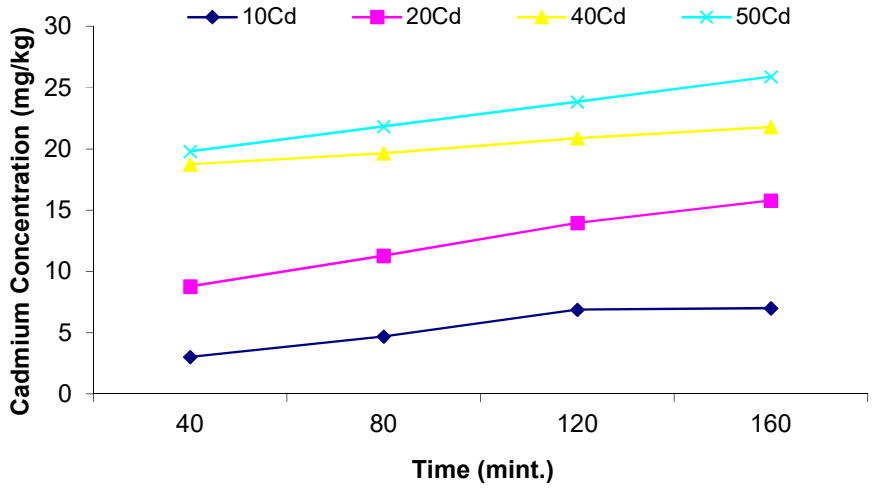

Figure 2: Time of attainment of cadmium adsorption equilibrium at pH of 7.0, 10mg kg^{-1} and temperature of 25^{o}C and centrifugation speed of 200 rpm per unit mass of cocoa shell.

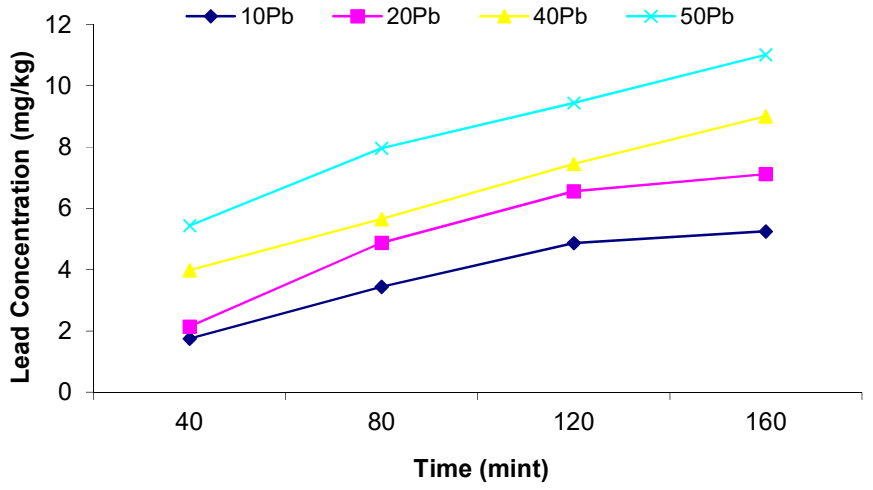

Figure 3: Time of attainment of lead adsorption equilibrium at pH of 7.0, 10mg kg^{-1} and temperature of 25^{o}C and centrifugation speed of 200 rpm per unit mass of cocoa shell.

Kinetic treatment of experimental data

The mechanism of adsorption for the heavy metals was subjected to both pseudo-first order Lagergren, (1898)[23] and pseudo second order Ho and Mckay (1999)[24] equations at the initial metal concentrations of 10 mg kg^{-1}

Pseudo first order or Lagergren equation

$\text{Log } [Q_e - Q] = \log Q_e - k_1/2.303_t$ ……..(2)

A linear plot of log $[Q_e - Q]$ against 't' indicates the conformity with the model

Q_e = mass of metal adsorbed at equilibrium (mg kg^{-1})

Q= mass of metal adsorbed at time "t" (mg kg^{-1})

"t"= time for adsorption (hrs)

k_1 = equilibrium rate constants for 1st order

Pseudo second order or Ho (2004) equation

$t/Q_e = 1/k_2Q_e^2 + t/Q_e$ ……..(3)

A linear plot of t/Q_e against't' indicates conformity with the model

Q_e = mass of metal adsorbed at equilibrium (mg kg^{-1})

"t"= time for adsorption (hrs)

k_2 = equilibrium rate constants for 2nd order.

First order kinetics for Mn^{2+}, $Cd^{2+}$and Pb^{2+} onto maize cob are shown in Figure 4, 5, 6.

Figures 7, 8, and 9 illustrates the pseudo second order (Ho) equations of Mn^{2+}, Cd^{2+}, and Pb^{2+} respectively at the initial metal concentrations of 10 mg kg^{-1}.

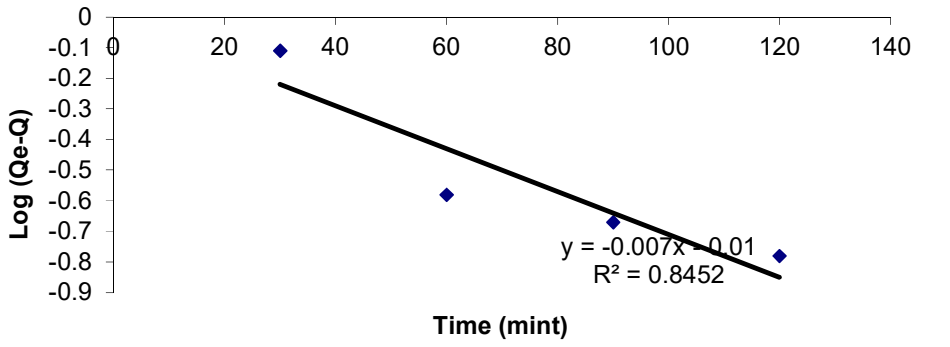

Figure 4: Lagergren pseudo first order kinetic plot for manganese at pH of 7.0, initial metal concentration of 10mg kg^{-1} and temperature of 25°C per unit mass of cocoa shell.

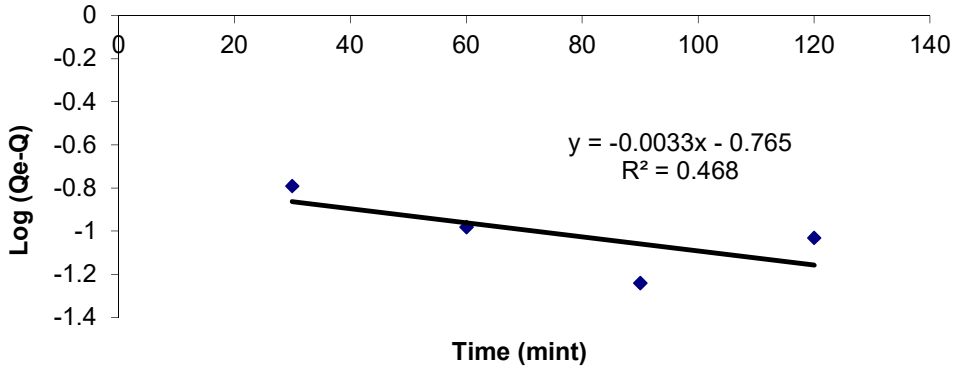

Figure 5: Lagergren pseudo first order kinetic plot for cadmium at pH of 7.0, initial metal concentration of 10 mg kg^{-1} and temperature of 25°C per unit mass of cocoa shell.

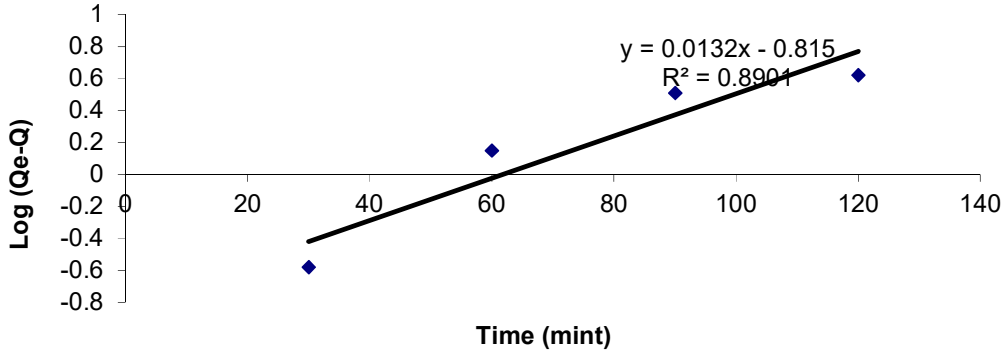

Figure 6: Lagergren pseudo first order kinetic plot for lead at pH of 7.0, initial metal concentration of 10 mg kg^{-1} and of 25°C per unit mass of cocoa shell.

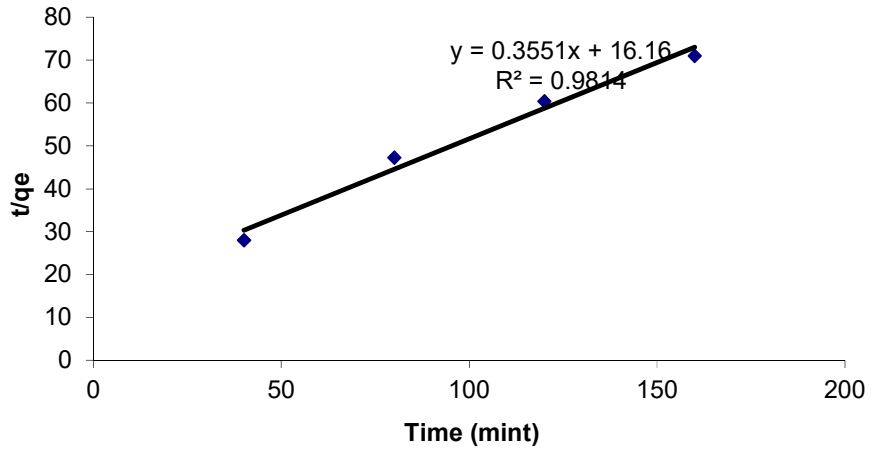

Figure 7: Ho pseudo second order kinetics plot for manganese at pH of 7.0, initial metal concentration of 10 mg kg^{-1} and 25°C per unit mass of cocoa shell.

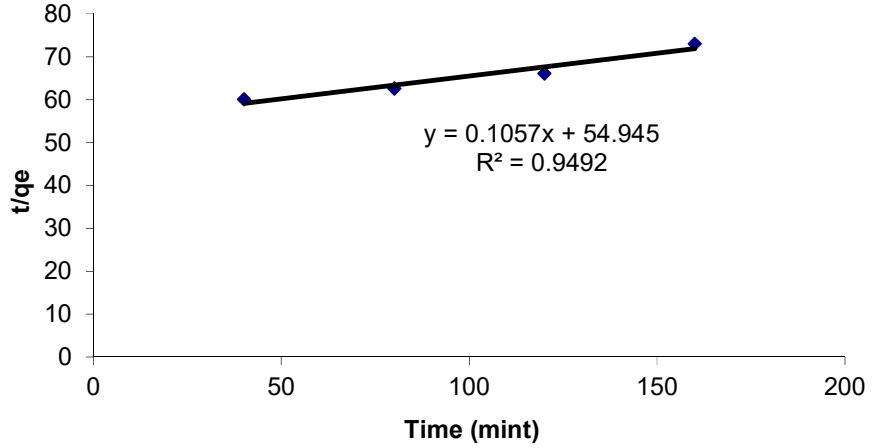

Figure 8: Ho pseudo second order kinetics plot for cadmium at neutral pH, initial metal concentration of 10 mg kg^{-1} and 25°C per unit mass of cocoa shell.

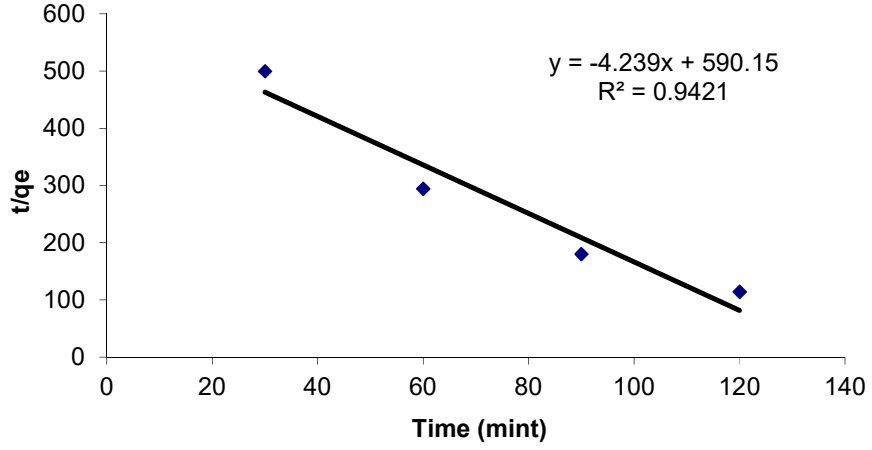

Figure 9: Ho pseudo second order kinetic plot for lead at neutral pH, initial metal concentration of 10 mg kg^{-1} and 25°C per unit mass of cocoa shell.

The rate of the metals sorption has the highest conformation with pseudo second order (Ho) rate model each, with coefficient of determination (R^2) of 0.98, 0.95and 0.94 for Mn^{2+}, Cd^{2+}, and Pb^{2+} respectively.

Adsorption isotherms

The adsorption characteristics of manganese, cadmium and lead was determined by fitting the adsorption data into both Freundlich (1926) and Langmuir (1918) equations respectively.

Freundlich isotherm: This is use for modeling the adsorption on heterogenous surfaces. This can be explained by the equation

$Q_e = K_f C_e^{1/n}$ **……**(4)

The linear form of equation (4) can be written as:

$\text{Log } Q_e = 1/n \log C_e + \log k_f$……..(5)

Q_e = the quantity of ions absorbed per unit weight of absorbent.

C_e = the equilibrium concentration of the adsorbate after adsorption has taken place.

"K_f" = Freunlich constant; and "1/n" = adsorption intensity.

Mn^{2+}, Cd^{2+} and Pb^{2+} adsorption isotherm using Freundlich approach in the study is presented as a function of the equilibrium concentration of metal ions in the aqueous medium at neutral pH, 25ºC and contact time of 160 minutes is shown in Figure 10, 11 and 12. These adsorptions gave a linear fit form of the model with the coefficient of determination (R^2) of 0.96, 0.96 and 0.96 for Mn^{2+}, $Cd^{2+}$and Pb^{2+} which are strong correlation.

The Freundlich adsorption co-efficients (k_f and 1/n) were numerical values that characterized the cocoa shell surface for its affinity for the metals. All the metals exhibited a slope (1/n) defined as adsorption intensity which is less than unity thereby exhibiting a favourable condition for the cocoa shell surface which agrees with Horsfall and Abia (2003) [25]. The 1/n that was less than unity implies that the surface site heterogeneity was predominant for the adsorption of the metals on cocoa shell that is, there was broad distribution of adsorption of the ions on the cocoa shell. The adsorption capacity (k_f) for Mn^{2+}, $Cd^{2+}$and Pb^{2+} by cocoa shell were positive value which predicted that the quantity adsorbed on cocoa shell corresponds to complete heterogenous layer coverage.

Langmuir adsorption isotherm:

This model suggests that the uptake occurs on homogenous surface by monolayer sorption with interaction between sobbed molecules. The model assumed uniform energies of adsorption onto the surface. Langmuir isotherm can be defined according to the following

$\mathbf{Q_e == V_m k C_e / 1 + k C_e}$……(6)

Q_e = the quantity of ions absorbed per unit weight of absorbent.

C_e = the equilibrium concentration of the adsorbate after adsorption has taken place.

V_m is the monolayer capacity and "k" is the equilibrium constant.

The linear form of equation (6) can be written as follow:

$\mathbf{C_e/Q_e = 1/kV_m + C_e/V_m}$……(7)

The sorption of the metals ions (Mn^{2+}, Cd^{2+} and Pb^{2+}) on cocoa shell also showed linearity with Langmuir linear equation. This indicates that the adsorption in Mn^{2+}, Cd^{2+} and Pb^{2+}did occur at the homogeneous surface molecules to each other as well in the plane of the active site cocoa shell.

CONCLUSION

This study clearly suggest that the use of cocoa shell as sorbent is much economical, effectual and more viable. It can be efficiently used to remove ions from aqueous solution. The different operational parameters observed during the process of investigations reveal that the adsorption of manganese, cadmium and lead ions was dependent on initial rate concentrations, ionic strength and contact-time with same magnitude in their removal but different adsorption capacities.

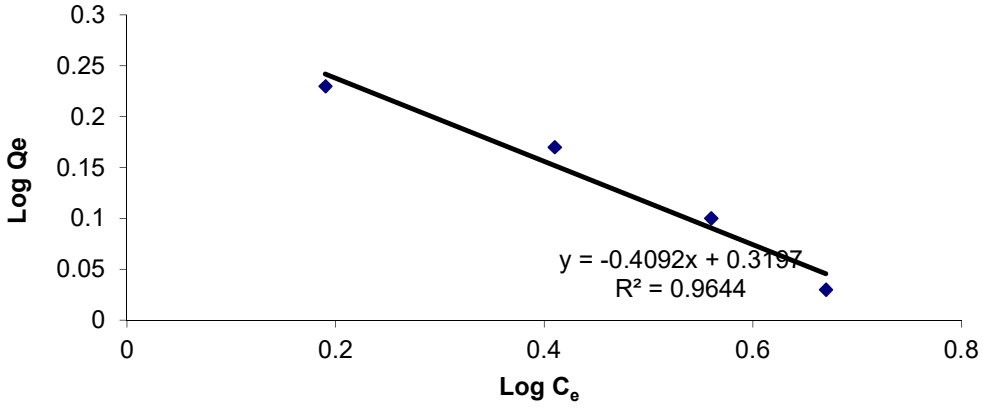

Figure 10: Freundlich adsorption isotherm for manganese at neutral pH, 10 mg kg^{-1} initial concentration and 25ºC per unit mass of cocoa shell.

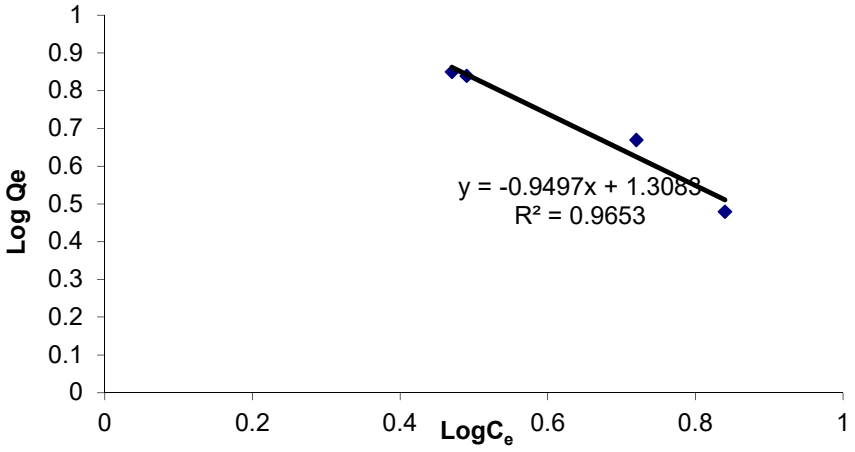

Figure 11: Freundlich adsorption isotherm for cadmium at neutral pH, initial concentration of 10 mg kg^{-1} and 25^{o}C per unit mass of cocoa shell.

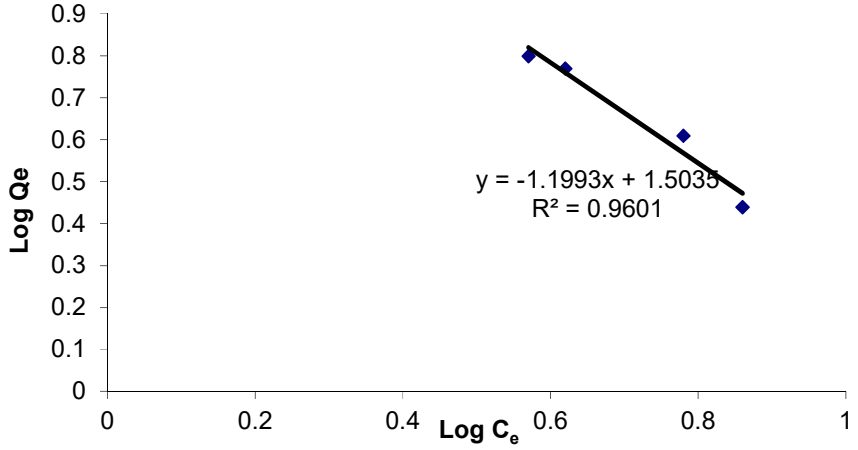

Figure 12: Freundlich adsorption isotherm for lead at neutral pH and initial concentration of 10 mg kg^{-1} and 25^{o}C per unit mass of cocoa shell.

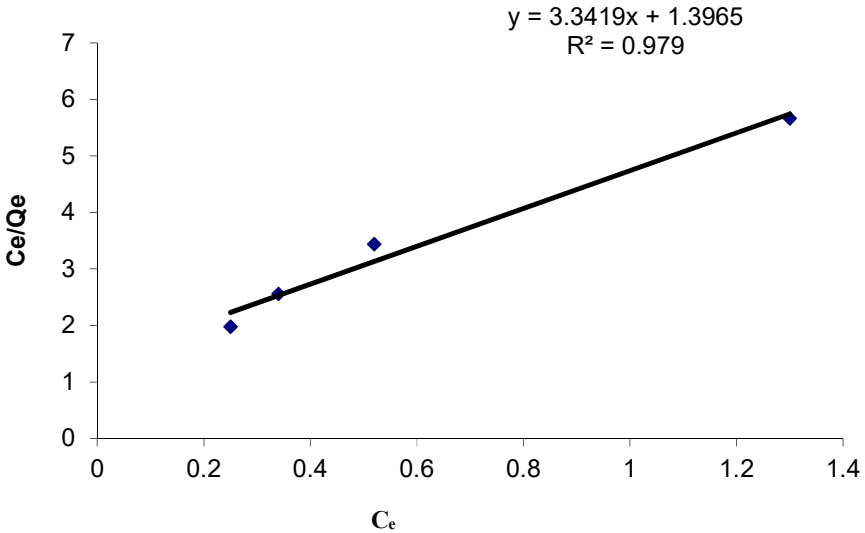

Figure 13: Langmuir adsorption isotherm for manganese at neutral pH and initial concentration of 10 mg kg^{-1} and 25^{o}C per unit mass of cocoa shell.

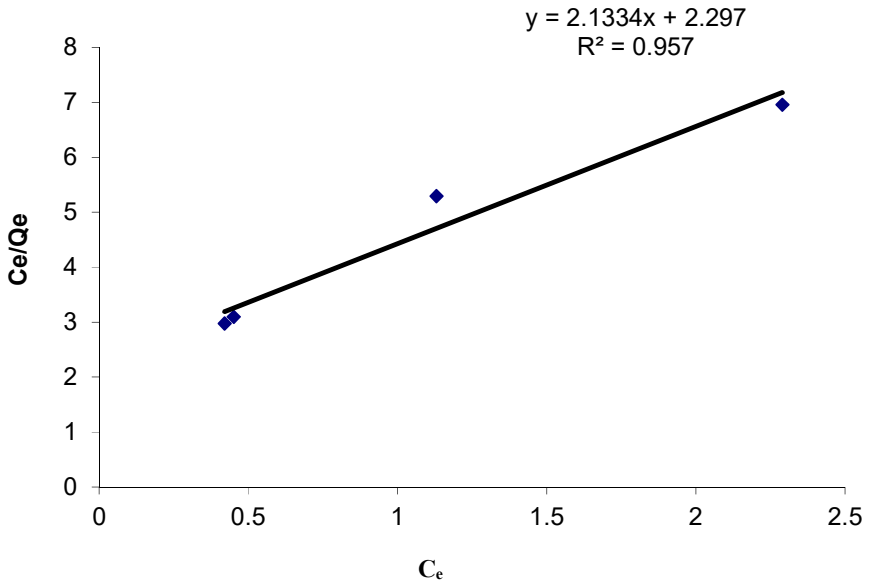

Figure 14: Langmuir adsorption isotherm for cadmium at neutral pH and initial concentration of 10 mg kg^{-1} and 25^{o}C per unit mass of cocoa shell.

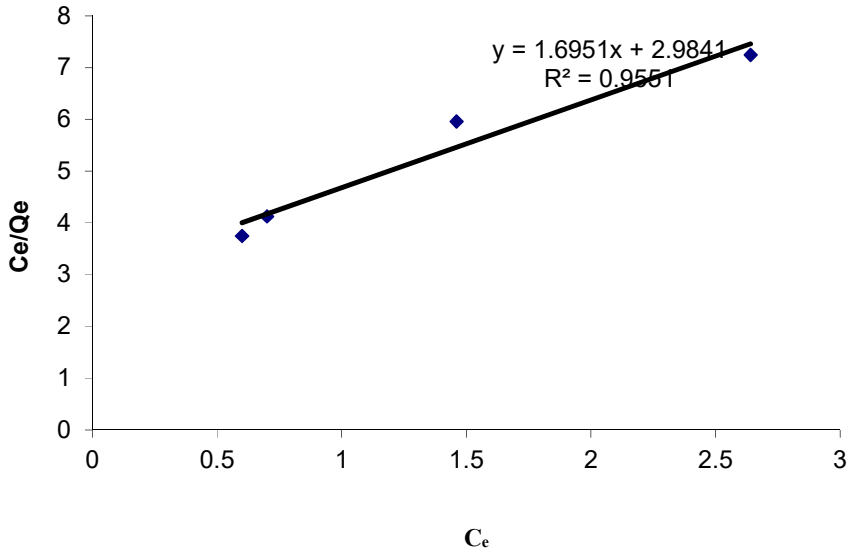

Figure 15: Langmuir adsorption isotherm for lead at neutral pH and initial metal concentrations of 10 mg kg^{-1} and 25^{o}C per unit mass of cocoa shell.

The long contact time of 160 minutes at which equilibrium for manganese, cadmium and lead ions was reached indicated that the predominant mechanism is physisorption and the kinetic of their reactions is best described by pseudo- second order rate model. It is common to describe the goodness of it in terms of R^2, which is the square of the correlation coefficient. Both Langmuir and Freundlich isotherms shows an adequate fit of experiment data in the whole range of concentrations generally giving the R^2 values higher than 0.90. The ability of these models to represent the experiment data could have been due to the fact that the isotherms take into account adsorbent-adsorbate interactions. The adsorption of the metals ions conform with Langmuir and Freundlich isotherm of both heterogeneous and homogenous adsorptions on the adsorbent surface. The adsorption capacities decreases from Mn^{2+}, $Cd^{2+}$and Pb^{2+} respectively. As a result of this study, it may be concluded that cocoa shell may be used as alternative and effective material for elimination of heavy metal pollution from waste waters since it is low cost, abundant and locally available adsorbent.

.

REFERENCES

1. Ho, Y, S. and Mckay, G.,1999. Pseudo-second order model for sorption process. *J.of Process Biochem*. 34(5), 451- 465 **(1999)**.
2. Horsfall, M. and Spiff, A.I., Equilibrium Sorption Study of Al^{3+}, Co^{2+} and Ag^{+} in Aqueous Solutions by Fluted Pumpkin (*Telfairia Occidentalis* HOOK) Waste Biomass. *Acta Chimica Slovinica*, 52, 174-181**(2005).**
3. Loubna, N., Ilhem, G. and Qualid Hamdacious, M., Batch sorption dynamic and equilibrium for the removal of cadmium ions from aqeous

phase wheat bran. *J.Hazardous Mate*. 149, 115 - 125 **(2007).**

4. Dakiky, M., Khamis M., Manassra, A and Mereb, M., Selective adsorption of chromium (iv) in industrial waste water using low- cost abundantly available adsorbents. *Adv. Env. Resources*. 6, 533 - 540**(2002).**
5. Hasan, S.H., Singh, K.K., Prakash, O., Talat, M. and Ho, Y.S., Removal of Cr(VI) from aqueous solutions using agricultural waste ‗maize bran. *J. of Hazardous Mate*. 152, 356 - 365(2008).
6. Oliveira, W.E., Franca, A.S., Oliveira, L.S. and Rocha, S.D., Untreated coffee husks as biosorbents for the removal of heavy metals from aqueous solutions. *J. of Hazardous Mate*. 152, 107- 108(2008).
7. Gao, H., Liu, Y., Zeng, G., Xu, W., Li, T. and Xia, W., Characterization of Cr(VI) removal from aqueous solutions by a surplus agricultural waste Rice straw.*J. of Hazardous Mate*. 150: 446-452**(2008)**.
8. Altundogan, H.S., Bahar, N., Mujde, B. and Tumen, F., The use of sulphuric acid - carbonization products of sugar beet pulp in Cr(VI) removal. *J. of Hazardous Mate*. 144, 255 - 264**(2007).**
9. Pagnanelli, F., Mainelli, S., Vegliò, F. and Toro, L., 2003. Heavy metal removal by olive pomace, Biosorbent characterisation and equilibrium modeling. Chemical Engineering Science, 58, 4709 - 4717**(2003).**
10. Maranon, E. and Sastre, H., Heavy metal removal in packed beds using apple wastes, Bioresources Techn. 38, 39 - 43**(1991**).
11. Ho, Y-S. and Ofomaja, A.E., Kinetic studies of copper ion adsorption on palm kernel fibre, *J. of Hazardous Mate*. B, 137: 1796-1802**(2006)**.
12. Zhu, C.S., Wang, L. P. and Chen, W.b., Removal of Cu(II) from aqueous solution by agricultural by-product: Peanut hull. J. of Hazardous Mate., 168, 739-746 **(2009).**
13. Demirbas, O., Karadag, A., Alkan, M. and Dogan, M., Removal of copper ions from queous solutions by hazelnut shell. J. of Hazardous Mate. 153,677- 684**(2008)**
14. Argun, M. E., Dursun, S., Ozdemir, C. and Karatas, M., Heavy metal adsorption by modified oak sawdust, Thermodynamics and kinetics. J. of Hazardous Mate.141,77 - 85**(2007).**
15. Fiol, N., Escudero, C. and Villaescusa, I., 2008. Chromium sorption and Cr(VI) reduction to Cr(III) by grape stalks and yohimbe bark. *Bioresources Techn*. 99, 5030-5036**(2008).**
16. Runping, H., Pan, H., Zhaohui, C., Zhenhui, Z. and Mingsheng, T., Kinetics and isotherms of Neutral Red adsorption on peanut husk. *J. of Env. Science*, 20, 1035-1041**(2008).**
17. Gardea Torresday, J.L.,Gonzalez, J.H.,Tiemann, K.J.,Rodriguez, O. and Gamez,G., Phytofilteration of hazardous cadmium, chromium, lead and zinc by biomass of Medicago sativa (alfalfa). *J. of Hazardous Mate*. 57 (1-3): 29-39**(1998).**
18. Cho, H., Dalyoung, O. Kwanh, k., A study on removal characteristics of heavy metals from aqueous solution by fly ash. J. of Hazardous Mate. B127,187-195**(2005).**
19. Horsfall, M., Abia, J.A and Spiff, A. I., Kinetic Studies on the adsorption of Cadmium, Copper and zinc ions from aqeous solution by cassava. (Manihot Sculenta Granz) tuber bark waste". J. Bioresource Techn. 97, 283 - 291**(2006).**
20. Naiya, T. K., Bhattacharya, A. K. and Das, S. K., Adsorptive removal of Cd(II) ions from aqueous solutions by rice husk ash. *Env. Progress in Chem. Eng*. 28, 535-546**(2009).**
21. Dermirbas, A., Adsorption of lead and cadmium ions in aqeous solutions modified lignin from Alkali glycerol delignication. J. Hazardous Mate. 109, 221-236**(2004).**
22. Okiemen, F.E., Maya, A.O. and Oriakhi, C.O.,Sorption of cadmium, lead, zinc Ions in Sulphur containing chemically modified Cellulosic Material Lust, *J. of Env. Anal. Chem.*32, 23-27**(1987).**
23. Lagergren, S., About the theory of so-called adsorption of soluble Substances Kungliga Svenska.Ventenskapsakademience.Handlingar 24,1-39**(1998).**
24. Ho.Y,S. and Mckay,G., Pseudo-second order model for sorption process. *J. of Process Biochem*. 34(5),451-465**(1999).**
25. Horsfall, M. and Abia, J.A., Sorption of cadmium (ll) and zinc (ll) ions from aqeous solution by cassava waste biomass (manihot Sculenta) Crainz Research. 37, 4913 - 4923**(2003).**

ISSN 214-453-2

INVESTIGATION INTO THE ADMIXTURE PROPERTIES OF BONE ASH: A FOCUS ON SETTING TIME OF ORDINARY PORTLAND CEMENT

M.O.A. MTALLIB AND D. TIJJANI
Department of Civil Engineering, Bayero University, Kano

ABSTRACT
This paper reports the findings of an investigation into the admixture potential of bone ash (BA) with a focus on the setting time of ordinary Portland cement (OPC). Cow bones are agricultural waste and constitute a sizeable proportion of solid waste in many cities of the world. Heaps of cow bones constitute aesthetic problem to the environment, unnecessary occupation of space and exude unpleasant odour that pollutes the environment. Cow bones need to be properly disposed to check the nuisance they constitute to the society. In the ever increasing endeavours to convert waste to wealth, investigation into the potentials of converting cow bones to beneficial applications in concrete becomes relevant. Bone vis-à-vis cow bone is mainly composed of compounds of calcium. The presence of calcium compounds in bone as well as in cement warrants effects of bone ash on cement to be envisaged. Cow bones were air-dried and incinerated to ash. The resulting ash was sieved through 75µm sieve. Based on weight of cement, 0%, 0.1%, 0.15%, 0.25%, 0.5, 1.0, 1.5%, 2.0%, and 2.5% of the ash were separately mixed with OPC to produce cement-bone ash (CBA). The required quantity of water determined from consistency test was added to the CBA mixture and mixed thoroughly to obtain CBA paste. The CBA paste was tested for setting time. Results show that BA decreases the setting time of OPC; the higher the content of BA, the faster is the reduction in the setting time of OPC. Reaction mechanisms are articulated and developed to explain reasons for the decrease in the setting time of OPC due to the addition of BA. It is concluded that BA is an accelerator; hence BA is recommended for use as an accelerator in concrete.

Keywords: *Admixture, Accelerator, Bone ash, Concrete, Economic disposal, Ordinary Portland cement, Properties, Safe disposal, Setting time, Solid waste.*

INTRODUCTION

Cement, aggregates, and water are the primary components of concrete. The properties of concrete both in the fresh and hardened states are largely dependent on the cement used. The commonest type of cement in use is the ordinary Portland cement (OPC). Sometimes, the properties desired of a given concrete in the fresh and/or hardened states are not achievable by using only the primary components of concrete. In such circumstances, admixture could be added to modify the properties of concrete in the fresh and/or hardened states. One of the properties of concrete that could be modified in the fresh state through the use of admixture is the setting time.

When water is added to cement, the process of setting of cement is initiated by chemical reaction of the cement and water. The chemical reaction that takes place between cement and water is referred to as hydration. Hydration of the cement results in the stiffening of the cement paste. The stiffening of the cement paste as it changes from fluid state to solid state is known as setting. The time it takes the cement paste to set is the setting time. Two types of setting times exist – the initial setting time and final setting time. The initial setting time is the period that elapses between when water is added to the cement and when stiffening of the cement paste becomes noticeable. The initial setting time of OPC should not be less than 45 minutes (BS EN 196-3: 2005+A1: 2008). The final setting time is the period that elapses between when water is added to the cement and when stiffening of the cement paste is completed. The final setting time of OPC should not be more than 10 hours (BS EN 196-3: 2005+A1: 2008). The setting of cement controls the setting of concrete. Therefore, the setting time of concrete can be modified through the modification of the setting time of cement by the addition of admixture.

Regular generation and dumping of solid wastes on authorized dumpsites, such as landfills, and on unauthorized dump places, such as roadsides, side drains, and undeveloped plots of land in residential areas lead to accumulation of solid waste in the environment. The resultant effects of the accumulated solid waste include unsightly surroundings, obstruction to pedestrians and traffic flow, air pollution, and ground water pollution due to leachates from the accumulated solid waste. Safe and economic disposal of solid waste in order to free the environment and the society of the menace constituted by accumulated solid waste have been issues of serious concern to individual countries and the entire world. Efforts have been made through researches to explore the possibilities of converting solid waste to advantageous applications in construction with a high level of success as a way of reducing solid waste accumulation in the environment. Numerous numbers of these researches (Tiamiyu, 1997; Al-Akhras and Samadi, 2004; Zain *et al*., 2004; Osinubi and Ijimdiya, 2005; Jimoh, 2006; Gbemisola, 2007), to cite but a few, have been undertaken to apply solid waste in soil and concrete to enhance their performances as construction materials. Specifically, the effects of solid waste on the hydration of OPC have also been investigated with beneficial results. Examples exist in

Hwang and Sheen (1991), de Rojas and Frias (1996), Hsiu-Liag *et al*. (2004), and Wang *et al*. (2004).

Generally speaking, bones are rigid organs that form part of the endoskeleton of vertebrates. They function to move, support and protect the various organs of the body, produce red and white blood cells and store minerals. While bone is essentially brittle, it does have significant degree of elasticity, contributed chiefly by collagen (Wikipedia). According to Encyclopedia Britannica (1981) and Wikipedia, the majority of bone is made of the bone matrix which has inorganic and organic parts.

The organic part of the bone matrix is mainly composed of type 1 collagen. Collagen is a fibrous protein. The organic part is also composed of various growth factors that include glycosaminoglycans, osleocalcin, bone sialo, protein, osteopontin and cell attachment factor (Wikipedia). Encyclopedia Britannica (1981) and Dunn Jr. (2009) present that the organic material makes up 30 to 35% of the bone. Of this amount collagen is about 95% (http://www.thepetcentre.com/xtra/bone.comp.html,2007; Dunn Jr., 2009). The other 5% of organic substances is composed of chondroithin sulphate, keratin sulphate and phospholipids. The collagen holds together calcium tetraoxophosphate (V) [$Ca_3(PO_4)_2$] and other calcium minerals in the bone (Encyclopedia Britannica, 1981).

The inorganic part amounts to 65 to 70% of the bone (Encyclopedia Britannica, 1981; Dunn Jr., 2009; Wikipedia). This inorganic part is composed of substances which are mainly of crystalline mineral salts and calcium present in a chemical arrangement called hydroxyapatite (HA) (Encyclopedia Britannica, 1981; Dunn Jr. 2009; Wikipedia). Hydroxyapatite (HA) is also known as osseous or phosphocalcic hydroxoapatite, is a complex compound of hydrated calcium tetraoxophosphate (V), chemically composed of 10 calcium atoms, 6 phosphorus atoms, 26 oxygen atoms, and 2 hydrogen atoms (Chai and Ben-Nissan, 1994; Garbuz *et al*., 1998; Azom, 2001; Dunn Jr., 2009; Teknimed, 2009; Wikipedia). The chemical formula of HA, according to Chai and Ben-Nissan (1994), Weng *et al*. (1994), Garbuz *et al*. (1998), Liao *et al*. (1999), Azom (2001), Dunn Jr. (2009), Teknimed (2009) is as given below.

$$Ca_{10}(PO_4)_6(OH)_2$$

The formula can also be written as $3Ca_3(PO_4)_2.Ca(OH)_2$

The formula indicates that 65 to 70% of bone is a mineral compound, HA, that is composed of nothing more than calcium, phosphorous, oxygen and hydrogen. However, Blincoe (1973) contends that in addition to calcium, other alkali earth elements are found in bone in small amounts. Pongkao *et al*. (1999) observed that HA is very close to our life as the main compound of bone and tooth minerals.

When cows are slaughtered for meat, the bones that remain after removing the flesh are usually stock-piled in heaps as waste in the vicinity of abattoirs. Some of the bones also find their ways into the environs of the abattoirs. Cow bones are agricultural waste and constitute a sizeable proportion of the accumulated solid waste in many cities. The heaps of cow bones constitute aesthetic problem to the environment and exude unpleasant odour that pollutes the environment. Therefore, cow bones need to be safely disposed to have a cleaner and healthier environment. In the ever increasing endeavours to convert waste to wealth, investigation into the potentials of converting cow bones to useful applications in concrete becomes apt. Cow bone is mainly composed of compounds of calcium; the presence of calcium compounds in bone as well as in cement warrants effects of bone ash on cement to be envisaged.

As noted earlier, hydrated calcium tetraoxophosphate (V), $Ca_{10}(PO_4)_6(OH)_2$, (i.e, HA), is the major composition of bone, accounting for 65-70% of the total composition of the bone. Similarly, calcium trioxocarbonate (IV), ($CaCO_3$), (i.e, calcium carbonate), is the primary raw material in the production of cement (Neville, 2003; Housecroft and Constable, 2006; Osei, 2007; Odesina, 2008). The produced cement is, therefore, basically composed of calcium compounds. The OPC consists of four main calcium compounds in the forms of dicalcium silicates (C_2S), tricalcium silicate (C_3S), tricalcium aluminate (C_3A), and tetra-calcium aluminoferite (C_4AF), (Cement and Concrete Association, CCA, 1979; Shirley 1980; Neville, 2003). It is, therefore, indicated that cement and bone have similar primary composition in calcium compounds. Literature search did not show any previous research on the use of BA as an admixture in concrete. This investigation, therefore is unveiling another area of interest in the continuous quest for safe and economically viable ways of getting rid of the solid waste in the environment, and finding local substitutes for ingredients in concrete.

On the basis of the similar compositional characteristics of cement and bone, it was reasoned in this study that the incineration of the cow bones to ash could produce elements and/or compounds in the resulting BA that could induce changes in the properties of cement. Consequently, the admixture potentials of BA, with a focus on the setting time of OPC, was investigated. If BA is found suitable as an admixture, another means of safely and economically disposing the cow bones would have been found. The incorporation of BA in concrete will not only assist in solving the cow bones disposal problem, but will also, as an admixture, help in improving on some of the properties of concrete. In addition, admixtures presently in use require a high level of technology to produce when compared to the simple incineration of the cow bones to produce the BA. Further more, admixtures are items of imports to many countries; this constitutes a drain on the foreign reserves of the importing countries. Cow bones are available in most countries as waste; the ash can

cheaply be produced by simple incineration; thus achieving economy in the acquisition of the BA. Suitability of BA as an admixture in concrete will not only contribute to environmental protection, it will also go a long way in reducing the consumption of energy in the production of admixtures, and will also help to conserve the foreign reserve of many countries by providing a local substitute for imported admixtures. Essentially, the conversion of solid waste to construction material, economy in the production of admixtures, and the protection of the environment are the main objectives of this study.

INVESTIGATION PROCEDURE

The materials used in this study include OPC, BA, and clean tap water. Cow bones were sourced from an abattoir. The bones were air-dried and incinerated to ash. The obtained ash was sieved through 75µm sieve. The ash passing the 75µm sieve was used in this study. Cement-bone ash (CBA) mixture was prepared by adding 0%, 0.10%, 0.15%, 0.20%, 0.25%, 0.5%, 1.0%, 1.5%, 2.0%, and 2.5% of BA by weight of cement to the OPC. The mixture was thoroughly mixed to achieve uniform distribution of OPC and BA in CBA. Consistency test was carried out in accordance with BS EN 196-3: 2005+A1: 2008 to determine the quantity of water required to produce a cement paste of normal consistency. The quantity of water determined from the consistency test was added to the CBA, and mixed thoroughly until a homogeneous mixture of CBA paste was obtained. Setting time test was carried out on the CBA paste in accordance with BS EN 196-3: 2005+A1: 2008

.

Presentation of Results

At standard weight of 400 g, the consistency of cement was obtained at water content of 30% by weight of cement as presented in Table 1.

Table 1: Results of the Consistency Test

Sample No.	Weight of water (g)	Water content (%)	Equivalent volume of water (ml)	Penetration of plunger from the bottom (mm)	Remark
1	400	20.0	80	4.0	Inconsistent
2	400	25.0	100	2.5	Inconsistent
3	400	30.0	120	6.0	Consistent
4	400	30.5	122	4.0	Inconsistent
5	400	30.25	121	4.0	Inconsistent

From the consistency test results, the water-cement ratio was calculated.

Weight of cement = 400 g
Water content = 30%
Water volume = 120 ml
Therefore, the water-cement ratio = 0.30

The results of the setting time test on the CBA paste are presented in Table 2.

Table 2: Results of Setting Time Test

BA content (%)	0	0.1	0.15	0.2	0.25	0.50	1.0	1.5	2.0	2.5
Initial setting time (mins)	71	69	67	63	60	57	55	50	48	46
Final setting time (mins)	151	149	149	147	138	120	115	105	101	92

DISCUSSION OF RESULTS

The results of the consistency test, Table 1, revealed that 30% (equivalent to 120 ml) of water by weight of cement is the quantity of water required to produce a standard cement paste of normal consistency of the OPC used. This represents 0.30 water/cement ratio.

As can be observed in Table 2 and Figure 1, the addition of BA to OPC decreases the setting time of OPC. As the content of BA in CBA increases, the decrease in the setting time of OPC increases. It can also be observed that the reduction in the setting time of OPC as the BA content increases is generally gradual for both initial and final setting times. That BA deceases the setting time of OPC indicates that BA is an accelerating admixture. The setting time for all the percentage contents of BA used in this research satisfy the required conditions for the setting time of OPC in accordance with BS EN 196-3: 2005+A1: 2008. It should be recalled that BS EN 196-3: 2005+A1: 2008 requires that the initial and final setting times of OPC should not be less than 45 minutes, and not greater than 10 hours, respectively. Since all the percentage contents of BA used in this research satisfy the required conditions for the setting time of OPC, it follows that any of the percentage contents used in this study can be deployed to accelerate the setting of OPC. The main condition that may guide the choice of a given percentage will be how rapid will be the required setting.

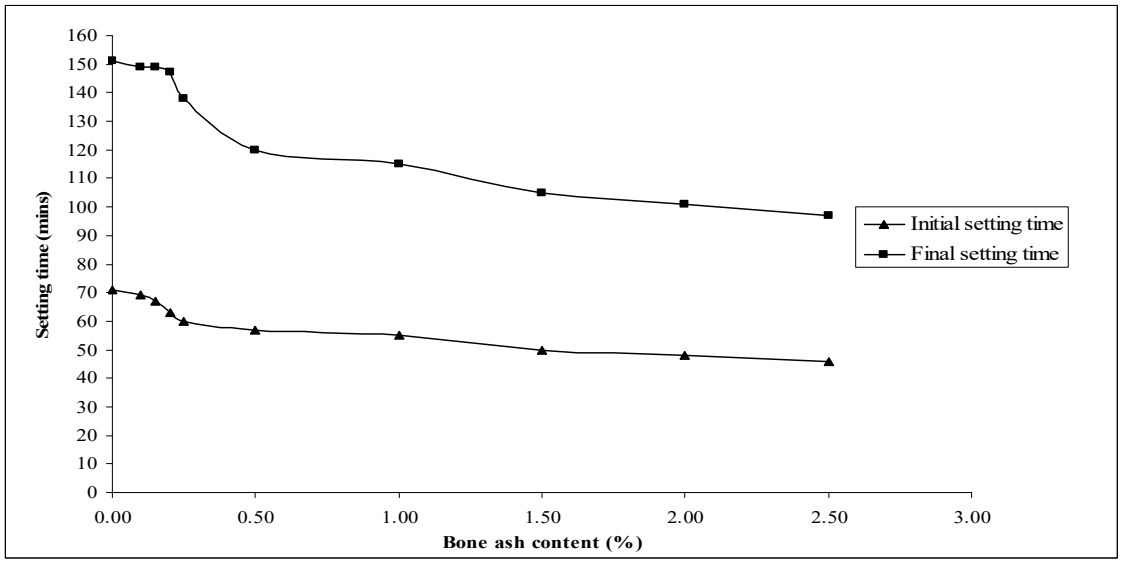

Figure 1: Setting Time Versus BA Content

Reaction Mechanisms

This study has identified BA as an accelerator**;** BA can, therefore, be used as admixture in concrete. To this extent, the main objectives of this study have been achieved. However, additional contribution is being made to articulate and develop reaction mechanisms to provide explanation for the accelerating effect of BA on the hydration of OPC.

Clearly, results have shown that BA has accelerating effect on the setting of OPC. However, the exact role BA plays in causing rapid hydration of OPC is not well understood. It is apt to mention at this juncture that the hydration of OPC itself is still not properly and completely understood. This statement is strongly backed by Bogue and Lerch (1934), and Neville (2003) who observed that the hydration of cement is not satisfactorily understood. In addition, Diamond (2004) states that the internal structures of hydrated cement pastes and concretes are poorly understood by most concrete engineers and technologists, and even by many researchers. Furthermore, Escalante-Garcia and Sharp (2004) remarked that the understanding of the chemistry of hydration of Portland cements remains an area of opportunity for many researchers. Probably because of these limitations, most literatures on accelerators and retarders stopped at the identification of a substance as an accelerator or as a retarder without providing adequate information on the intricacies of the reactions between the substance and the cement that resulted in the accelerating or retarding effect. In a sharp deviation from this trend, this study did not stop at only identifying that BA is an accelerator but has gone a step further to develop reaction mechanisms, from the much that is known about the setting of cement, to explain the likely reactions that would result in the increase in the hydration of the OPC with the addition of BA.

To start with, OPC is polymineralic. The polymineralic nature of OPC would influence the effect of BA on the rate of hydration of OPC. Different matrices of hydrated cement paste would result under different conditions and compositional characteristics. The reasons for the kind of matrix of hydrated cement paste under a given set of conditions and compositional characteristics are not sufficiently understood. This reflects Bougue and Lerch (1934) that posits that the products of hydration reaction may influence one another, or may themselves interact with other components in the system. The polymineralic nature of cement and the heterogeneous phase distribution of cement, coupled with compositional characteristics of cement and hydration conditions make the hydration process of cement difficult to be properly and completely understood. Since the hydration of cement is still far from being satisfactorily understood, and since complex reactions are involved among the cement compounds, and between the cement compounds and admixture during hydration, it will be difficult to realistically present stoichiometrically, the mechanisms being developed in this study to explain these complex reactions between the cement compounds and BA constituents that will lead to the accelerating effect of BA on the cement. Notwithstanding the foregoing limitations, attempt has been made in this paper to provide explanations of the plausible reasons for the increase in the rate of hydration of the cement due to the addition of BA.

The main active compounds of the cement are dicalcium silicate (C_2S), tricalcium silicate (C_3S), tricalcium aluminate (C_3A), and tetracalcium aluminoferrite (C_4AF). The quantities and reactivity of the four main compounds of cement have been presented (Taylor, 1985; Harisson *et al*., 1997; Stutzman, 2004; Kjellsen and Justnes, 2004). It should be made clear, however, that in addition to these main active compounds, minor oxides such as sodium oxide (Na_2O), potassium oxide (K_2O), manganese (III) oxide (Mn_2O_3), tin oxide (T_iO_2), and magnesium oxide (MgO) are also present in OPC. While the main OPC compounds play the dominant role in the hydration of OPC, the minor oxides are also important in the

hydration of OPC. Neville (2003) explains that K_2O and Na_2O are referred to as minor oxides because of the quantities present, but they play vital role in the hydration of cement. The setting of cement proceeds by selective hydration of the cement compounds. During the selective hydration of the cement compounds, the C_3S and C_2S dominate the process of hydration at the early stage. Between the C_3S and C_2S, the C_3S is more dominant in the early period of cement hydration.

It is posited in this study that during incineration of the bones to ash, decomposition of the complex hydrated calcium tetraoxophosphate (V), $Ca_{10}(PO_4)_6(OH)_2$, (i.e, HA), which is the main compound in bones, will take place to produce anhydrous calcium tetraoxophosphate (V) (apatite), calcium oxide (CaO), and a loss of the bound water in the compound. The proposed process in this study is represented in equation (1).

$$Ca_{10}(PO_4)_6(OH)_2 \xrightarrow{heat} 3Ca_3(PO_4)_2 + CaO + H_2O \quad \ldots\ldots\ldots\ldots \quad (1)$$

This study believes that the collagen which is an organic material mainly of fibrous protein will be burnt off during the ashing of bones. This belief is in line with Hortling *et al*. (1999) that observed that heated bones have no carbon. Therefore, the main constituents of BA are the complex compound of calcium tetraoxophosphate (V) and calcium oxide.

$$3Ca_3(PO_4)_2 + CaO$$

Studies that have been conducted on the decomposition of HA show that HA is thermally unstable (Chai and Ben-Nissan, 1994; Weng *et al*., 1994; Liao *et al*., 1999; Azom, 2001; Barralet *et al*., 2002). According to Azom, (2001) HA decomposes at temperature from 800-1200ºC depending on its stoichiometry. It begins to dehydroxylate at about 800ºC to form oxyhydroxyapatite. This process is gradual and takes place over a range of temperatures. When bone is thermally decomposed, the resulting ash consist mainly of complex products on which, so far, there is no consensus opinion. As presented in Chai and Ben-Nissan (1994), two mechanisms have been proposed for the decomposition of HA as follows equations 2 & 3:

$$Ca_{10}(PO_4)_6(OH)_2 \xrightarrow{heat} 2\beta\text{–}Ca_3(PO_4)_2 + Ca_4P_2O_9 + H_2O \quad \text{----------(2)}$$

$$Ca_{10}(PO_4)_6(OH)_2 \xrightarrow{heat} 3\beta\text{–}Ca_3(PO_4)_2 + CaO + H_2O \quad \text{----------(3)}$$

It can be seen that in (2), the products of thermal decomposition of HA are 2-β apatite, CaO, and water; while in (3), the products of thermal decomposition of HA are 3-β apatite, CaO, and water. In both equations, the water component is lost during thermal decomposition; this agrees with the position of this study. Of equations (2) and (3), equation (3) (except for the inclusion of 3β) is in consonance with the proposed decomposition mechanism presented in equation (1) in this study. Therefore, the proposed equation (1) in this study for the thermal decomposition of bones is accepted and adopted for the explanation of how BA accelerates the setting of OPC.

When water is added to the mixture of OPC and BA, a reaction process that causes a shift in the normal hydration of OPC is set up. Faster rate of hydration is induced in OPC by the BA. That the reaction of the OPC and BA in the presence of water results in the reduction of the setting time of OPC suggests, in the opinion of this study, that reaction products with decrease in C_2S content and an increase in the C_3S content which favours the fast setting of OPC are encountered. With the reduction in the C_2S and an increase in the C_3S, the hydration of CBA paste will proceed faster than that of OPC paste alone. Hence BA accelerates the setting time of OPC. In addition, this paper posits that during the hydration of the CBA paste, the apatite activity is negligible, while the CaO remains the main active compound in the BA. The CaO of BA reacts with the major components of the cement resulting in reaction products that favours the acceleration of the hydration of OPC. The proposed reaction equations in this paper of the CaO of BA with the main compounds of OPC in the presence of water are as presented in equations (4) to (7).

$$2Ca_2SiO_4 + CaO + 5H_2O \rightarrow 2CaO.SiO_2.H_2O + 3Ca(OH)_2 \ldots\ldots\ldots\ldots(4)$$

$$3Ca_3SiO_5 + CaO + 10H_2O \rightarrow 3CaO.SiO_2.H_2O + 7Ca(OH)_2 \ldots\ldots(5)$$

$$3Ca_3Al_2O_6 + CaO + 10H_2O \rightarrow 3CaO.Al_2O_3.H_2O + 7Ca(OH)_2 \ldots\ldots\ldots..(6)$$

$$4Ca_4Al_2Fe_2O_{10} + CaO + 17H_2O \rightarrow 4CaO.Al_2O_3.Fe_2O_3.H_2O + 13Ca(OH)_2 \ldots.(7)$$

Equations (4) to (7) show the typical products of the hydration of OPC which are composed of the respective hydrates of dicalcium silicates, (4); tricalcium silicates, (5); tricalcium aluminate, (6); tetracalcium aluminoferrite, (7). The product in common to the four equations is calcium hydroxide $Ca(OH)_2$. The typical products of hydration of cements which are calcium silicate hydrates (C-S-H) and calcium hydroxide (CH), as clearly presented in equations (4) to (7), have been described as the dominant products of hydration (Neville, 2003; Escalante-Garcia and Sharp, 2004; Kjellsen and Justnes, 2004; Scrivener, 2004).

At the early stage of hydration, the C-S-H and CH are produced mainly by the selective hydration of C_3S and

C_2S. Between the C_3S and C_2S, the C_3S reacts first and dominates the reaction within the first few days of hydration (Neville, 2003; Scrivener, 2004). Kjellsen and Justnes (2004) described C_3S as the most important phase of cement hydration. The C-S-H gel resulting from these reactions is reported to be principally responsible for the mechanical properties of hydrated cement (Escalante-Garcia and Sharp, 2004; Scrivener, 2004). Therefore, this paper considers that the formation of the C-S-H and CH, and their chemical behaviours during the hydration process are also very vital in the explanation of how the accelerating effect is produced in OPC by BA.

It should be noted that complete hydration of the cement grains is not instantaneous; it takes place over a long period of time and is dependent on some factors. Information on the gradual process of hydration of cement are presented in Harrison *et al*. (1997), Diamond (2001), Diamond (2004), Escalante-Garcia and Sharp (2004), Kjellsen and Justnes (2004), Scrivener (2004), and Stutzman (2004). As soon as the C-S-H and CH start forming, further hydration will be influenced by the micro-structural characteristics of the formed C-S-H and CH. The deposition of the C-S-H and CH phases in the microstructure of the hydrated cement is quite distinct; C-S-H is deposited mainly around the cement grains, while CH is precipitated in the water filled pores. The C-S-H and CH solids resulting from hydration will bridge the spaces between the cement grains. When the C-S-H and CH solids bridge the spaces between the cement grains, the hydration process is affected. When higher quantities of C-S-H and CH are present in the cement paste, there will be faster consumption of the C_3S at the early stage of hydration with the result that no substantial solids will be available to bridge the spaces between the cement grains. Therefore, the surfaces of the cement grains will constantly be exposed for hydration. This will result in a rapid hydration process; consequently, a decrease in setting time will be observed.

From the foregoing explanations, the implication of equations (4) to (7), developed in this paper for the reaction mechanisms, is that, although the typical hydration products of OPC (i.e., C-S-H and CH) can be formed with or without the CaO of BA since CaO is inherent in cement, but with the addition of the CaO from BA, there will be higher quantity of CaO in the CBA paste than that of OPC paste alone. Therefore the high quantity of CaO in CBA paste provides additional C-S-H and CH for the rapid consumption of C_3S in OPC which resulted in the acceleration of hydration of OPC. Hence the setting time of OPC is decreased when mixed with BA.

CONCLUSIONS

From the results of this study, the following conclusions are drawn.

(i) Bone ash is an accelerator.

(ii) The higher the content of BA, the greater the accelerating effect.

(iii) For all the percentages of BA contents used in this study, the requirements of BS EN 196-3: 2005+A1: 2008 are satisfied for both the initial and final setting times of OPC.

REFERENCES

Al-Akhras, N.M., and Smadi, M.M (2004). Properties of tire ash mortar. Cement and Concrete Composites, Elsevier Ltd., Vol. 28, Issue 7. Pp. 821-26.

Azom (2001). Hydroxyaptite-properties and applications. http://www.azom.com/details.asp?ArticleID=107 (Accessed 13/12/2016)

Barralet, J., Knowles J.C., Best S., and Bonfield W (2002). Thermal decomposition of synthesized carbonate hydroxyapatite. Journal of Material Science in Medicine, Vol. 13, No. 6. Pp. 529-533.

http://www.biomedexperts.com/Abstracts.bone/15348582/thermal_decomposition_of_sythesised_carbonate_hydrooapatite (Accessed 15/01/2017)

Bogue, R.H and Lerch, W (1934). Hydration of Portland cement. Industrial and Engineering Chemistry. Easter Pa. 26, No, 8. Pp 837-847.

BS EN 196-3:2005+A1:2008: Methods of testing cement. Determination of setting times and soundn**ess** European Standard, European Committee for Standardization, Brussels, Belgium

Blincoe, C. Lesperance, A.L and Bohman V.R (1973). Bone magnesium, calcium and strotium concentrations in range cattle. Journal of Animal Science. American Society of Animal Science, Vol. 36, No. 15. Pp. 971-975. http://jas.fass.org/cgi/reprint/36/5/971.pdf (Accessed 19/12/2016)

CCA (1979). Concrete practice. Cement and Concrete Association. Wexham Springs, Slough SL3 6PL.

Chai, C and Ben-Nissan, B (1994). Hydroxyapatite – Thermal stability of synthetic hydroxyapatites International Ceramic monographs, Vol.1 No.1. Pp 79-85.

http://www.azom.com/details.asp? ArticleID=1462. (Accessed 19/01/2017)

de Rojas, M.I.S and Frias, M (1996). The pozzolanic activity of different materials, its influence on the hydration heat in motars. Cem. Concr. Res. 26: Pp. 203-213.

Diamond S (2001). Calcium hydroxide in cement paste and concrete - a microstructural appraisal. In: Skalny, J, Gabauer, J, and Odler, I (editors). Materials Science of Concrete. Special Volume: Calcium Hydroxide in Concrete. Westerville. The American Ceramic Society. Pp. 37-58.

Diamond S (2004). The microstructure of cement paste and concrete – a visual primer. Cement and Concrete Composites, Elsevier Ltd., Vol. 26, Issue 8. Pp. 919-933.

Dunn Jr. T.J. (2009). The Nutritional Aspects of Bone Composition. The Petcenter . http://www.thepetcenter.com/home.aspx (Accessed 15/12/2016)

Encyclopedia Britanica (1981). 15th edition. William Benton, London.

Escalante-Garcia J.I and Sharp J.H (2004). The chemical composition and microstructure of hydration products in blended cements. Cement and Concrete Composites. Elsevier Ltd., Vol. 26, Issue 8. Pp. 967-976.

Garbuz, V.V. Dubok, V.A. Kravchenko, L.F. Kurochkin, V.D. Ul'yanchich N.V and Kornilova V.I (1998). Analysis of the chemical composition of a bioceramic based on hydroxoapatite and tricalcium phosphate. Materials Science Institute, Ukraine Academy of Science, Kiev No. 3-4 (400). Pp 74-76.

http://www.springerlink.com/index/23607R107m5m6.pdf (Accessed 17/12/2016)

Gbemisola M. B (2007). Effects of lime-rice husk ash on the engineering properties of lateritic soils. M. Eng Thesis, Department of Civil Engineering, Bayero University, Kano. 87pp.

Harrisson, A.M. Taylor, H.F.W and Winter, N.B (1997). Electron optical analyses of the phases in a Portland cement clicker with some observations on the calculation of quantitative phase composition. Cem. Concr. Res. 15:775.

Hortling, A. Mannonen, R and Rasanen, J (1999). Bone China of Lapland in Finland. Proceedings No. 60, Vol. 2. European Ceramic Society, U.K. (Paper Presented at the 6th Conference and Exhibition of the European Ceramic Society, June 20-24. Brighton Conference Centre U.K. Pp. 1-3. http://www.ulah.fi/arkisto/elokuvat/hortling/bonechina.pdf

(Accessed 21/01/2017)

Housecroft, C.E and Constable, E.C (2006). Chemistry. 3rd edition. Pearson Education Limited, Edinburgh Gate, Harlow, Essex CM20 2JE, England. Pp. 568, 705.

Hsiu-Liang, C. Yun-Sheng, T and King-Ching, H (2004). Spent FCC catalyst as a pozzolanic material for high performance mortars. Cement and Concrete Ccomposites. Elsevier Ltd., Vol. 26, Issue 6. Pp. 657-664.

http://www.thepetcentre.com/xtra/bone.comp.html(2007). The Nutritional Aspects of Bone Composition. (Accessed 07/02/2017)

Hwang, C.L and Sheen, D.H (1991). The effect of blast-furnace slag and fly ash on the hydration of Portland cement. Cem. Concr. Res; 21. Pp. 410-425.

Jimoh A.A (2006). Investigation into the engineering properties of rice-husk ash stabilized lateritic soils. M. Eng Thesis, Department of Civil Engineering, Bayero University, Kano. 73Pp

Kjellsen, K.O and Justnes, H (2004). Revisiting the microstructure of hydrated tricalcium silicate – a comparison to Portland cement. Cement and Concrete Composites. Elsevier Ltd. Vol. 26. Issue 8. Pp. 947-956.

Liao, C. Lin, F. Chen, K and Sun, J (1999) Thermal decomposition and reconstitution of hydroxyapatite in air atmosphere. Biomaterials, Elsevier Science B.V. Vol. 20 Issue 19. Pp.1807-1813. http://www.linkinghub.elsevier.com/retrieve/pii/50142961299000769 (Accessed 07/02/2017)

Neville, A.M (2003). Properties of concrete. 4th Edition (Second India Reprint). Pearson Education, Delhi, India. Pp. 18-19, 37-53.

Odesina, I.A (2008). Essential chemistry for senior secondary schools, 2nd edition. Tonad Publishers Limited, Ikeja, Lagos.

Osei, Y.A (2007). New school chemistry for senior secondary schools. Revised edition. Africana First Publishers Limited, Onitsha, Nigeria.

Osinubi, K.J and Ijimdiya, T.A (2005). Economic utilization of an agro-industrial waste-Bagasse ash. Book of Proceedings, 4th Nigerian Materials Congress, NIMACON 2005, November 2005, Zaria. Pp 36-40.

Pongkao, D. Lorprayoon, C and Condradt R (1999). Dissolution/precipitation behaviour of hydroxyapatites prepared from cattle bone ash. Bioceramics volume 12, edited by H. Ohgushi, G.W. Hastings and T. Yoshikawa (proceedings of the 12th International Symposium on ceramics in medicine). Nara, Japan, October, 1999. World Science Publishing Co. Plc. Ltd.

http://www.203.158.6.22:8080sutir/bitstream/123456789/697/bib164.pdf (Accessed 21/12/2016)

Scrivener, K.L (2004). Backscattered electron imaging of cementitious microstructures: understanding and quantification. Cement and Concrete Composites. Elsevier Ltd. Vol. 26, Issue 8. Pp. 935-945.

Shirley, D.C (1980). Introduction to concrete. Cement and Concrete Association, Wexham Springs, Slough SL3 6PL.

Stutzman, P (2004). Scanning electron microscopy imaging of hydraulic cement microstructure. Cement and Concrete Composites. Elsevier, Ltd., Vol. 26, Issue 8. Pp. 957-966

Taylor, H.W.F (1985). Cement chemistry. 2nd edition. Thomas Telford. 459pp

Teknimed (2009). Hydroxoapatite.

http://www.teknimed.com/en/pagelibre000104a1.html. (Accessed 25/02/2017)

Tiamiyu, I. A (1997). Strength characteristics of cement-rice husk ash concrete. B. Eng Project, Department of Civil Engineering, Bayero University, Kano. 52pp

Wang, K.S. Lin, K.K. Lee, T.Y and Tzeng, B.Y (2004). The hydration characteristics when C_2S is present in MSW1 fly ash slag. Cement and Concrete Composites. Elsevier Ltd., Vol. 26, Issue 4. Pp. 323-330.

Weng, J. Liu, X. Zhang, X and Ji, X (1994). Thermal decomposition of hydroxyapatite structure induced by titanium and its dioxide. Journal of materials science and letters. Vol. 13. No. 3. Pp 156-161.

http://www.springerlink.com/content/rq4q5138853619r2/ (Accessed 25/02/2017)

Wikipedia- Bone. The free encyclopedia. http://en.wikipedia.org/wiki/Bone (Accessed 17/12/2016)

Zain, M.F.M. Islam, M.M. Radin, S.S and Yap, S.G (2004). Cement-based solidification for the safe disposal of blasted copper slag. Cement and Concrete Composites. Elsevier Ltd., Vol. 26, Issue 7. Pp. 845-851.

ISSN 214-453-2

PHOTO-DEGRADATION OF DIRECT YELLOW 96 IN UV/TIO_2 AND UV/H_2O_2 USING FACTORIAL DESIGN

A. C. OKEME[1], A. A. KOGO[2], N. YUSUF[3] AND A. GIWA[2]
[1]Entrepreneural Development Centre, Federal Polytechnic Idah, Kogi State
[2]Department of Polymer and Textile Science, Ahmadu Bello University, Zaria, Nigeria
[3]Department of Chemical and Petroleum Engineering, Bayero University, Kano, Kano State
[challyok@yahoo.com, 08037459185]

ABSTRACT
In this research, factorial design have been employed to study the influence of four important factors; pH, catalyst dosage, irradiation time and dye concentration in the treatment of C.I. Direct Yellow 96 dyestuff using UV/TiO_2 and UV/H_2O_2 photo-degradation processes. The results indicate that the adsorbent dosage and irradiation time exhibit a significant positive effect on the efficiency of decolourization, whereas the initial dye concentration and pH of dye solution show a significant negative effect in UV/TiO_2 for the dye. Under UV/TiO_2, maximum degradation of 73% was obtained at dye concentration of 5mg/l, pH 4, reaction time of 90min and catalyst dose of 2g/l. Under UV/H_2O_2 the irradiation time and initial dye concentration exhibit a significant positive effect on the efficiency of decolourization, whereas the pH of dye solution and adsorbent dosage show a significant negative effect for the dye. However, the UV/H_2O_2 gave a maximum degradation of 58% at dye concentration of 5mg/l, pH 4, reaction time of 90min and H_2O_2 catalyst dose of 25mM. Hence, both methods can be adopted as a preliminary treatment process for dye wastewaters.

Keywords: *Photo-degradation, dye, photoreactor, UV/TiO_2 and UV/H_2O_2*

INTRODUCTION

Coloured industrial effluent is the most obvious indicator of water pollution and the discharge of highly coloured synthetic dye effluents is aesthetically displeasing and cause considerable damage to the aquatic life. Over 700,000 tons of approximately 10,000 types of dyes and pigments are produced annually worldwide (Giwa *et al.,* 2012). From this amount, about 20% are discharged as industrial effluents during the textile dyeing and finishing processes without pre-treatment (Carneiro *et al.,* 2007).

Dyeing wastewater causes serious environmental problems due to its high colour, large amount of suspended solids (SS), and high chemical oxygen demand (COD) (Kim *et al.,* 2004). The impact of these dyes on the environment is a major concern because of the potentially carcinogenic properties of the chemicals (Parsons. 2004). Also, some dyes can undergo anaerobic decolouration to form potential carcinogens (Alam et al. 2010). Consequently, there is a considerable need to treat these coloured effluents before discharging them into various water bodies. The increase of public concern as well as tighter regulations has challenged the environmental research community to explore new lines in reducing environmental problems associated with such wastewater.

At present, the industrial methods for dye waste treatment include adsorption, precipitation, electrical remediation, oxidation, and biological degradation. But all these ways cost much money, and/or create secondary contamination. Currently, chemical methods such as advanced oxidation processes (AOPs) seem more promising. AOPs predominantly involve the generation of very powerful and non-selective oxidizing species, the hydroxyl radicals (OH) for the destruction of refractory and hazardous pollutants observed in industrial wastewaters, surface waters and ground waters. The photo catalytic method such as TiO_2 photo catalysis has been shown to be efficient for degradation and mineralization of various organic pollutants in water at room temperature and normal pressure. The method has potential to be used for treatment of industrial or domestic wastewater on a large scale (Alfano *et al.,* 2000) and also ultraviolent photolysis combined with hydrogen peroxide (UV/H_2O_2) is one of the most appropriate AOP technologies for removing toxic organics from water because it may occur in nature itself. This process involves the production of reactive and non-selective hydroxyl radicals (OH) and can initiate the decolourisation reactions by reacting with the dye molecules.

The objective of this study is to investigate the effect of UV/TiO_2 and UV/H_2O_2 in the treatment of C.I. Direct Yellow 96 textile dyestuff. The effects of the key operating variables, such as pH, catalyst dosage, irradiation time and dye concentration on photo degradation process. Interactions between these factors were also studied.

EXPERIMENTAL

Materials

The dye C.I. Direct Yellow 96 (DY96) was obtained from Sigma. Titanium dioxide (Degussa P25) and H_2O_2 (30% w/w) was utilized as a photo-catalyst. Distilled water was used to prepare experimental solutions. The pH of the solutions were adjusted using H_2SO_4 and NaOH. The chemical structure, physical and chemical properties of the Direct Yellow 96 dye according to manufacturer are shown in Figure 1 and Table 1.

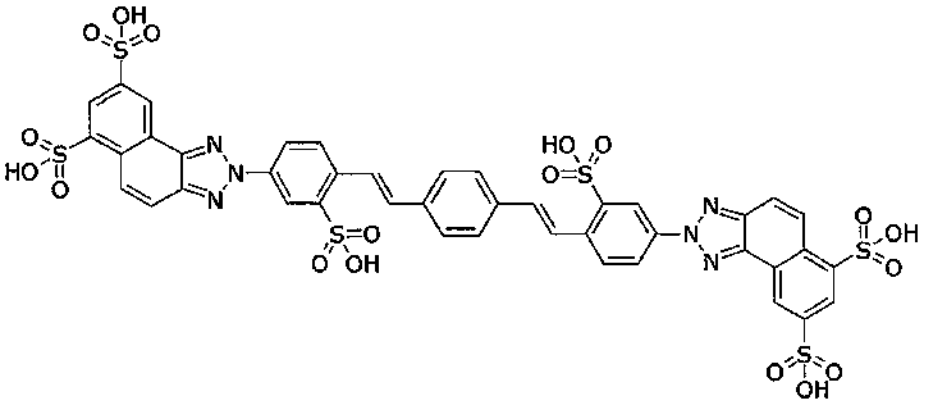

Fig. 1: C.I. Direct Yellow 96 (Diphenyl Brilliant Flavine)

Table 1: Chemical and Physical Properties of DY96

Properties	Values
Molecular Weight	1275.59 g/mol
Hydrogen Bond Donor Count	8
Hydrogen Bond Acceptor Count	23
Rotatable Bond Count	15
Exact Mass	1274.51 g/mol
Monoisotopic Mass	1274.51 g/mol
Topological Polar Surface Area	395 A^2
Heavy Atom Count	86
Formal Charge	4
Complexity	2030
Covalently-Bonded Unit Count	5

Photoreactor

The photocatalytic activities of the photocatalysts were performed in a 400 ml jacketed glass reactor fitted with a 9W 5" long Philips (PL-S 9W/10/2P Hg) bulb. The samples were centrifuged (6000 rpm, 10 min) and filtered through a millipore filter (0.45 μm) membrane and analyzed for the concentration of the C.I. Direct Yellow 96 in the solution using computer software attached to UV-Vis Spectrophotometer. Photocatalytic degradation processes were performed using a 200 ml solution containing a specified concentration of the selected dye. Samples were withdrawn from sample points and analyzed for degradation. Photo-degradation of dye solutions was checked and controlled by measuring the maximum absorbance of dyes by UV-Vis Spectrophotometer.

Design of Experiments

The experimental design consisted of four variables with two levels using MINITAB software (version 16). Because experiments from the degradation are time consuming, a half fraction design of 8 trials was used. Tables 2 and 3 display the Factors and their Uncoded Levels of low and high values of trials for the design of experiment (DOE).

Table 2: Factors and their Uncoded Levels for C.I. Direct Yellow 96 using UV/TiO_2.

Factor	Name	Low	High
A	Concentration (mg/l)	5	25
B	pH	4	8
C	Time (mins)	0	90
D	Dose (g/l)	0	2

Table 3; Factors and their Uncoded Levels for C.I. Direct Yellow 96 using UV/H_2O_2

Factor	Name	Low	High
A	Concentration (mg/l)	5	25
B	pH	4	8
C	Time (mins)	0	90
D	Dose (mM)	5	25

RESULTS AND DISCUSSION

To measure the percentage degradation which is a function of absorbance of the aqueous dye solution before and after exposure to the UV light, percentage colour disappearance was calculated using the following equation:

$$Decolorization\ (\%) = \frac{(Absorbance)_0 - (Absorbance)_t}{(Absorbance)_0}$$

where $(Absorbance)_0$ is the absorbance before irradiation and $(Absorbance)_t$ is the absorbance at time t. The results obtained are shown in Tables 4 and 5 for both UV/TiO_2 and UV/H_2O_2 processes.

Table 4: Design of Experiment for C.I. Direct Yellow 96 using UV/TiO_2

Run Order	Dye Conc. (mg/l)	pH	Time (mins)	Dose (g/l)	Initial Abs	Final Abs	Degradation (%)
1	5	4	90	2	0.74	0.20	72.97
2	5	4	0	0	0.70	0.70	0.00
3	5	8	90	0	0.20	0.20	0.00
4	25	8	0	0	0.38	0.38	0.00
5	25	4	90	0	0.40	0.40	0.00
6	5	8	0	2	0.75	0.75	0.00
7	25	8	90	2	0.40	0.26	35.00
8	25	4	0	2	0.28	0.28	0.00

Table 5: Design of Experiment for C.I. Direct Yellow 96 using UV/H_2O

Run Order	Dye Conc. (mg/l)	pH	Time (mins)	Dose (mM)	Initial Abs	Final Abs	Degradation (%)
1	5	8	90	5	0.32	0.30	6.25
2	25	8	0	5	0.48	0.48	0
3	25	4	0	25	0.46	0.46	0
4	25	4	90	5	0.48	0.20	58.33
5	5	4	0	5	0.32	0.32	0
6	25	8	90	25	0.46	0.32	30.43
7	5	4	90	25	0.42	0.20	52.38
8	5	8	0	25	0.32	0.32	0

The Normal Plot displays whether the effect of the factor is positive or negative on the response. The Normal Plots for the responses are shown as Figures 2 and 3. A positive effect means that as factors increases, degradation percentage increases. Whereas a negative effect indicates that as factor increases, the degradation in percent decreases.

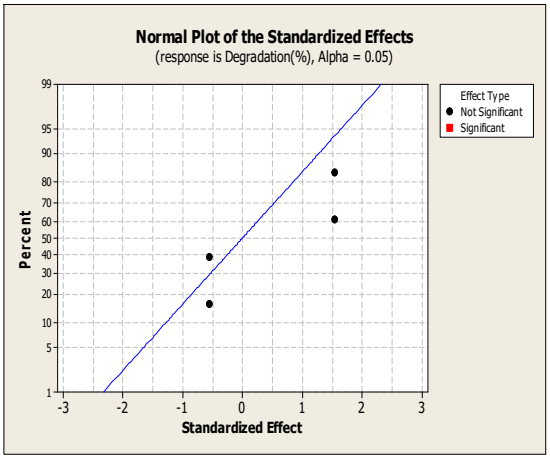

Fig 2: Normal Plot of DY96 degradation (%) under UV/TiO_2

The Normal Plot in Fig. 2 shows Time and Dose with a positive effect and pH and Concentration having a negative effect this implies that as Time and Dose increases, degradation percentage increases. Whereas a negative effect indicates that as pH and Concentration increases, the degradation in percent decreases.

The Normal Plot in Fig 3 shows Time and Concentration with a positive effect and Dose and pH having a negative effect.

A main effect is the difference in the mean response between two levels of a factor as shown in Figures 4 and 5.

The main effect plot fig 4 also shows that as concentration increases from 5mg/l-25mg/l there is decrease in degradation, pH in acidic region favours increase in degradation, the more the time of loading, the higher the degradation and increase of dosage from 0g/l-2g/l leads to increase in degradation.

The main effect plot Fig 5 also shows that as concentration increases from 5mg/l - 25mg/l there is increase in degradation, pH in acidic region favours increase in degradation, the more the time of loading, the higher the degradation and increase of dosage from 5mM - 25mM leads to decrease in degradation.

Figures 6 and 7 shows interaction plot of degradation for the direct dye. Each point in the interaction plot shows the mean degradation at different combinations of factor levels. If the lines are not parallel, the plot indicates that there is an interaction between the two factors

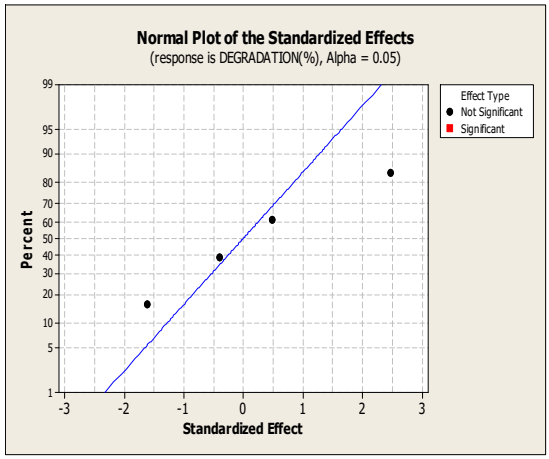

Fig. 3: Normal Plot of DY96 degradation (%) under UV/H_2O_2

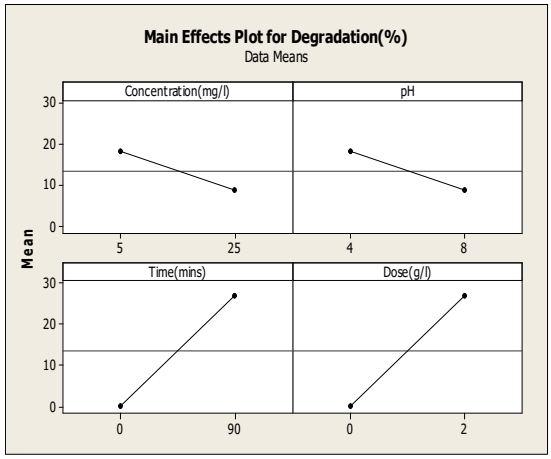

Fig 4: Main Effects Plot for Direct dye Degradation (%) (UV/TiO_2)

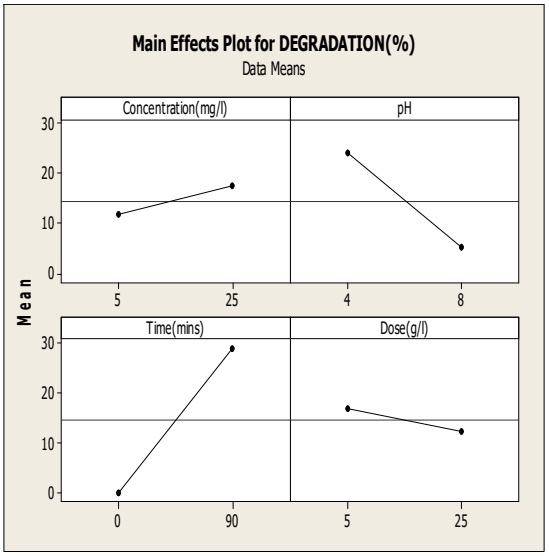

Fig. 5: Main Effects Plot for Direct dye Degradation (%) (UV/H_2O_2)

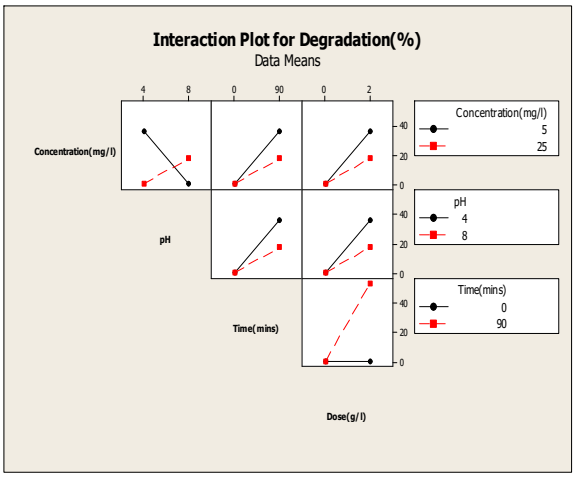

Fig. 6: Interaction Plot for Direct dye Degradation (UV/TiO_2)

For fig 6, at a concentration 5mg/l an increase of pH from 4 to 8 at 90mins with 2g/l TiO_2 leads to decrease in the adsorption efficiency by approximately 40%. At concentration of 25mg/l an increase of pH from 4 to 8 at 90mins with 2g/l TiO_2 leads to decrease in the adsorption efficiency by approximately 20%.

From above explanations it can be seen that pH plays a major role in degradation of the direct yellow 96 dye. Increase in pH from the low to high point decreases the adsorption efficiency by 37.97% similar trend was reported for a direct dye by Toor *et al.,* 2006. Adsorption rate increase, as expected with increase in TiO_2 dosage. Increase of catalyst dosage from 0-2g/l increases adsorption rate. This is due to the fact that increase in absorbent dosage increases area available for adsorption. At low initial concentration adsorption in all cases are favored. The effect of TiO_2 dosage was more noticeable at lower initial concentration. These results support the previous findings related to the effect of each factor on photocatalytic degradation. Similar results were found by Ray *et al.,* 2009.

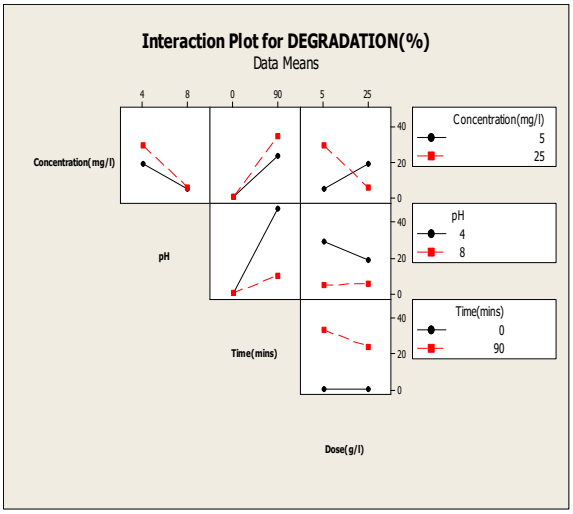

Fig. 7: Interaction Plot for Direct dye Degradation (UV/H_2O_2)

For Fig 7, which is an Interaction Plot shows that at a concentration of 5mg/l an increase of pH from 4 to 8 leads to decrease in the adsorption efficiency by approximately 5%, while an increase in time of exposure from 0-90mins increases the adsorption efficiency by approximately 40%. An increase in dosage from 5mM to 25mM H_2O_2 leads to reduction in the adsorption efficiency by approximately 20%. At 90mins time of exposure 5mM dose of H_2O_2 had an adsorption efficiency of 40% while 25mM dose of H_2O_2 had an adsorption efficiency of 20% at a concentration 25mg/l an increase of pH from 4 to 8 leads to decrease in the adsorption efficiency by approximately 10%.

For degradation of Direct Yellow 96 in this case, increase in pH from low to high point decreases the adsorption efficiency by 47.22%. According to some authors Critenden *et al.,* 1999 and Oppenlader *et al.,* 2003 the photochemical degradation rate of H_2O_2 is variable under certain pH conditions and this can affect the UV/H_2O_2 reaction to degrade different contaminants. Under alkaline conditions, hydrogen peroxide deprotonates with formation of the H_2O_2/HO_2^- equilibrium. The HO_2^- species reacts with a non-dissociated molecule of H_2O_2 according to reaction (1), which leads to dioxygen and water, instead of producing hydroxyl radicals under UV radiation. Therefore, the instantaneous concentration of 'OH is lower than expected.

$$H_2O_2 + HO_2^- \longrightarrow H_2O + OH^- + O_2 \ldots\ldots (1)$$

It was also verified that the efficiency of the processes increased at 5mM of hydrogen peroxide dosage where the remove rate were higher, after this point the efficiency decreased because of high presence of H_2O_2 in the reaction medium. When the hydrogen peroxide concentration becomes high, the excess hydrogen peroxide consumes hydroxyl radicals and it performed like hydroxyl radical scavengers. At high initial concentration adsorption in these cases was favored.

PREDICTION OF THE RESPONSE

Minitab software calculates the coefficients and constants for response equations. The response equations

can be used as models for predicting responses at different operating conditions (factors). The coefficients and constants for the dye are shown in Table 6 and 7.

Table 6: Estimated Coefficients for direct dye (UV/TiO_2) Degradation (%) using data in uncoded units

Term	Coef
Constant	7.8619
Concentration(mg/l)	-0.474625
pH	-2.37312
Time(mins)	0.299917
Dose(g/l)	13.4962

Table 7: Estimated Coefficients for direct dye (UV/H_2O_2) Degradation (%) using data in uncoded units

Term	Coef
Constant	27.6037
Concentration(mg/l)	0.285625
pH	-4.72687
Time(mins)	0.322306
Dose(mM)	-0.235125

In simple or multiple linear regression, the size of the coefficient for each independent variable gives the size of the effect that variable is having on dependent variable, and the sign on the coefficient (positive or negative) gives the direction of the effect. In regression with a single independent variable, the coefficient tells how much the dependent variable is expected to increase (if the coefficient is positive) or decrease (if the coefficient is negative) when that independent variable increases by one. In regression with multiple independent variables as this, the coefficient tells how much the dependent variable is expected to increase when that independent variable increases by one, holding all the other independent variables constant.

However, since this is a first order, linear model, the coefficients can be combined with the operating parameters to determine equations. The equations from this model are shown below:

Degradation (%) (UV/TiO_2) =7.862 - 0.475(Conc.) - 2.373(pH) + 0.300(Time) + 13.496(Dose)

Degradation (%) (UV/H_2O_2)=27.604 + 0.286(Conc.) - 4.727(pH) + 0.322(Time) - 0.235(Dose)

CONCLUSION

This study showed that factorial experimental design approach is an excellent tool and could successfully be used to develop empirical equation for the prediction and understanding the photocatalytic degradation efficiency of the Direct Yellow 96. The results obtained indicates that UV/TiO_2 treatment gave a maximum degradation of 73% at dye concentration of 5mg/l, pH 4, reaction time of 90min and catalyst dose of 2g/l, while UV/H_2O_2 treatment gave a maximum degradation of 58% at dye concentration of 5mg/l, pH 4, reaction time of 90min and H_2O_2 catalyst dose of 25mM. The results obtained shows that degradation rate can be influence by operational parameters such as pH, irradiation time, catalyst loading and dye concentration apart from the presence of electron acceptors and other additives. This process is an efficient and environmentally friendly technique for effluent treatment of industrial wastewater containing dye solution from textile industry since the dyes were mineralized into sampled and eco-friendly compounds of carbon (IV) oxide and water.

REFERENCE

Alam M.Z., Ahmad S., Malik A. and Ahmad M., (2010). "Mutagenicity and Genotoxicity of Tannery Effluents Used for Irrigation at Kanpur, India," *Ecotoxicology and Environmental Safety*, Vol. 73, No. 7, pp. 1620-1628.

Alfano OM, Bahnemann D, Cassano AE, Dillert R (2000) "Photocatalysis in water environments using artificial and solar light"Catalysis today,– Elsevier Volume 58, Issues 2–3, 12, pp 199–230

Patrıcia A. Carneiro, Maureen K. Sakagami, Maria and Valnice B, (2007) "Chemical characterization of a dye processing plant effluent—Identification of the mutagenic components," Mutation Research 626 pp135–142

Critenden J.C, Hu S, Hand D. W. and Green S. A. (1999). A kinetic model for UV/H_2O_2 process in a completely mixed batch reactor, water Res. 33 p1543-1548.

Giwa A., Nkeonye P. O., Bello K. A. and Kolawole E. G. (2012). Photo catalytic decolourisation and degradation of CI Basic blue 41 using TiO_2 Nanoparticles. Journal of Environmental Protection 3: p1063-1069.

Kim H, Hao O J, and Chiang PC (2004) – "Decolorization of wastewater" Critical reviews in environmental - Taylor & Francis Journal 30 p 123

Oppenlander T. (2003).Photochemical purification of water and air, advanced Oxidation processes (AOPs) principles, reaction mechanisms, reactor concepts, wiley-VCH verlag, weinheim, Germany, p 368

Parsons S. "Advanced Oxidation Processes for Water and Wastewater," IWA Publishing, London, 2004.

Ray S., Lalman J. A., and Biswas N. (2009). Using the Box-Benkhen technique to statistically model phenol photocatalytic degradation by titanium dioxide nanoparticles. *Chem. Eng. J.*, 150, 15–24.

Toor A.P., Verma A., Jotshi C.K., Bajpai, P.K. and Singh V. (2006). "Photocatalytic degradation of Direct Yellow 12 dye using UV/TiO 2 in a shallow pond slurry reactor" Dyes and pigments 68 (1), p 53-60.

ISSN 214-453-2

GOLD CYANIDATION AND CHARACTERIZATION OF ITAGUNMODI GOLD DEPOSIT USING CYANIDE FROM CASSAVA

[1,2*]O.D. OGUNDARE, [1]A.R. ADETUNJI AND [1]M. O. ADEOYE

[1]Department of Materials Science and Engineering, Obafemi Awolowo University Ile Ife Nigeria.
[2]Engineering Materials Development Institute Akure Nigeria.
[suppiedee@yahoo.com, aderade2004@yahoo.com, madeoye@oauife.edu.ng]

ABSTRACT

This work has investigated gold cyanidation and characterization of Itagunmodi gold deposit using cyanide from cassava. The gold ore was subjected to selective removal of associated minerals, treated to varied concentrations of cyanide extracted from cassava and precipitation of the gold. The precipitated gold was characterized using optical microscope, SEM - EDX, EDXRF and XRFS. The result showed that after 24 hours of cyanidation using analar grade sodium cyanide of 60 mg/l, 10 g Itagunmodi gold ore concentrate yielded 0.096 g (96 mg) gold. Also, under the same condition, using cassava based cyanide concentration of 60 mg/l, 10 g Itagunmodi gold ore concentrate yielded 0.08 g (80 mg) gold. This work has shown that sourcing cyanide from cassava waste for gold leaching is the appropriate alternative to the conventional cyanidation.

Keywords: *gold cyanidation, Itagunmodi, cassava based cyanide*

INTRODUCTION

The oxidation of gold is a prerequisite for its dissolution in alkaline cyanide solution. Although gold is inert to oxidation, it is widely accepted that, in the presence of a suitable complex agent such as cyanide, gold is oxidized and dissolved to form the stable complex ion [Au $(CN_2)^-$]. Oxygen is reduced and hydrogen peroxide is formed as an intermediate product in the first step and becomes the oxidizing agent in the second step, leading to the following chemical reactions which proceed in parallel (De Andrade Lima and Hodouin, 2005; Senanayake, 2005) equation 1 and 2. Cyanidation techniques used in the gold industry today include heap or valley fill leaching followed by carbon adsorption (carbon-in-column adsorption), agitation leaching followed by carbon-in-pulp (CIP), or agitated carbon-in-leach (CIL). *In situ* leaching of gold is being researched by the Bureau of Mines, but is not used commercially at this time. Cyanidation is best suited to fine-grain gold in disseminated deposits. Heap or valley fill leaching is generally used to beneficiate ores containing less than 0.04 oz/t. CIP and CIL techniques, commonly referred to as tank or vat methods, are generally used to beneficiate ores containing more than 0.04 oz/t. These gold beneficiation cut-off values are dependent on many factors, including the price of gold and an operation's ability to recover the precious metal (van Zyl et al. 1988).

MATERIALS AND METHODS

All chemical reagents used in this work were of analytical grade and all stock solutions were prepared using distilled water.

Experimental Approach

The samples were collected from 2 pits from Itagunmodi in Atakumosa West LGA of Osun State. The pits were dug to 7 feet deep and 6 feet in width. Shovel, head pan as well as sample bags were used in collecting the samples. The samples were a mixture of stones (granite), pebbles, clay and water. 500 kg of samples from the two pits were collected and brought into the laboratory for beneficiation. Each gold ore as obtained from the mining site was soaked in water for three (3) days in plastic container. The slurry was stirred daily to allow the lumps to break down and highly dense gold grain to settle to the bottom. The particles of ore mineral were separated from those of the gangue by simply hand picking the gangue and other physical impurities.

The gold ore, obtained from Itagunmodi gold ore deposit, was weighed and other physical impurities were removed. The procedure for selective removal of associated minerals was carried out by successive addition of concentrated hydrogen tetraoxosulphate (VI) acid (H_2SO_4), concentrated hydrogen chloride (HCl) and sodium hydroxide (NaOH). The gold ore samples were exposed to varied concentrations from 7.5 mg/l to 60 mg/l of cyanide (CN^-) at intervals of 7.5 mg/l CN^- from cyanide solution obtained from cassava and sodium cyanide (NaCN) analar grade respectively. Acid washing was carried out on the aurocyanide solution in order to precipitate the gold by addition of concentrated H_2SO_4. Also, HCl was added to remove the co-precipitated iron. The precipitate was thereafter dried at 850°C. A second stage of acid washing was carried out by adding concentrated hydrogen trioxonitrate (V) acid (HNO_3) in order to remove any remaining gangue in the gold precipitate.

The chemical equation for the process is represented as follows (equation 1 – 4).

$$2Au_{(s)} + 4CN^-_{(aq)} + O_{2(g)} + 2H_2O_{(aq)} \longrightarrow 2Au(CN)^-_{2\,(aq)} + H_2O_{2(aq)} + 2OH^-_{(aq)} \quad (1)$$

$$2Au_{(s)} + 4CN^-_{(aq)} + H_2O_{2(aq)} \longrightarrow 2Au(CN)^-_{2\,(aq)} + 2OH^-_{(aq)} \quad (2)$$

The summation of the two partial reactions is presented in Eq. (3), as proposed by Elsner:

$$4Au_{(s)} + 8CN^-_{(aq)} + O_{2(g)} + 2H_2O_{(aq)} \longrightarrow 4Au(CN)^-_{2\,(aq)} + 4OH^-_{(aq)} \quad (3)$$

$$4NaAu(CN)_{2(aq)} + 4NaOH_{(aq)} \longrightarrow 4Au_{(s)} + 8NaCN_{(aq)} + 2H_2O_{(aq)} + O_{2(g)} \quad (4)$$

RESULT AND DISCUSSION

The results of gold cyanidation tests carried out to leach gold using various lixiviants and precipitants are depicted in Figure 1. It can be observed that as the concentration of the lixiviants increased, the gold yield obtained increased. It should be noted that further refining of the earlier gold yield obtained by acid leaching (H_2SO_4) has led to increased gold yield. This is because HNO_3 is a more powerful oxidizing agent than H_2SO_4. This result is part of the work published by Ogundare *et al.,* (2014).

The reaction mechanism governing the gold cyanidation process can be summarized as follows (equation 5 and 6).

After 24 hours of cyanidation using analar grade sodium cyanide of 60 mg/l, 10 g Itagunmodi gold ore concentrate yielded 0.096 g (96 mg). Also, under the same condition, using cassava based cyanide concentration of 60 mg/l, 10 g Itagunmodi gold ore concentrate yielded 0.08 g (80 mg). It is of interest to note that cyanidation is more effective in gold recovery than amalgamation process.

This work has been able to prove that sourcing cyanide from cassava waste for gold leaching is the appropriate approach. Although Mitchell *et al.* (1997) claims that both cyanidation and amalgamation processes have the same environmental impact, it may be that the authors have not taken into consideration the biodegradability of spent cyanide which makes it pose lesser environmental impact.

The percentage yield of gold from Itagunmodi gold ore, Ilesa- Nigeria and those from the other countries are as presented in Table1:

$$2Au_{(s)} + 4CN^-_{(aq)} + H_2O + {}^1/_2O_{2\,(g)} \longrightarrow 2[Au(CN)_2^-]_{(aq)} + 2OH^-_{(aq)} \quad (5)$$

$$2\,[Au(CN)_2^-]_{(aq)} + 2OH^-_{(aq)} + H_2SO_{4(aq)} \longrightarrow 2Au_{(s)} + SO^-_4 + 4HCN_{(l)} \quad (6)$$

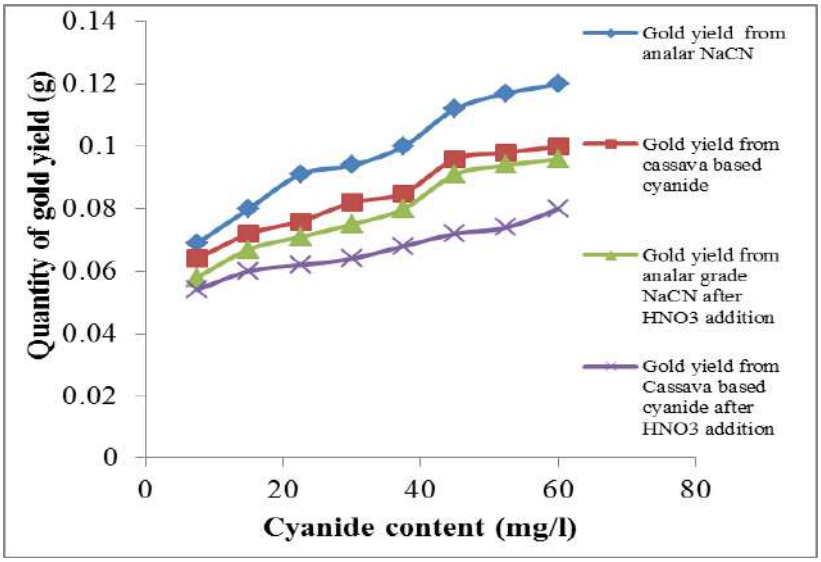

Figure 1: Effect of cyanide content on the quantity of gold yield through analar grade NaCN and cyanide solution from cassava.

These results have shown that the Itagunmodi (Nigeria) gold ore deposit is richer in native gold than those of Ijero Ekiti (Nigeria), Igun (Nigeria), Australia and Saudi Arabia deposits. According to Lewis and Martin (1983); and Robinson (1983), Australia and Saudi Arabia deposits contain mainly gold in the form of gold sulphide. The sulphide ore did not allow the direct attack of the gold particles by the cyanide solution in the ore because gold particles were locked in the sulphides. Extraction of gold from Igun deposit did not pass through acid leaching after cyanidation to unlock the residual gold particles. Baba *et al.* (2011) have reported a study on the dissolution kinetics and solvent extraction of total gold from Ijero-Ekiti (Nigeria) gold ore deposit by hydrochloric acid leaching followed by extraction with Tributylphosphate (TBP) in kerosene. In this work, double acid washing procedure has been employed. On the gold yield, with 60 mg/l cyanide content of analar grade sodium cyanide, 0.96 % gold was recovered while with 60 mg/l cyanide content of cassava based cyanide, 0.8 % was recovered. In terms of gold recovery efficiency, the performance of analar grade sodium cyanide is greater than cassava based cyanide by a difference of 0.16%.

Comparing Plates 1 (a) and 2 (b), it can be observed that the gold leached through sodium cyanide analar grade and cyanide solution from cassava has a lot of similarities. It can be observed that the gold grains have curved edges with rough surfaces due to corrosive effects from the cyanidation procedures. Also, it can be observed that gold grains leached through sodium cyanide analar grade and cyanide solution from cassava as shown in Plates 1 (a) and 1 (b) have irregular shapes and without impurities. This attests to the fact that gold leached through sodium cyanide analar grade and cyanide solution from cassava have same quality.

Table 1: Comparison of the percentage yield of gold from Itagunmodi gold ore with other deposits

Country	Yield (mg/100 g of ore)	%Yield
Itagunmodi, Atakumosa LGA (Nigeria)	96/80	0.96/ 0.8
Ijero Ekiti (Nigeria) (Baba *et al.*, 2011)	85.28	0.85
Itagunmodi, Atakumosa LGA (Nigeria) (Adetunji, 1991)	27.2/16.48	0.27/0.16
Igun, Atakumosa LGA (Nigeria) (Mesubi *et al.*, 1991)	33.00	0.330
Papua, Australia (Robinson, 1983)	2.86	0.00286
Mahd Adh Dhahab Saudi Arabia (Lewis and Martin, 1983)	2.60	0.00260

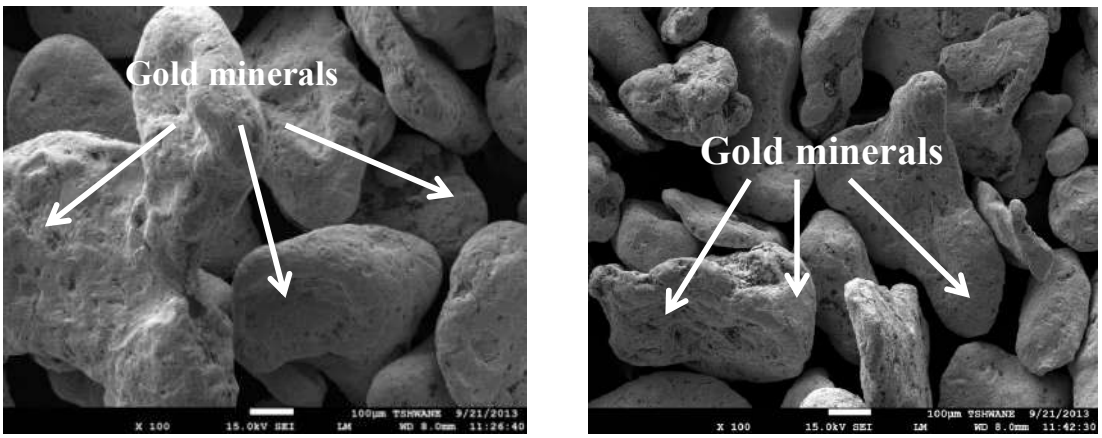

(a) (b)

Plate 1: SEM micrographs of the precipitated gold grains (a) through sodium cyanide, (b) through cyanide solution from cassava

The result of the attached EDX (Table 2) showed the composition of the ore and the presence of gold elements (6.4 wt. %). Other associated elements discovered are carbon, nitrogen, aluminium, copper, potassium, titanium and iron. These are in tandem with elements/ compounds found when XRFS was used for the same purpose as described in Table 3. However, the difference in the values obtained between the attached EDX and XRFS may be due to the variation in the distribution of the gold and its associated minerals at the point of sample testing. In order words, exactly the sample portion of the ore may not have been examined even when thoroughly mixed.

The chemical analysis (Table 3) showed that Itagunmodi gold ore and gold extract contain magnesium, aluminium, silicon, phosphorus, sulphur, potassium, calcium, titanium, vanadium, chromium, manganese, cobalt, iron, nickel, copper, zinc, arsenic, yittirium, lead, tungsten, gold, silver and rhobium. The presence of these associated minerals has been earlier reported by (Ariyibi *et al.,* (2011); Elueze, (1997); Mesubi *et al.,* (1999). One striking feature is that the high quantity of iron (Fe) discovered in the ore (23 %) may be as a result of the large composition of laterite sand in the ore during mining process. The high

quantity of iron was observed to have been drastically reduced after cyanidation process to 0.56 % and 0.89 % respectively in gold leached using 60 mg/l analar sodium cyanide and gold precipitated using 60 mg/l cyanide solution from cassava. Also, titanium oxide which was found in high quantity (31%) in the ore has been reduced after the cyanidation process to 0.3 % and 0.5 % respectively. However, it is surprising to observe a sudden increase in the amount of tungsten oxide from 6 % in the ore to about 102 % and 91% respectively.

Table 2: Energy Dispersive X-Ray (EDX) Analysis attached to Scanning Electron Microscope of the gold ore and precipitated gold

a. Itagunmodi Gold Ore

Element	Weight%	Atomic%
C K	15.39	28.53
O K	37.06	51.59
Al K	6.95	5.73
Si K	4.20	3.33
Ti K	5.74	2.67
Fe K	5.38	2.15
Cu L	6.32	2.22
Zr L	12.56	3.07
Au M	6.40	0.72
Totals	100.00	

b. Leached gold by analar NaCN

Element	Weight%	Atomic%
C K	5.55	30.03
N K	2.96	13.65
O K	5.75	23.35
Al K	0.86	2.08
Ti K	0.85	1.15
Fe K	0.84	0.97
Cu L	1.93	1.98
Au M	81.00	26.71
Po M	0.26	0.08
Totals	100.00	

c. Leached gold by CN^- from cassava

Element	Weight%	Atomic%
C K	9.65	43.80
N K	3.50	13.62
O K	5.57	18.93
Al K	0.39	0.79
Fe K	0.70	0.69
Au M	80.19	22.19
Totals	100.00	

Table 3: Energy dispersive-x ray fluorescence spectrometry (EDXRFS) of the precipitated gold

	Gold ore	Gold Extracted using 60 mg/l Sodium Cyanide Analar	Gold Extracted using 60 mg/l Cassava based cyanide
Element	Content (ppm)	Content (ppm)	Content (ppm)
Mg	0.0478	0.4507	0.3081
Al	0.6538	0.7153	0.5887
Si	2.1584	0.6043	0.5367
P	0.4485	2.2342	2.0426
S	0.3998	7.0327	6.1424
K	0.0000	0.0000	0.0000
Ca	0.2197	0.0593	0.0757
Ti	30.9081	0.2533	0.5112
V	0.2328	0.0079	0.0114
Cr	0.0000	0.0021	0.0011
Mn	0.7312	0.0099	0.0201
Co	0.0039	0.0030	0.0000
Fe	23.1568	0.5682	0.8987
Ni	0.0609	0.0412	0.0450
Cu	0.0661	0.0646	0.0875
Zn	0.1021	0.2687	0.2682
As	0.0000	0.0000	0.0000
Pb	0.0156	0.0000	0.0000
W	6.1191	102.4461	90.5610
Au	19.0095	208.6410	191.9714
Ag	0.0362	0.0186	0.0240
Rb	0.0091	0.2900	0.2619

CONCLUSION

1. After 24 hours of cyanidation and cyanide content of 60 mg/l on 10 g gold ore concentrate, the analar grade sodium cyanide yielded 0.096 g gold while the cassava based cyanide yielded 0.08 g gold.
2. The SEM revealed similar curved edges, irregular shapes, purity and quality for the precipitated gold from cyanide solution from cassava and sodium cyanide analar grade.

REFERENCES

1. Adetunji, A.R. (1991): "Use of Cyanide Solution from Cassava for the Extraction of Gold", M.Sc Thesis, Department of Materials Science and Engineering Obafemi Awolowo University Ile Ife Nigeria.
2. Ariyibi, E.A, Folami, S.L, Ako, B.D, Ajayi, T.R and Adelusi, A.O. (2011), "Application of the principal component analysis on geochemical data: A case study in the basement complex of Southern Ilesa area, Nigeria". Arab Journal of Geosciences. pp. 239 – 247.
3. Baba, A.A., Adekola, F.A., Ojutemieden, D.O. and Dada, F.K. (2011): "Solvent Extraction of Gold from Hydrochloric Acid-Leached Nigerian Gold Ore by Tributylphosphate" Chemical Bulletin of "Politechnica" University of Timisoara, Romania, Vol. 56 No 70, pp. 29 -37.
4. De Andrade Lima, L.R.P. and Hodouin, D. (2005): "A Lumped Kinetic Model for Gold Ore Cyanidation," Hydrometallurgy, Vol. 79, pp.121-137.
5. Elueze, A.A. (1997), "Geological and geochemical studies in the Ilesa schist belt in relation to gold mineralization", M.Phil. Thesis (Unpublished), Department of Geology and Mineral Sciences, University of Ibadan.
6. Mesubi, M.A., Adekola, F. A., Bello, A. A., Adekeye, J.I.D. And Bale, R.B. (1999), "Extraction of Gold from Igun Gold Ore Deposit in Atakumosa Local Government Area, Osun State, Nigeria". Nigeria Journal of Pure and Applied Science Vol. 14 pp. 935 -945.
7. Mitchell, C.J., Evans, E.J. and Styles, M.T. (1997): "A review of gold particle size and recovery methods", British Geological Survey Technical report. www.overseasgeologyseies/gold accessed 18th February 2011
8. Ogundare, D. O., Mosobalaje, O. A., Adelana, R. A., Olusegun, O. A. (2014): "Beneficiation and Characterization of Gold from Itagunmodi Gold Ore by Cyanidation". Journal of Minerals and Materials Characterization and Engineering, 2, 300-307.
9. Robinson, P.C. (1983), "Mineralogy and treatment of refractory gold from the Porgera deposit, Papau New Guinea", Australia Mineral Processing and Extractive Metallurgy, Institution of Mining and Metallurgy, Transactions, Section C, Vol. 92 No 6 pp. 87 - 91.
10. Senanayake, G. (2005): "Kinetics and Reaction Mechanism of Gold Cyanidation: Surface Reaction Model via Au(I)-OH-CN Complexes," Hydrometallurgy, Vol. 80,pp. 1-12.
11. Van Zyl, D.J.A., I.P.G. Hutchison, and J.E. Kiel (editors) (1988): "Introduction to Evaluation, Design and Operation of Precious Metal Heap Leaching Projects". Littleton, CO: Society for Mining, Metallurgy, and Exploration, Inc.

NIGERIAN JOURNAL OF MATERIALS SCIENCE AND ENGINEERING
NJMSE
ISSN 214-453-2

HEAVY METALS STATUS OF SOIL AROUND WASTE DUMPSITES IN UGHELLI METROPOLIS, DELTA STATE

C. K. OJEBAH[*], A. UWAGUE[**] AND O. G. EDEMA[***]

*,**Department of Science Laboratory Technology, Delta State Polytechnic, Ozoro, Delta State.
***Department of Science Laboratory Technology, Federal Polytechnic, Auchi, Edo State.
[ckojebah@gmail.com]

ABSTRACT

This study investigated the heavy metal status of soils around waste dumpsites in Ughell, metropolis, Delta State, Nigeria. Two different dumpsites were used for this study. For the metal analysis, soil samples were collected at 0-15cm depth. The soil samples were air dried for five days and sieved. 2.0g of the soil sample was digested with $HNO_3/HClO_4$ mixture and analysed for heavy metals (Fe, Pb, Cd, Zn, Cu and Mn) concentration using Atomic Absorption Spectrophotometer (AAS) Buck 200A model. The result obtained ranged from18.23-32.31mg/kg for Fe; 1.28-1.36mg/kg for Pb; 4.72-6.23mg/kg for Cd; 13.6-17.62mg/kg for Zn; 1.32-1.35mg/kg for Cu and 26.36-29.82mg/kg for Mn. The mean concentration of all the metals in the two sampling stations is in the order: Mn>Fe>Zn>Cd>Cu>Pb. The results when compared with the control site were quite higher indicating the metal enrichment of soil from the waste in the dumpsites. The results were within DPR target value except cadmium. The level of Cadmium in the present study calls for concern, considering the location of the sites and toxicity of cadmium. All hands must therefore be on deck to check the effect of these metals now and in the future in order to promote a healthy environment for sustainable development.

***Keywords**; heavy metals, dumpsites, soil, concentration, waste, samples*

INTRODUCTION

The ever increasing population coupled with the desire of most people for a higher material standard of living are resulting in worldwide pollution on a massive scale (Manahan, 2005). Municipal solid wastes normally termed as garbage or trash is an inevitable by-product of human urban settlements (Abah *et al.,* 2015). Large arable expanse of land have been transformed to dumpsites over time due to high population density and increasing urbanization rates and industrial processes which promote waste accumulation (Solomon *et al.,* 2015; Begum, *et al.,* 2009). Usually, these wastes are never screened or sorted out and consequently, heavy metals eventually find their way into the soil from metal scraps, agricultural and industrial wastes (Quek et al., 1998) deposited on the dumpsites, making it almost impossible for plants survival and healthy human habitation (Solomon *et al.,* 2015).

Heavy metals are chemical elements mostly with density greater than 4g/cm^3 found in all kinds of soils, rocks and fresh water ecosystem (Adelekan and Abegunde 2011). Heavy metals in high concentration are harmful to the environment because of their potential toxicity to biota and indirect threat to human health from groundwater contamination and accumulation in food crops (Martinez *et al.,* 2000). Most of the heavy metals are extremely toxic because of their solubility in water; they are known to accumulate in living organisms and even at low levels they can result in long term cumulative health effect (Njagi *et al.,* 2016). The concentrations of heavy metals are associated with biological and geochemical cycles and are influenced by anthropogenic activities such as agricultural practices, transport, industrial activities and waste disposal (Lund, 1990; Abollino *et al.,* 2002).

The levels of heavy metals in the environment have been seriously increased during the last decades due to human activities (Bin *et al.,* 2001). Some heavy metals are essential to maintain human metabolism. Heavy metals are very harmful because of their non biodegradable nature, long biological half lives and their potential to accumulate in different body parts (Manahan, 2005; Wilson and Pyatt 2007). Excessive accumulation of heavy metals in agricultural soils, through waste water irrigation results in soil contamination as well as food quality and safety (Muchuweti *et al.,* 2006). Heavy metals such as cadmium, lead, copper; zinc and nickel are carcinogenic or have toxic effects on humans and the environment (Trichopoulous, 2001; Tutkdogan *et al.,* 2002; Kocasoy and Sachim 2007). Anthropogenic releases can increase the concentrations of these metals relative to their normal background values making the heavy metals to be considered as serious pollutants because of their toxicity, persistence and nondegradable conditions in the environment, thereby constituting threat to humans and other forms of biological life (Tam and Wong, 2000; Nwuche and Ugoji, 2008; Aina et al., 2009; Mohiuddin *et al.,* 2010; Adelekan and Abegunde 2011).

This present study was embarked upon to determine the concentration of heavy metals in soils around some waste dumpsites in Ughelli metropolis and ascertain the extent to which the soil is contaminated by the heavy metals investigated.

MATERIALS AND METHODS

Study Area

Ughelli is the administrative headquarters of Ughelli North local government area of Delta State. Ughelli is situated at latitude 5.49°N and longitude 6.01°E and lies

at an altitude of 27 meters above the sea level. Ughelli is an oil rich town accommodating many oil companies. It is one of the commercial towns in Delta State. Indiscriminate dumping activities have led to the pollution of the soil.

Sample Collection and Preparation

Soil samples around dumpsites located in two different locations; Oteri road and Patani road within Ughelli metropolis were collected at 0 – 15cm depth using a stainless steel soil augur. A third sample was collected from another location that was not a dumpsite to serve as a control. Samples were collected in clean polythene bags and taken to the laboratory for analysis. The samples were air dried in the laboratory for four days at room temperature and large objects (sticks, stones plastics, etc) removed (Asiagwu et al., 2007). The dried samples were crushed into fine powder using agate mortar and pestle and thereafter sieved through a 100 mesh screen to obtain a homogenous particle size ($\leq 150\mu m$). The soil particles that penetrated the screen were used for the experimental work.

METHODS

Digestion

2 grams of each soil sample was measured and put in a separate beaker. 10ml of nitric/perchloric acid 2:1 was added to the sample. The samples were digested at 105˚C for 1 hour. Next HCl and distilled water 1:1 ratio was added to the digested sample and transferred to the digester again and the mixture were heated for 30minutes. The digestate was removed from the digester and allowed to cool to room temperature. The digests were filtered into 50ml standard flask using Whatman No 1 filter paper and made up to the mark after quantitatively transferring reinsates with distilled water. The filtrates were transferred into clean dry plastic containers for storage prior to AAS analysis.

Metal Analysis

Determination of heavy metals was done using Atomic Absorption Spectrophotometer (Buck 200A model).

RESULTS

The results of the heavy metal analysis are presented in table 1 and figure 1. The results of the vertical distribution of heavy metals determined in soil (in mg/kg) around waste dumpsites in Ughelli showed high concentration of the metals in Patani road than Oteri road. The mean concentration of all the metals in the sampling stations follows in the order: Mn>Fe>Zn>Cd>Cu>Pb (Table 1). Iron result ranged from 18.23/kg – 32.31mg/kg with a mean concentration of 25.25mg/kg as shown in table 1. The iron result was lower than 10.71mg/kg recorded for the control. The concentration of iron was comparable with those obtained from soils in Kaduna metropolis which were in the range of 19.56 - 25.47 mg/kg of dry soil (Ajibola and Ozigis, 2005) (Table 2). Iron result varied significantly with the range of 22.01– 525.50 mg/kg obtained by Njagi et al (2016) for Kadhodeki dumpsite in Kenya and 185.57 - 213.97mg/kg reported for Akure metropolis by Anietie and Labunmi, (2015) (Table 2). Iron result was lower than the 1000mg/kg permissible limit by USEPA (1986) for soil as shown in table 3.

Lead result ranged from 1.28 – 1.36mg/kg with an average value of 1.32mg/kg. The result obtained was greater than the 0.06mg/kg recorded for the control. Lead result in this study was lower than the range of 19.79 – 60.22mg/kg obtained by Njagi *et al.,* (2016) for Kadhodeki dumpsite in Kenya. However the result was within the range of 0.101-2.003mg/kg reported by Odhiambo *et al.*, (2015) for Narok Kenya and 0.24 - 2.15mg/kg reported by Amadi and Nwankwoala, 2013 for Aba (Table 2). Lead result in this study was lower than the 85mg/kg target value by DPR (2002) (Table 3).

The concentrations of cadmium ranged from 4.72 – 6.23mg/kg with a mean value of 5.48mg/kg. The result was higher than the 0.35mg/kg obtained for the control as shown in table 1. Cadmium result obtained was higher than the range of 0.105 - 1.005mg/kg obtained by Odhiambo *et al.*, (2015) and 0.18 - 2.60mg/kg by Amadi and Nwankwoala, 2013 for Narok Kenya and Aba respectively. However the result was lower than the range of 28.56 - 40.17mg/kg obtained by Anietie and Labunmi, (2015) for Akure metropolis Table 2. The result obtained in this present study was quite higher than the target value of 0.80mg/kg set by DPR (2002). Cadmium gets accumulated in the intestine, liver and kidney when ingested by humans and chronic exposure may lead to proximal tubular disease and osteomalacia (Pascual *et al.,* 2004).The level of cadmium obtained in this study calls for concern considering the toxicity of cadmium.

Zinc concentration ranged from 13.16 – 17.62mg/kg with a mean value of 15.39mg/kg. Zinc result obtained was higher than 4.35mg/kg in the control. Zinc concentration was above the range of 0.728 - 4.654mg/kg reported by Odhiambo *et al.,* (2015) and 2.40 - 28.50mg/kg by Amadi and Nwankwoala, (2013) for Narok Kenya and Aba respectively. Similarly result obtained was very much below the range of 128.11 – 289.27mg/kg reported by Njagi et al., (2016) for Kadhodeki dumpsite in Kenya and 86.29 - 95.28mg/kg by Anietie and Labunmi, 2015 for Akure metropolis (Table 2). Zinc result was below the 146mg/kg target value permitted by DPR, (2002) for soil and sediments (Table 3).

Table 1 Distribution of metals (mg/kg) of soil around waste dumpsite in Ughelli metropolis

Sample location	Metal concentration (mg/kg)					
	Fe	Pb	Cd	Zn	Cu	Mn
Oteri road dumpsite soil	18.23	1.28	4.72	17.62	1.32	29.82
Patani road dumpsite soil	32.31	1.36	6.23	13.16	1.35	26.36
Mean	25.27	1.32	5.48	15.39	1.34	28.09
Control site soil	10.71	0.06	0.35	4.35	0.38	4.28

Table .2 Comparison of the Range of Heavy Metals (mg/kg) of Dumpsite Soils in Present Study with that of Other Researchers

Metal	Concentration (mg/kg)	
	Present study	**Previous studies**
Fe	18.23 - 32.31	22.01 - 525.50[a]
		185.57 - 213.97[b]
		19.56 - 25.47[c]
Pb	1.28 - 1.36	40.66 - 56.16[b]
		0.101 - 2.003[d]
		0.24 - 2.15[e]
Cd	4.72-6.23	28.56 - 40.17[b]
		0.105 - 1.005[d]
		0.18 - 2.60[e]
Zn	13.16-17.16	40 - 336[a]
		86.29 - 95.28[b]
		0.728 - 4.654[d]
		2.40 - 28.50[e]
Cu	1.32-1.35	43.02 - 2089.61[a]
		31.34 - 52.48[b]
		1.06 - 15.98[e]
Mn	26.36-29.82	5490.60 - 14419.10[a]
		0.30 - 92.10[e]

[a]Njagi *et al.*, 2016; [b]Anietie and Labunmi, 2015; [c]Ajibola and Ozigis, 2005; [d]Odhiambo *et al.*, 2015; [e]Amadi and Nwankwoala, 2013

Table 3: Department of Petroleum Resources (DPR, 2002) Target Value

Metal	Target values (mg/kg)
Cadmium	0.8
Chromium	100
Copper	36
Nickel	35
Lead	85
Zinc	146
Cobalt	20
Manganese	100-300*
Iron	1000*

* USEPA (1986)

DISCUSSION

Copper concentrations ranged from 1.32 – 1.35mg/kg with an average value of 1.34mg/kg (Table 1). The result was above the 0.38mg/kg for the control. Copper result was within the range of 1.06 - 15.98mg/kg reported by Amadi and Nwankwoala, (2013) for Aba but lower than the range of 31.34 – 52.48mg/kg reported by Anietie and Labunmi, (2015) for Akure metropolis. The result was also very much lower than the range of 143.02 – 2089.61mg/kg reported by Njagi *et al.,* (2016) for Kadhodeki dumpsite in Kenya. Copper concentration was below the 36mg/kg target value permitted by DPR (2002).

Manganese concentration ranged from 26.36 – 29.82mg/kg with a mean concentration of 28.09mg/kg. The result was high compared to the 4.28mg/kg obtained for the control. The result was lower than the range of 5490.60 – 14419.10mg/kg reported by Njagi *et al.,* (2016) for Kadhodeki dumpsite, Kenya. The concentration of the metal was within the 100 - 300mg/kg acceptable value by USEPA, (1986) for soil.

The results obtained in both sites are far above the values obtained from the control site. This is an indication that metal enrichment in the soil was caused by waste present in sampled dumpsites as shown in table 1.

CONCLUSION

The concentration of the heavy metals obtained in this study follow the sequence: Mn>Fe >Zn>Cd>Cu>Pb for soil around "Oteri road dumpsite" and Fe> Mn>Zn>Cd>Pb>Cu for soil around "Patani road dumpsite". It is worthy of note that the heavy metal concentration obtained though elevated as a result of waste present in the dumpsites were below DPR permissible target limits except cadmium. Cadmium result obtained in this study calls for concern. Therefore all hands must be on deck to put things right in order to promote a healthy environment for sustainable development.

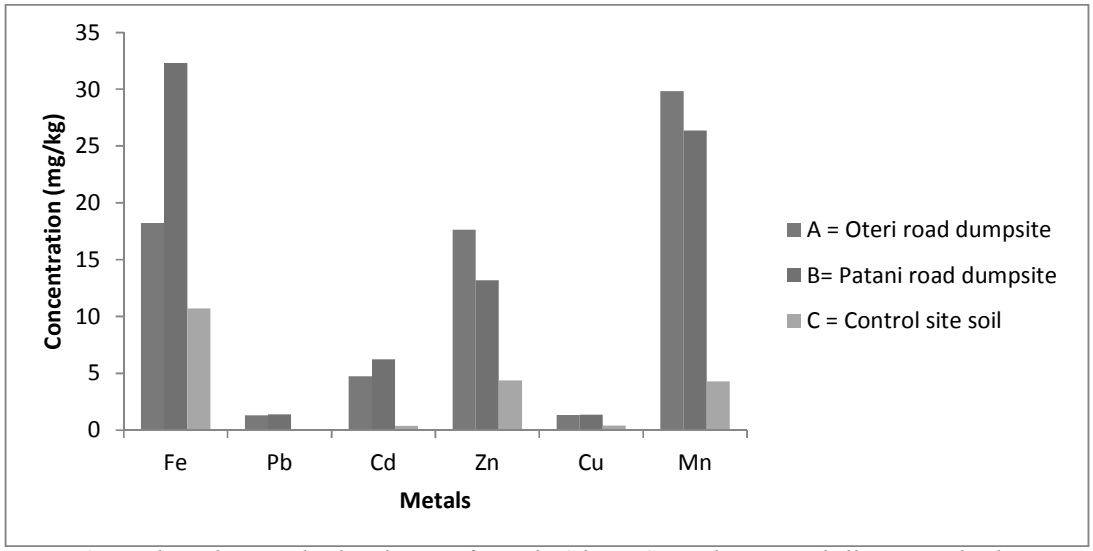

Figure 1 Bar chart showing the distribution of Fe, Pb, Cd, Zn, Cu, and Mn in Ughelli Metropolis dumpsites

REFERENCES

Abah, J., Mashebe, P., Onjefu, S.A., and Malu, S. P. (2015). Assessment of the In-situ Concentrations of Some Heavy Metals in Surface Soil Dusts at the Katima Mulilo Urban Waste Dumpsite, Namibia. *International Journal of Advanced Scientific and Technical Research, 4(5):88-100*

Abollino, O., Aceto M, Maladrino M, Mentastic E, Sarzanini, C and Patrella, F (2002). Heavy Metals in Agricultural Soils from Piedmont Italy, Distribution, Speciation and Chemometric Data Treatment. *Chemosphere 49: 545-557*

Adelekan, B. A. and Abegunde, K. D. (2011). Heavy metals contamination of soil and groundwater at automobile mechanic villages in Ibadan, Nigeria. *Inter. Journal of the Physical Sciences. 6 (5):1045-1058.*

Aina, M., Matejka, G., Mama, D., Yao, B., and Moudachirou, M. (2009). Characterization of stabilized waste: evaluation of pollution risk. *Int. J Environ. Sci. Technol. 6(1):159-165*

Ajibola V. O. and Ozigis I. (2005). Partitioning of some heavy metals in Kaduna street soils. J. of Chemical Society of Nigeria, 30(1), 62-66

Amadi, A. N and Nwankwo, H. O. (2013). Evaluation of Heavy metal in soil from Enyimba Dumpsite in Aba, South Eastern Nigeria.Using Contamination Factor and Geo-Accumulation Index. *Energy and Environmental Research, 3(1):125 - 134*

Anietie, O. V and Labunmi, L. (2015). Surface Soil Pollution by Heavy Metals. A Case Study of two Refuse Dumpsites in Akure Metropolis. *International Journal of Scientific Technology research 4; 71-74*

Asiagwu, A. K, Ilabor, S. C, Omuku, P. E and Onianwa, P. C (2007). Concentration and Speciation Patterns of Some Heavy Metals in Stream Sediments in an Urban City in Nigeria. *Biosciences, Biotechnology Research Asia 4(2)513-520*

Begum, A., Ramaiah, M., Harikrishna, Khan, I. And Veena, K. (2009). Analysis of Heavy Metals Concentration in Soil and Litchens from Various Localities of Hosur Road, Bangalore, India. *E.J. Chem., 6(1): 13-22*

Bin, L., Qinquan, W., Benli, H. and Shuping, L. (2001). Evaluation of the results from a Quassi-Tessier's Sequential extraction procedure for heavy metal speciation in soils and sediments by ICP-MS. *JJAC, 17:1561-1563..*

Department of Petroleum Resources (DPR) (2002). Environmental guidelines and standards for the petroleum industry in Nigeria (revised edition). Department of Petroleum Resources, Ministry of Petroleum and Natural Resources, Abuja, Nigeria.

Kokasoy, G and Sahim, V (2007). Heavy metal removal from industrial wastewater by Chinoptilolit. *J. Environ. Sci. health Part A 42:2139 - 2146*

Lund, W (1990). Speciation Analysis. Why and How? *Fresenius Journal of Anal. Chem. 337:557-564*

Manahan, S. E. (2005). Environmental Chemistry 8th Edition, Lewis Publisher, Boca Ration, Florida.

Martínez C.E., Motto H.L.(2000). Solubility of lead, zinc and copper added to minerals soils. *Environ. Pollut., 107, 153-158.*

Mohiuddin, K. M., Zakir, H. M., Otomo, K., Sharmin, S., and Shikazono, N (2010). Geochemical Distribution of Trace Metal Pollutants in Water and Sediments of Downstream of an Urban River. *Int. J. Environ. Sci. Technol., 7(1):17-28*

Muchuweti, M., Birkett, J. W., Chinyanga, E., Zvauya R., Scrimshaw, M. D and Lester, J.N (2006). Heavy metal content of vegetables irrigated with mixture of wastewater and sewage sludge in Zimbabwe: Implications for human health. *Agric. Ecosyst. Environ. 112:41-48.*

Njagi, J. M., Akunga, D. N., Njagi, M. M., Ngugi, M. P., and Njagi, E M.N. (2016). Heavy Metal Pollution of the Environment by Dumpsites: A Case of Kadhodeki Dumpsite. *Int. J. Life. Sci. Scienti.Res.,*2(2):191-197

Nwuche, C. O. and Ugoji, E. O. (2008). Effects of Heavy Metal Pollution on the Soil Microbial activity. *Int. J. Environ. Sci. Tech. 5(3):409-414*

Pascual, B., Gold-Bouchot, G., Ceja-Moreno, V., & del Ri'o-garci'a, M. (2004). Heavy metal and hydrocarbons in sediments from three lakes from san Miguel, Chiapas, Mexico. *Bull. Environ. Contam. Toxicol., 73*, 762-769.

Quek S.Y., Wase D.A.J., Forster C.F., (1998). The use of sago waste for the sorption of lead and copper. *Water SA, 24 (3), 251-256.*

Solomon E. Shaibu, Folahan A. Adekola, Halimat I. Adegoke, Nasir Abdus-Salam (2015). Heavy Metal Speciation Patterns of Selected Dumpsites in Ilorin Metropolis. *International Journal of Chemical, Material and Environmental Research, 2 (1): 1-11*

Tam, N. F. Y. and Wong, Y. S. (2000). Spartial Variation of Heavy Metals in Surface Sediments of Hong Kong Mangroove Swamps. *Environ. Pollution, 100(2):195-205.*

Trichopoulos, D. (2003). Epidemiology of cancer. In cancer Principles and practice of oncology, De vita, V. T (Ed). *Lippincott Company, Philadeiphia, pp 231 – 258.*

Turdogan, M. K, Kilicel, F., Kara, K., Tuncer, I., and Uygan, I. (2002). Heavy metals in soil, vegetables and fruits in the endemic upper gastrointestinal cancer region of Turkey. *Environ. Toxicol. Pharmacol., 13:175-179*

USEPA (1986). Test methods of evaluation of solid waste in contaminated land policies in some industrialized countries. (W.J.F Visser, ed) *Pp 38 - 41TCB report RO2 UK..*

Wilson, B. and Pyatt, F. B (2007). Heavy metal dispersion, persistence and bioaccumulation around an ancient copper mine situated in Anglesey UK. *Ecotoxical. Environ. Safety 66:224-231*

NIGERIAN JOURNAL OF MATERIALS SCIENCE AND ENGINEERING
NJMSE
ISSN 214-453-2

EVALUATION OF COMPACTED BLACK COTTON SOIL – SAWDUST ASH MIXTURES AS ROAD CONSTRUCTION MATERIAL

I. MANNIR, P. YOHANNA AND K. J. OSINUBI
Department of Civil Engineering, Ahmadu Bello University, Zaria, Kaduna State. Nigeria
[paulyohanna45@yahoo.co.uk]

ABSTRACT
This study was aimed at the evaluation of the stabilization potential of sawdust ash (SDA) on black cotton soil. Soil samples were treated with up to 10 % SDA content by dry weight of soil compacted with reduced British Standard light (RBSL) energy. Index properties of the natural soil showed that the soil belongs to A-7-5 (36) in American Association of State Highway Transportation Officials (AASHTO) classification system and CH in Unified Soil Classification System (USCS) classification system. The natural soil has liquid limit, plasticity index and free swell values of 60.0, 32.4 and 50.0 %, respectively. These properties suggest a soil that cannot be used for engineering purpose in its natural state and requires improvement. The liquid limit, plastic limit and linear shrinkage decreased to minimum values of 54 %, 24.4 %, and 14.2 %, respectively, while plasticity index increased to 14.2 % at 10 % SDA content. Also optimum moisture content (OMC) increased to a maximum value of 30 % while maximum dry density decreased to a minimum value of 0.86Mg/m^3 at 10 % SDA content. Peak unsoaked California bearing ratio (CBR) value of 4 % was recorded at 2% SDA content. On the other hand peak 7 days unconfined compressive strength (UCS) value of 90kN/m^2 was recorded at 8 % SDA content. This value fell of specification requirement of the CBR value to be used as sub-base or base material. The durability of samples determined by immersion in water recorded peak resistance to loss in strength of 48.24 % (i.e., loss in strength of 51.76 %) at 8 % SDA content. The results recorded indicate that black cotton soil compacted with RBSL energy cannot be used as a road pavement material, but for low load bearing structures such as road shoulders and pedestrian walkways. However, SDA can be beneficially used as an admixture in road construction when a higher compactive effort is used.

Keywords: *Black cotton soil, Saw dust ash, Stabilization, Durability, California bearing ratio.*

INTRODUCTION

The increase in world population, industrialization and economic development led to a global demand for reduction in the rising cost of waste disposal. Increase in waste generated led to a global research towards economic utilization of wastes for engineering purposes. The safe disposal of industrial and agricultural waste products demand urgent and cost effective solutions because of their debilitating effects on the environment and the health hazards that they constitute. Nearly all industrial activities lead to depletion of natural resources, a process that may result in the accumulation of by-products and/or waste materials. In most cases there are problems associated with the disposal of these waste heaps. Continuous generation of waste arising from industrial by-product and agricultural residue, create acute environmental problems both in terms of their treatment and disposal (Oriola and Moses, 2010).

Black cotton soils are problem soils with expansive behaviour having potential for shrinking or swelling under changing moisture condition (Ola, 1983). Such unusual behavior with changing moisture conditions causes damage to structures, buildings and pavements .They are produced from the breakdown of basic igneous rocks where seasonal variation of weather is extreme. The soils are formed under conditions of poor drainage from basic rocks or limestone under alternating wet or dry climatic conditions. These soils are problematic when used as building foundation and pavement sub-grades. They constitute the major problem soils in north eastern Nigeria where they occupy an estimated area of 104,000 km^2 in the north eastern part of the country (Ola, 1983; Osinubi *et al.,* 2011).

Osinubi and Katte, (1997) referred to soil stabilization as the alteration or control of any soil property. Because of the swelling and shrinkage properties of black cotton soils with changing moisture condition, there is need for improving its engineering properties. Different techniques for improving the engineering properties of the soil have been developed by various researchers such as improvement of black cotton soil with agricultural and industrial waste with pozzalanic properties. Factors normally considered in the use of such options include availability, cost, accessibility, location and workability. Materials that have been used to improve such black cotton soils include cement and lime, pozzolanic admixture like bagasse ash, sawdust ash, locust bean waste ash etc (Moses, 2008).

Lime and Portland cement are industrial manufactured additives which have been in use for improving soil properties (Nerville, 2000). The use of industrial manufactured additives such as cement and lime has always been restricted due to the high cost of purchasing them. There is need for cheaper but efficient materials to be used for soil stabilization, Recent studies have also focused on the use of industrial and agricultural waste as possible admixtures for improving

black cotton soils (Ferguson, 1993; Osinubi and Stephen, 2005; Roy *et.al.,* 2007; Osinubi and Ijimdiya, 2008; 2009; Osinubi and Mustapha, 2009; Srirama and Rama, 2008; Amadi, 2010; Osinubi and Oyelakin, 2012; Eberemu and Sada, 2013; Osinubi *et al.*, 2015; Eberemu *et al.*, 2016). Sawdust is an industrial waste in the timber industry and poses a nuisance to the health and environment when not properly managed (Elinwa and Abdulkadir, 2012). The waste is disposed indiscriminately most of time by incineration with the formation of sawdust ash which poses environment hazard due to the toxic nature of the smoke it emits (KEPA, 2012).

The study was aimed at the evaluation of the stabilization potential of sawdust ash (SDA) on black cotton soil. The objective was to determine the changes in the strength properties of the soil with varying stepped concentration of sawdust ash when the reduced British Standard light compaction energy is used.

MATERIALS AND METHODS

Materials

Soil: Black cotton soil (BCS) used for the study was sourced from Deba Local government Area of Gombe state, Nigeria. Soil sample was collected by method of disturbed sampling. The soil was air-dried, pulverized and passed through British Standard (BS) No. 4 sieve (4.75 mm aperture) as required for laboratory test (Head, 1982).

Sawdust ash: The sawdust ash used for this study was procured locally from a timber shed situated in Bakori town of Katsina state, Nigeria. The sawdust collected was air-dried and burnt under atmospheric condition. The ash was then passed through the BS No. 200 sieve (75µm aperture to meet the requirement of ASTM C618-78 (2013)

Methods

Index Properties: Laboratory tests were performed to determine the index properties of the natural soil and soil–SDA mixtures in accordance with British Standards BS 1377 (1990) and BS 1924 (1990), respectively.

Compaction: Compaction tests were carried out in accordance with BS 1377 (1990) to determine the compaction characteristics of black cotton soil – SDA mixtures. Specimens were prepared in stepped concentrations of 0, 2, 4, 6, 8 and 10 % SDA by dry weight of soil. Specimens were compacted with reduced Proctor energy that involves a 2.5 kg rammer falling 300 mm onto three layers in a British Standard mould, each receiving fifteen (15) blows.

Unconfined compressive strength: The unconfined compression tests were performed on the soil samples according to BS 1377: (1990) Part 7 test 2 using the reduced Proctor compactive effort, at their respective OMCs.

California bearing ratio: The California bearing ratio (CBR) tests were conducted in accordance with BS 1377 (1990) and BS 1924 (1990) for the natural and treated soils, respectively.

Durability: The durability assessment (under adverse field conditions) of the soil sample was determined by resistance to loss in strength when immersed in water. It was expressed as the ratio of UCS of the specimen wax-cured for 7 days and de-waxed top and bottom before being soaked for another 7 days to the UCS of the specimen cured for 14 days:

$$\text{Resistances to Loss in Strength} = \frac{\text{UCS(7Days cured + 7 Days)}}{\text{UCS(14 Days cured)}}$$

RESULTS AND DISCUSSION

Index properties: The natural soil was classified as A-7-5(36) soil based on AASHTO Classification system (AASHTO, 1986), CH soil based on Unified Soil Classification System (USCS) (ASTM, 1992). Some geotechnical properties of the natural black cotton soil are given in Table 1.

Table 1: Properties of the natural black cotton soil

Properties	Quantity
Percentage Passing No. 200 Sieve (75 µm aperture)	91.4
Natural moisture content, %	16.1
Specific gravity	2.46
Free swell %	50.0
Liquid limit, %	60.0
Plastic limit, %	27.6
Plasticity index, %	32.3
Linear shrinkage, %	16.5
Maximum dry density, Mg/m^3	1.36
Optimun moisture content, %	26.0
UCS (7 days), kN/m^2	52.87
CBR (unsoaked), %	3
CBR (soaked), %	2

Effect of Sawdust Ash on Black Cotton Soil

Specific gravity: The specific gravity decreased with increase in sawdust ash treatment as indicated in Fig. 1. The reason for this trend of decrease is due to low specific gravity of SDA (2.20) replacing the soil with higher specific gravity. However, with increment in sawdust ash content, the proportioning of the sample result in decreased quantity of soil and increased sawdust ash, thereby leading to a continuous drop in specific gravity with higher SDA content.

Cation exchange capacity: The cation exchange capacity (CEC) which measures the amount of positively charged cations a soil can hold had decreased with increase in sawdust ash content as shown in Fig 1. The CEC values decreased from 38.3 Cmol/kg for the natural soil to 20.4 Cmol/kg at 10 % SDA treatment. The decrease in CEC value was as a result of decrease in the clay size fraction of the soil (Warrick, 2002;

Salahedin, 2013; Osinubi *et al.*, 2015). The decrease in CEC value could also be attributed to the reduction in pH of black cotton soil by SDA that had a higher calcium hydroxide content that supplied free Ca^{2+} required for the cation exchange between the clay mineral particles. This agrees with the findings of Akinmade, (2008) who worked on stabilization of black cotton soil using locust bean waste ash.

Atterberg limits

Liquid limit: The variation of liquid limit of BCS with SDA content is shown in Fig. 2. The results indicated a decrease in liquid limit from 60 % for the natural soil to a value of 54 % for the soil treated with 10 % SDA, the overall decrease in liquid limit could be attributed by the flocculation and aggregation of clay particles and the accompanying reduction in surface area and increase in strength(Al karagooly, 2012). This decrease may also be due to flocculation and agglomeration arising from cation exchange reactions where by Ca^{+} in the additives reacted with ions of lower valence in the clay structure. This is in agreement with the findings of Al-Zoubi (2008), Portelinha et.al. (2012) and Ramesh et al. (2013).

Plastic limit: The variation of plastic limit of BCS with SDA is shown in Fig. 2. There was increase in plastic limit from 27.6% for the natural soil to a value of 31.1% at 4% SDA. This atteration of soil character probably occurred due to bi-valent calcium ion supplied by the SDA replacing less firmly attached monovalent ions in the double layer surrounding clay particles (Koteswara,2004)

Plasticity index: The result for plasticity index of black cotton soil treated with sawdust ash is as presented in Fig 2. Plasticity index decreased to a minimum at 4 % sawdust ash content and thereafter increased with increase in sawdust ash content. This trend was as a result of substitution of finer particles of the soil with ash, and shows less workability resulting in a higher probability of existance of macropore and poor interlift of the soil (Osinubi *et al.,* 2011).

Linear shrinkage: The variation of linear shrinkage of BCS with SDA content is shown in Fig. 3. Linear shrinkage value range from 16.54 % to 14.2 % and the trend shows that shrinkage is highly dependent on the amount of fines in the soil. Linear shrinkage occur as the water surronding the individual soil particles of the specimen is removed, the particles move closer together more movenment are experience in finear particles than coaser particles (Osinubi *et al*., 2011)

Compaction characteristics

Maximum dry density*:* The variation of maximum dry density (MDD) of BCS with SDA content is shown in Fig. 4 The MDD values decreased on addition of SDA to a value of 0.86 Mg/m^3 at 10 % SDA content. The decrease in MDD with addition of SDA was probably due to the lower specific gravity of the SDA occupying spaces with lattice there by decreasing the MDD.Similar behaviour was observed by Phanikumar *et al.,* (2004), Osinubi and Stephen, (2007), Jadhao and Nagarnaik (2008) as well as Kumar and Puri (2013).

Optimum moisture content: The variation of optimum moisture content (OMC) of black cotton soil with sawdust ash (SDA) content is shown in Fig. 4. The OMC of the natural soil was 26% and it increased to a value of 30.0 % at 10 % SDA content. The increase in OMC agrees with the results reported by Osinubi and Katte (1997). They attributed the increase to the amount of water required for pozzolanic reactions to take place.

Strength characteristics

Unconfined compressive strength: The variation of unconfined compressive strength (UCS) of black cotton soil with sawdust ash SDA content at 7, 14 and 28 days curing periods is shown in Fig. 5. It was observed that the UCS of the SDA treated black cotton soil initially increased up to 8 % SDA content and thereafter decreased for all the curing periods considered, Peak UCS values of 104.23, 174.83 and 175.50 kN/m^2, respectively, were obtained at 8 % SDA content. The increased UCS values could be attributed to ion exchange at the surface of clay particles as the Ca^{2+} in the stabilizer reacted with the lower valence metallic ions in the clay microstructure which resulted in agglomeration and flocculation of the clay particles (Koteswara, *et al.,* 2012).

***California bearing ratio*:**The results presented in Fig. 6 show the variation of soaked and unsoaked California bearing ratio (CBR) of black cotton soil with sawdust ash content. The CBR values of the natural soil is 3% for both unsoaked and soaked conditions. The unsoaked CBR value increased to a peak value of 4 % at 2 % SDA content and progressively decreased to 3 % at 8 % SDA content, then increased to 4 % at 10 % SDA content. For the soaked condition CBR value decreased to a minimum value of 2 % at 2 % SDA and progressively increased to 3 % at 10 % SDA content. There was a a marginal improvement with higher SDA content. The reason for the slight improvenment in the strength for the unsoaked condition was due to inadequate amount of calcium available for the formation of calcium silicate hydrate (CSH), which is the major compound responsible for the strength gain.(Koteswara Rao, *et al.,* 2012) The Nigerian General Specifications (1997) recommends that a CBR value of 180% should be attained in the laboratory for cement stabilized material to the constructed by the mix in place method. Although the SDA treated black cotton soil did not meet the criterion specified for use as base course material, SDA can be used in admixture stabilization with a more potent stabilizer(i.e cement or lime) in order to reduce cost of construction.

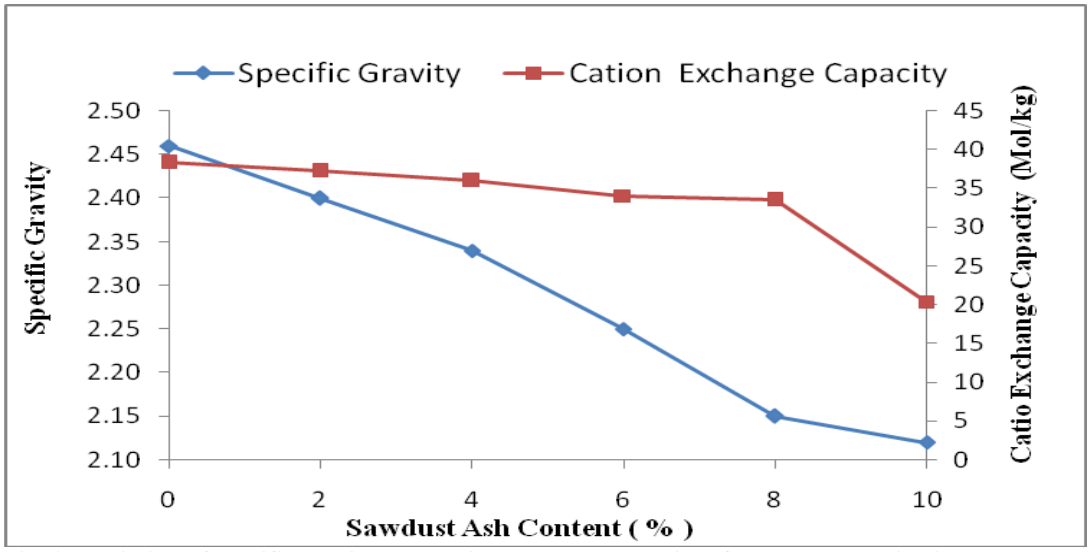

Fig. 1: Variation of specific gravity and cation exchange capacity of black cotton soil with sawdust ash content.

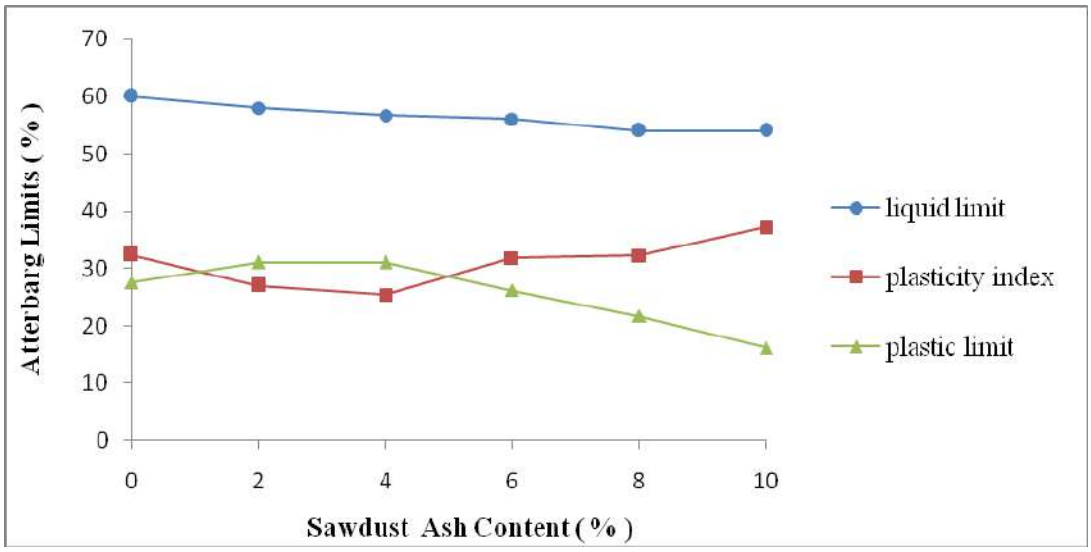

Fig. 2: Variation of Atterbarg limits of black cotton soil with sawdust ash content

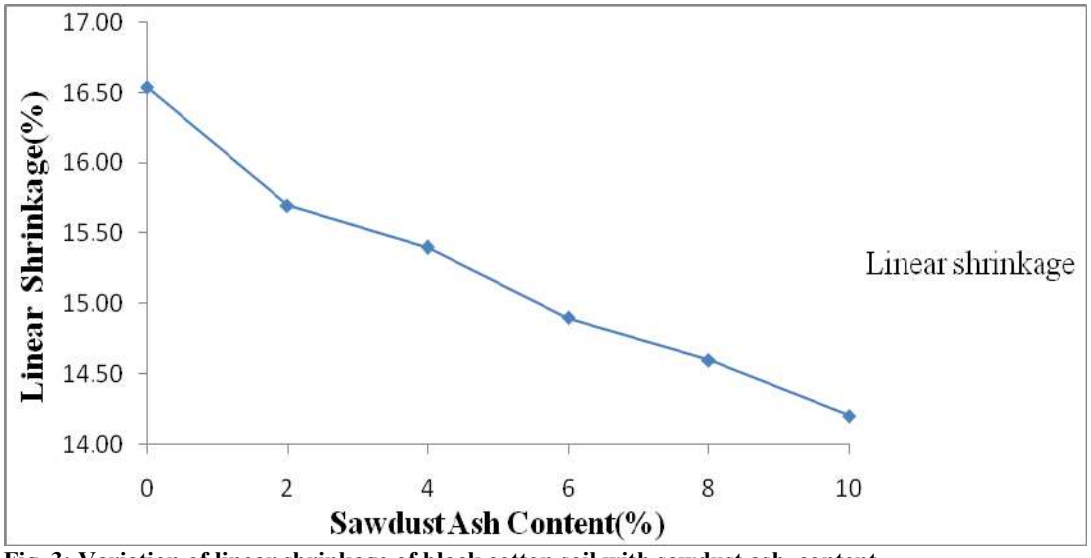

Fig. 3: Variation of linear shrinkage of black cotton soil with sawdust ash content

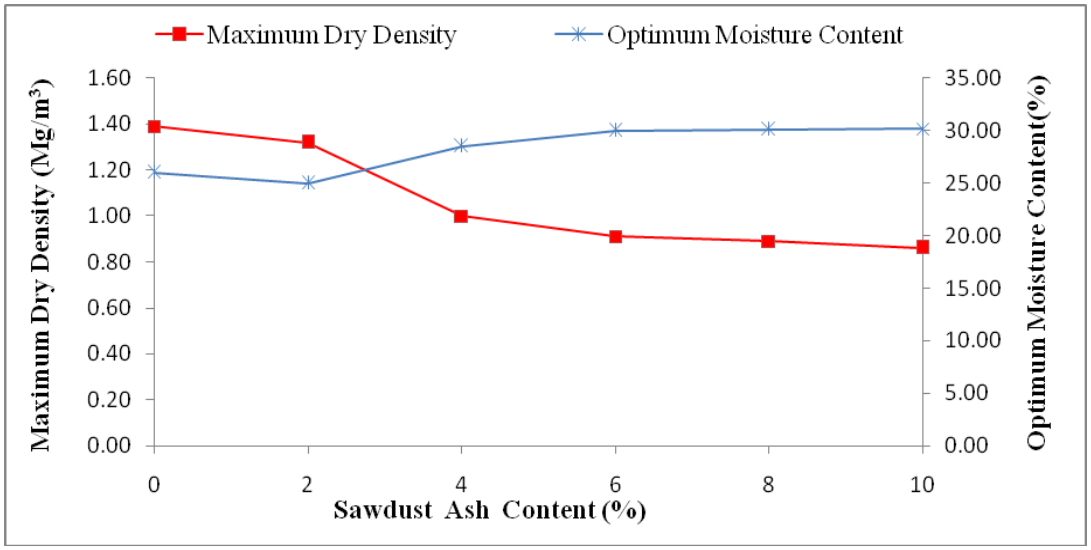

Fig. 4: Variation of maximum dry density and optimum moisture content of black cotton soil with sawdust ash content.

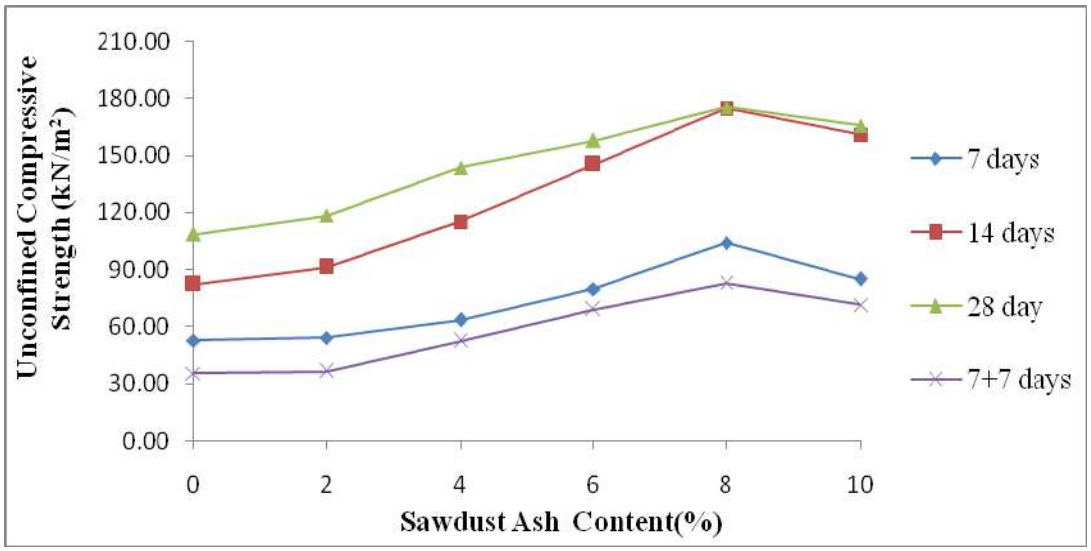

Fig. 5 Variation of unconfined compressive strength of black cotton soil with sawdust ash content.

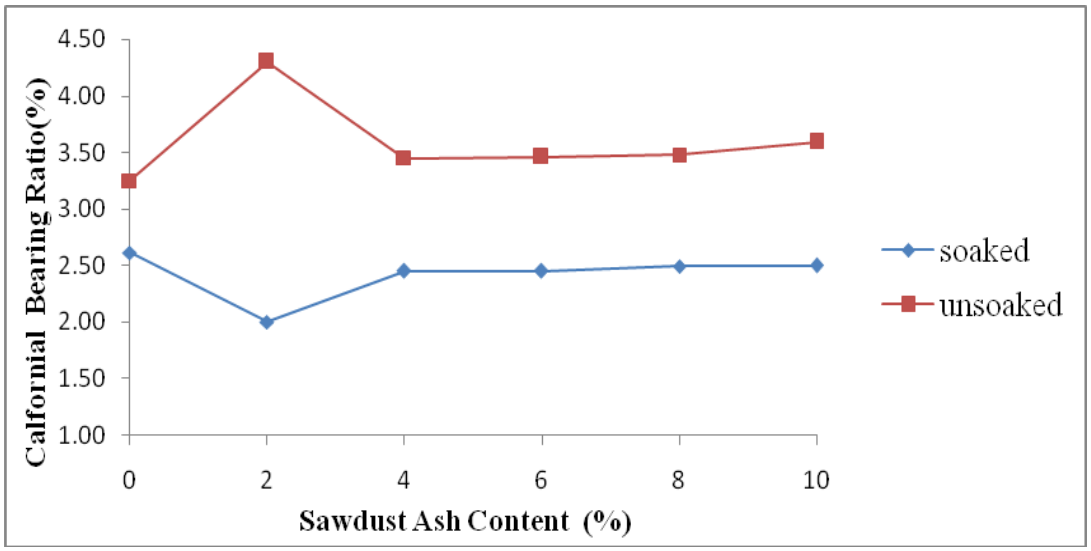

Fig. 6. Variation of California bearing ratio of black cotton soil with sawdust ash content

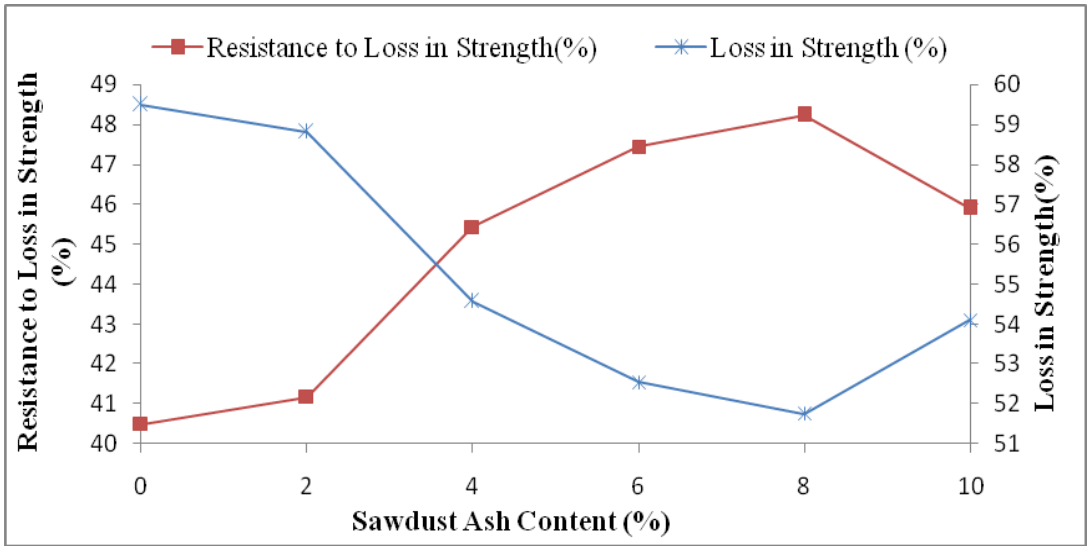

Fig. 7: Variation of loss in strength and resistance to loss in strength of black cotton soil with sawdust ash content.

***Durability*:** The resistance to loss in strength for the black cotton soil shows the variation of the durability of black cotton soil with sawdust ash content as shown in Fig. 7. The resistance to loss in strength increased as SDA content increased to a peak value of 48.24 % (i.e, 51.76 % loss in strength) at 8 % SDA content and thereafter decreased for the range of SDA content considered. The recorded loss in strength was more than the maximum 20 % allowable loss in strength (Osinubi *et al.,* 2009). Regardless of the harsher 7 days immersion period used in this study, the SDA stabilized blackcotton soil did not meet the durability requirement for use in pavenment construction.

CONCLUSION

Results of preliminary investigations conducted on the natural properties of the soil showed that the soil is classified as A-7-5(36) subgrade of the AASHTO classification system, CH soil according to USCS. The natural soil was highly silty and clayey with 96.6 percent passing BS sieve No. 200, with a liquid limit of 60%, plastic limit of 27.6% and plasticity index 37.37%. The liquid limit decrease to a minimum value of 50 % at 10 % S D A, the plastic limit, plasticity index and linear shrinkage at a minimum value at 10 % S D A with the values 24.4 %, 14.2% and 14.2 % respectively. Addition of sawdust ash significantly improvesd the index properties, compaction and strength characteristic of black cotton soil under study. Addition of sawdust ash brought about an improvement in the compaction parameters of the study soils, by increasing the optimum moisture content of the soils with decrease in the corresponding value of the maximun dry density. There was a general increase in the UCS value with SDA content and curing period. The CBR value of the treated soil (unsoaked) recorded a peak value of 4 % at 6 % SDA content. This value is significantly lower than the CBR value of 180% recommended by the Nigerian General Specification (1997). It implies that SDA cannot be used as a stand-alone stabilizer for black cotton soil in road construction work. but could used in areas where less strength is required such as shoulders and pedestrian walkways. The benefit of the technique includes the reduction of the cost of stabilization when it is used as an admixture and the adverse enviromental impact of sawdust waste.

REFERENCES

AASHTO (1986): Standard Specification for Transportation Material and Method of Sampling and Testing 14th Edition Am. Assoc. of state Hwy and transp. Official Washington D.C.

Akinmade, O. B. (2008). "*Stabilization of Black Cotton Soil using Locust Bean Waste Ash*".Unpublished M.Sc thesis, Civil Engineering Department, Ahmadu Bello University, Zaria.

Al karagooly, Y. H (2012) Effect of Cement Kiln Dust on Some Properties of Soil. *Journal of Babylon University/Engineering Sciences*, 20(4): 110-117.

Amadi, A (2010) Evaluation of Changes in Index Properties of Lateritic Soil Stabilized with Fly Ash. *Leonardo Electronic Journal of Practices and Technologies.*17: 69-78

ASTM (1992) "Standard specification for fly Ash and Raw or calcined natural pozzolana for use as a mineral admixture in portland Annual Book of ASTM standard philadelphia U.S.A.

ASTM C618-78(2013) Standard Specification for Determination of Compacting Factor Bristish Institution London.

Al-Zoubi, M. S. (2008) "Undrained Shear Strength and Swelling Characteristics of Cement Treated Soil" *Jordan Journal of Civil Engineering,* 2(1): 53-62.

BS 1377(1990).*Method of Testing Soils for Civil Engineering Purpose*. British Standard Institute, BSI, London.

BS1924 (1990) *Method of Test for Stabilized Soils.* British Standard Institute BSI London.

Eberemu, O.A and Sada, H. (2013) "*Compressibility Characteristics of Compacted Black Cotton Soil Treated with Rice Husk Ash*" *Nigerian Journals of Technology* Vol. 32 No 3 pp 507-521.

Eberemu, A.O., Omajali, D.I and Abdulhamid, Z. (2016) Effect of Compactive Effort and Curing Period on the Compressibility Characteristics of Tropical Black Clay Treated with rice Husk Ash. *Journal of Geotechnical and Geological Engineering*, Vol 34(1), pp 313-322. DOI 10.1007/s10706-015-9946-9.

Elinwa A U. and Abdulkadir (2012); Characterizing sawdust ash for use as an inhibitor for reinforcement corrosion.

Ferguson, G. (1993). Use of Self-Cementing Fly Ash as a Soil Stabilizing Agent, Geotechnical Special Publication No. 36*, American Society of Civil Engineers*, New York, United State of America.

Head K.H. (1982); Manual of soil laboratory testing Vol.1 pentech press London Plymouth.

Jadhao, P.D and Nagarnaik, P. B. (2008) Influence of Polypropylene Fibers on Engineering Behavior of Soil−Fly Ash Mixtures for Road Construction. *Electronic Journal of Geotechnical Engineering*, 13: 1-11.

KEPA (2012); A guide to environment heath issue in kaduna state vol 24 N0. 4 Kaduna state Environmental protection agency.

Koteswara Rao, D. (2004), The performance studies on Geo-grid as reinforcement in the flexible pavement construction, IGC-2004(9).

Koteswara Rao, D, Anusha, M., Pranav, P.R.T., Venkatesh, G. (2012)" A Laboratory Study on Stabilization of Marine Clay using Sawdust Ash and Lime. *International Journal of Engineering science.* 2,(4): 851 – 862

Kumar,B and Puri,N.(2013) Stabilization of Weak Pavement Subgrades using Cement Kiln Dust *International Journal of Civil Engineering and Technology*, 4(1): 26-37.

Moses, G. (2008) "Stabilization of Black Cotton Soil with Ordinary Portland Cement Using Bagasse Ash as Admixture" *IRJI Journal of Research in Engrg,* 5(3): 107-115.

Neville, A.M. (2000). *Properties of Concrete.* 4th ed. (low-price ed.). Pearson Education Asia Publication, England, Produced by Longman Malaysia

Nigerian General Specifications (1997), *Road and Bridges Federal Ministry of Works*. Abuja Nigeria.

Ola, S. A. (1983). 'The Geotechnical Properties of Black Cotton Soils of North Eastern Nigeria.' In S. A. Ola (ed.) *Tropical Soils of Nigeria in Engineering Practice.* Balkama, Rotterdam, pp. 160-178.

Oriola, F. and Moses, G. (2010) "Groundnut Shell Ash Stabilization of Black Cotton Soil" *Electronic Journal of Geotechnical Engineering*, 15: 415-428.

Osinubi, K. J. and Katte, V.Y. (1997). Effect of elapsed time after mixing on grain size plasticity characteristics soil-lime mixes. *Nigeria Society of Engineers Technical Transactions*, 32(4): 65-76.

Osinubi, K. J. and Stephen, T. A. (2005). Economic utilization of an agro-industrial waste – bagasse ash. *Proceedings of the 4th Nigerian Materials Congress "NIMACON 2005"*, Zaria, Nigeria, 17 –19 November, pp.36-40

Osinubi K.J., and Stephen T.A (2007)"Influence of compactive effort on bagasses ash treated black cotton soil Nigerian. *Journal of Soil and Environmental Research*..7: 92-101.

Osinubi, K. J. and Ijimdiya, T. S. (2008). Laboratory investigation of engineering use of baggasse ash. *Nigerian Society of Engineers Technical Transactions*. 43(1): 1-17.

Osinubi, K. J. and Ijimdiya, T. S. (2009). Laboratory Investigation of Desiccation Characteristics of Black Cotton Soil Treated with Bagasse Ash. *Proceedings of Bi-monthly Meetings/Workshops organized by Zaria Chapter of Materials Society of Nigeria*, pp. 61– 68.

Osinubi, K. J. and Mustapha, A. M. (2009). Optimal use of bagasse ash on cement stabilized laterite. *Nigerian Society of Engineers Technical Transactions*, Vol. 44, No 1, pp. 1 – 16.

Osinubi, K.J., Ijimdiya, T. S. and Nmadu, I. (2009). 'Lime Stabilization of Black Cotton Soil using Bagasse Ash as Admixture.' *Advanced Materials Research*, Vols. 62 – 64, pp. 3 – 10. In: *Advances in Materials Systems Technologies II* Online http://www.scientific.net Trans Tech Publications, Switzerland.

Osinubi, K. J, Oyelakin, M. A and Eberemu, A. O. (2011). Improvement of Black Cotton Soil with Ordinary Portland Cement - Locust Bean Waste Ash Blend. *Electronic Journal of Geotechnical Engineering,* 16: 619-627.

Osinubi, K. J and Oyelakin M. A. (2012). 'Optimising Soil-Cement-Ash Stabilization Mix for Maximum Compressive Strength: A Case Study of the Tropical Clay Sub-base Material Stabilized with Cement-locust Bean Waste Ash.' *Proeedings of West Africa Built Environment Research Conference (WABER 2012) Conference.* Editors Dr. Samuel Laryea, Dr. Sena A. Agyepong, Dr. Roine Leiringer and Prof. Will Hughes. July 24 -26, Abuja, Nigeria. Vol. 2, pp. 1207 – 1218.

Osinubi, K. J, Yohanna, P and Eberemu, A. O. (2015) Cement Modification of Tropical Black Clay Using Iron Ore Tailing as Admixture. *Journal of Transportation Geotechnics*.Vol 5pp 35- 49. http://dx.doi.org/10.1016/j.trgeo.2015.10.001 Elsevier Publishing Company.

Phanikumar B.R., Radhey S. and Sharma (2004) Effect of flyash on Engineering properties of Expansive Soil. *Journal of Geotechnical and Geoenvironmental Engineering*: 130(7): 764-767.

Portelinha, F. H. M., Lima, D. C, Fontes, M. P. F.and Carvalho, C. A. B (2012) Modification of a Lateritic Soil with Lime and Cement:An Economical Alternative for Flexible Pavement Layers. *Journal of Soil and Rock*, 35(1): 51-63.

Ramesh, H.N, Krishnaiah, A.J and Supriya,M.D (2013) Role of Moulding Water Content on the Strength Properties of Red Earth treated with Mine tailings. *International Journal of Scientific and Engineering Research*, l4(5): 47-50.

Roy, S., Adhikari, G.R, and Gupta, R.N (2007).'Use of gold mill tailings in making bricks: *a feasibility study.' Waste Management and Research*, No. 25, pp. 475-482.

Salahedin, M. (2013) Effects of CEC on Atterberg limits and Plastic Index in Different Soil Textures .*International Journal of Agronomy and Plant Production*, 4 (9): 2111-2118.

Srirama, R. and Rama, R. (2008). Swell - Shrink Behaviour of Expansive Soils Under Stabilized Fly Ash Cushions. T*he 12th International Conference of International Association for Computer Methods and Advances in Geomechanics* Goa, India pp 1539-1546.

Warrick, A.W (2002).Soil physics companion (ed). CRC Press LLC. Boca Raton, London, New York Washington, D.C. P: 19.

NIGERIA JOURNAL OF MATERIALS SCIENCE AND ENGINEERING

A Publication of Materials Science and Technology Society of Nigeria (MSN) RC: 54708

ISSN: 214-453-2

CALL FOR PAPERS/GUIDE FOR AUTHORS

AIM: *T*o improve the international exchange of scientific research in materials science and engineering.

INTRODUCTION

The Journal of Materials Science and Engineering (NJMSE) publishes reviews, full-length papers, and short Communications recording original research results on, or techniques for studying the relationship between structure, properties, and uses of materials. The subjects are seen from international and interdisciplinary perspectives covering areas including metals, ceramics, glasses, polymers, electrical materials, composite materials, fibers, nanostructured materials, nanocomposites, biological, biomedical materials, etc. The NJMSE is now firmly established as the leading source of primary communication for scientists investigating the structure and properties of all engineering materials in Nigeria.

UNIQUENESS OF THE JOURNAL

NJMSE is introduced to publish research findings on current topical issues of interest to both public and private sectors. The scope of the Journal focuses on theoretical and empirical research in the Materials Science and Engineering. Findings from multidisciplinary research covering diverse areas of interest with potential impact on the public and private sectors of both the national and international communities will be priorities of the journal.

GUIDE FOR AUHORS

NJMSE welcomes research papers covering original work that has good potential for practical application. Submission of a manuscript will be held to imply that the work being reported is original and that the result has not been published previously nor been under considerations for publication elsewhere.

MANUSCRIPT PREPARATION

The format of the typescript should be as follows:

The official language of the journal is English. When writing do not mix languages, use US English completely or use UK English completely. It is expected that before submission, the manuscript will have been thoroughly reviewed and written in simple clear expression. Manuscript should be typewritten with double-spacing and 2.54cm or 1inch margins on all sides. Manuscripts should be submitted in electronic form and e-mailed directly to the Managing Editor in MS-Word format. Manuscripts should be arranged in the following order: title page, abstract, introduction, materials and methods, results and discussion, conclusions, acknowledgements, references. The manuscripts should follow the format listed below.

Title: The title page should contain the title [concise but clear expression, written in bold, lower case], followed by the authors [initials then surname, block letters throughout], and followed by their institutional affiliations and their e-mail addresses. In case of many authors, please indicate the corresponding author

Abstract: An abstract of not more than 350 words should be supplied immediately before the beginning of the paper (Graphical abstracts are also acceptable).

Introduction: This should contain a brief review of literature, clearly stated objectives and justification for the study.

Materials and Methods: This should contain materials preparation procedure and major measurement patterns. Sufficient information should be provided to perform repetition of the experimental work.

Results and Discussion: The result section should contain appropriate tables, figures/illustrations**.** These should be pertinent to the work and should clearly indicate the degree of reliability of results. Tables should be numbered consecutively, with a short descriptive title in upper case (block letters) on top of the table. They should contain no vertical lines and no lines to separate the rows except the heading and the end of the table. Figures, micrographs, or illustrations must be clearly captioned, the captions at the bottom of each figure. Figures may not be used to repeat the information already presented in tables or text or vice versa. Micrographs and illustrations are considered as figures and must be labeled as such.

Conclusions: These should summarize any important conclusions emerging from the work.

Acknowledgements: These should be presented at the end of text and before the references. Technical assistance and advice may be acknowledged. Acknowledgments of financial support can also be stated in this section.

References:
Citing: Reference in the text should be made by the author's last name and year of publication, e.g. (Abel, 2007); (Abel and Babcock, 2007); (Bowen *et al*., 2007). Two papers by the same author in the same year should be distinguished by a suffix, (a, b, etc) e.g. (Madonna, 2006a); (Madonna, 2006b).
Listing: This should be in alphabetical order and should follow this format: Name(s) and initial(s) of author(s), (year of publication), exact title of paper (in quote), the title of periodical, Vol. (number)**:** initial and final page numbers. Please note that only name cited in the text can be used.
Serial: Briant, C.L. and Banerji, S.K. (1981). Tempered martensite embrittlement and intergranular fracture in an ultrahigh strength sulfur doped steel, Metall. Trans. A, 12A: 309-319.
Book: Samuels, L.E. (1982). Metallographic polishing by mechanical methods, 3ed., American Society for Metals, Metals, Park, Ohio..
Proceeding: Olorunnisola, A.O. (2006). The potentials of bamboo as novel building and furniture production materials in Nigeria, pp.180-185. In *Proc. Nigerian Materials Congress (NIMACON 2006),* (B. Babatope and W.O. Siyanbola, eds.), organized by Materials Society of Nigeria, 15-18 November 2006, Abuja, Nigeria

Heading and sub-heading: All headings and sub-headings should be numbered and started from the left hand margin. All headings should be in upper case while sub-headings should be in lower case except the first letter.

Equations: Equations should be distinctly typed using Microsoft equation. Avoid powers of "e" and use "exp". Equations should be numbered consecutively by Arabic numerals in parenthesis at the right margin. In the text, such equation should be cited as equation (1) etc.

Units and symbols: Symbols, units and nomenclature should conform to the recommendations of the International Union of Pure Applied Chemistry (IUPAC). SI units should be used for physical quantities.

Peer-Review: All submitted manuscripts are subjected to a peer- review process and galley proofs will be sent to the first or corresponding author where necessary.

SUBMISSION OF MANUSCRIPTS
The Assessment fee is ₦ 5,000.00 only per article. All submitted articles MUST be accompanied with scanned Bank Tellers or On-line transfer receipt as evidence of payment. Send your article(s) and Bank Teller to: njmse@msn.ng Submission of manuscripts on-line is recommended in order to accelerate and simplify the refereeing process.

PRINTING COST/PAGE CHARGE
Corresponding Authors of accepted articles will be required to pay ₦12,000.00 only (All other countries $ 100 USD) and they will receive a free copy of NJMSE, while each additional copy will be sold for ₦ 4,000.00 only.

COPY RIGHT
Submission of an article for publication implies the transfer of the copyright of the manuscript from the author(s) to the publisher upon acceptance. Accepted papers become the permanent property of the publisher and may not be reproduced by any means without the written consent of the Editor-in-Chief.

Correspondence:

Dr. A. Giwa
Department of Polymer and Textile Science
Ahmadu Bello University
Zaria - Nigeria

Account Details
Name: Mat. Sc. & Tech. Soc. of Nig.
GTB A/C No. 0171794514

FOR: Nigerian Journal of Materials Science and Engineering (NJMSE)
Email: njmse@msn.ng; GSM: 08051990880

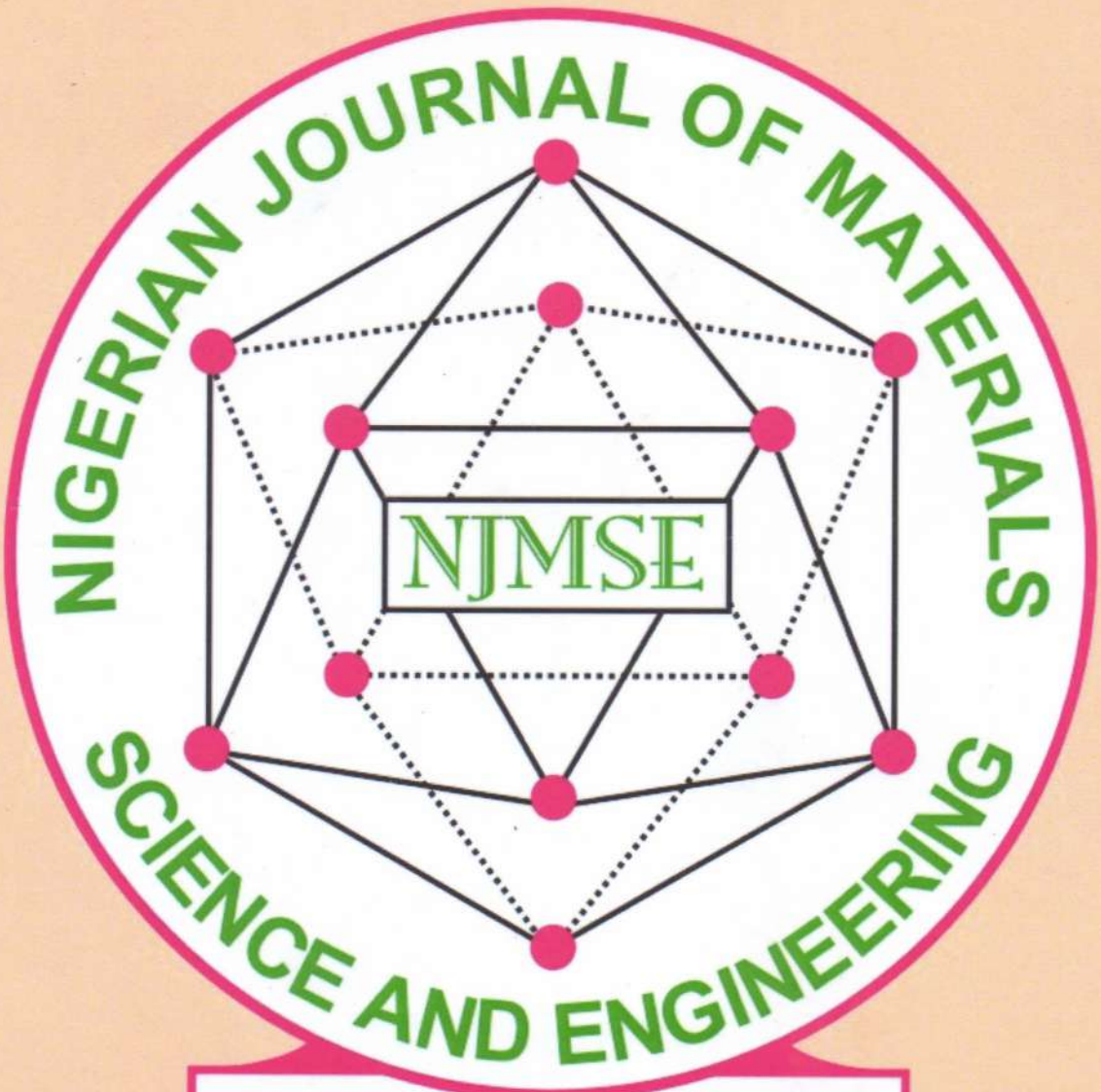

ISSN 214-453-2